
Barrow Alaska Coastal Erosion Feasibility Study

Appendix D: Hydraulics and Hydrology



Barrow, Alaska



**US Army Corps
of Engineers**

Alaska District

PAGE INTENTIONALLY LEFT BLANK

PREFACE

The following 2019 Hydraulics and Hydrology Appendix for the Barrow Alaska Coastal Erosion Feasibility Study is based on the 2010 Hydraulics Appendix that was reviewed by Dr. Robert Dean in 2007.

The Barrow Alaska Coastal Erosion Feasibility Study began in July 2017. The Hydraulics and Hydrology Appendix for the study was scheduled to meet the 3x3x3 paradigm. The data from the 2010 Hydraulics Appendix was to be updated to include recent wind and wave hindcasts and use improved models that were available. The Tentatively Selected Plan (TSP) was scheduled for February 2019 and Agency Decision Milestone (ADM) for October 2019. In March, 2018, 8 months into the schedule, the TSP was moved up 7 months to June 2018 and the feasibility study schedule was reduced by 6 months. With the updated TSP date, new data to update the 2010 Hydraulics Appendix work would not be available before TSP. The team made a risk informed decision to use the data and design from the 2010 Hydraulics Appendix. In June 2018 the schedule was reduced by another 6 months, making the feasibility study schedule a two year study. The original schedule for updating the hydraulic modeling and analyses could not be shifted and still allow sufficient time to perform all data collection and design analyses before ADM. The reduced schedule and reliance upon the 14 year old data and analyses performed for the 2010 Barrow Storm Damage Reduction Hydraulic Appendix was a risk-informed planning decision accepted by the Project Delivery Team (PDT), Pacific Ocean Division (POD), the Regional Integration Team (RIT), and Office of Water Project Review (OWPR) on June 25, 2018. To mitigate the risk of using the 2010 Hydraulics Appendix data, the team continued with the modeling update and agreed that the design would be revisited in Pre-Engineering and Design (PED) to reflect the updated modeling results. The alternatives in the following 2019 Hydraulic and Hydrology Appendix reflect the alternatives developed for the current study. This appendix does not include any design changes associated with model updates or updated design guidance because the modeling updates were not available at the time of report submission.

The 2010 Hydraulic Appendix included the development of a wind and wave hindcast that was used to determine the forcing for nearshore wave modeling and wind surge modeling. The nearshore waves and wind surge (including inverted barometric pressure and approximated tide) were used as inputs for the wave run-up model (SBEACH). The run-up elevation was then used in addition to the total water level (tide + wind surge + wave setup) to calculate the depth-limited wave height at the toe of the structure. The depth-limited wave height was used to calculate run-up associated with a permeable risk reduction structure and as the basis for determining armor rock size based on wave forces. The wind and wave hindcast, wave transformation, total surge, total water level modeling, run-up modeling and calculations, and armor rock size selection presented in the following Hydraulic and Hydrology Appendix is from the 2010 Hydraulic Appendix and has not been updated. No tidal determination had been performed by the time modeling completed in 2004, but it is assumed that Mean Lower Low Water (MLLW) was used as the vertical datum for the 2010 Hydraulic Appendix and all data that was not provided in MLLW was converted to MLLW.

While the risk-informed planning decision did not allow enough time to incorporate any new data or update the design analysis in the following 2019 Hydraulic and Hydrology Appendix, the PDT has continued to move forward with data collection and hydraulic modeling during the

feasibility phase. New LiDAR and tidal determination were collected in July 2018 and updated wind and wave hindcast, coupled wave transformation, and wind surge modeling began in August 2018. All future modeling efforts are being completed in Mean Higher High Water (MHHW), based on the 2018 tidal determination, to ensure that high tide is associated with model outputs. This effort will provide a total water level at the location where the toe of the proposed structure would be constructed. The updated modeled run-up in addition to the total water level will be used to determine the depth-limited wave height and run-up elevation, setting the crest elevation for the structure. This information would be used to complete the final design of the selected alternative if/when the project moves into the PED Phase.

Beach nourishment has been thoroughly studied as a possibility for Barrow starting in 1987 with a coastal survey program for Barrow and ending with the dredge sinking in August 2000. In the Coastal Survey Program for Barrow it was reported that the mean sediment diameter decreases in the offshore direction, with beach sediment being coarse sand (D_{50} of 0.31mm), nearshore sediment being fine sand (D_{50} of 0.23mm), and offshore being fine sand (D_{50} of 0.10mm). It also found that no location offshore had sufficient sediment with the same coarse sand that is typically found on the beach. The Wainwright and Barrow Beach Nourishment Project and Plan Review in 1992 found that there was no upland source of material available in the quantities and quality needed for beach nourishment and restoration. EM 1110-2-1100 (Part III) Chapter 2 suggests that the mean sediment diameter used for nourishment should be the same size or slightly larger than the existing material on the beach. The beach nourishment efforts that were performed by a dredge bought for Wainwright and Barrow had a difficult time producing high quantities of adequately sized material off of Barrow and the dredge sunk during the August 2000 storm event. Because sufficient analysis was conducted and yielded no adequately sized material in the quantities needed, beach nourishment was recognized as an alternative, but was eventually dropped from further consideration for the current study.

The 2019 Barrow Alaska Coastal Erosion Feasibility Study Hydraulics and Hydrology Appendix went through an Agency Technical Review (ATR) in September 2018, was reviewed for United States Army Corps of Engineers (USACE) Headquarter (HQ) policy conformance in October 2018, and went through a second ATR in May 2019. The 2019 Hydraulics and Hydrology Appendix has been updated according to the comments made during the review process. Major comments that were made during the reviews and will be addressed in PED include compliance with USACE Relative Sea Level Change (RSLC) guidance (ER 1100-2-8162 and ETL 1100-2-1) and addressing resiliency measures to comply with USACE Resilience guidance (ECB 2018-2). Design adjustments that will be investigated in PED include increasing armor rock size, raising the crest elevation, and buried toe options for the proposed structure. In response to ATR and HQ review comments on compliance of the 2019 Hydraulics and Hydrology Appendix to current RSLC guidance, new RSLC calculations are included in the 2019 Hydraulics and Hydrology Appendix.

To capture some of the uncertainty in the proposed crest height due to RSLC not being incorporated in the 2004 modeling and the currently proposed TSP, a sensitivity analysis was performed in order to bound the potential crest elevations (Section 14 Volume Sensitivity Analysis). An updated RSLC analysis was performed and is included in the body of the following Hydraulics and Hydrology Appendix (Section 6 Sea Level Change). All three RSLC curves (USACE Low, USACE Intermediate, and USACE High) were included in the sensitivity

analysis. In order to incorporate RSLC into the 2004 modeling results, RSLC was linearly added to the SBEACH total water levels reported in Table 16 of Section 10.4.1 (Total Water Level). Based on the updated total water level and the estimated elevation at the toe of the proposed structure, a new design wave height was calculated. The design wave height was set to the depth-limited wave height, with the wave height set to 78 percent of the water depth. Based on the new design wave height, a new run-up calculation was performed using wave run-up on permeable surfaces (Eq. VI-5-13 in EM 1110-2-1100) as described in Section 10.4.2 (Run-up for Low Lying Area Structure) and Section 10.4.3 (Run-up for Bluff Revetment) in the following Hydraulics and Hydrology Appendix. Based on engineering judgment, safety concerns of the community, and budget constraints, only the run-up associated with the RSLC at 50 years past construction was considered for the sensitivity analysis. The crest elevations used for the sensitivity analysis were 14.5ft MLLW, 15.5ft MLLW, and 17ft MLLW for the berm and revetted raised road and 19ft MLLW, 21ft MLLW, and 23ft MLLW for the revetment.

Ivu events occur when the shorefast ice is pushed onto the beach and the leading edge digs into the beach and buckle up into piles of ice blocks as high as 30 ft (Section 3.2 Ice Conditions). The North Slope Borough Hazard Mitigation Plan (HMP) describes the risk of an ivu event as rare and a credible probability with limited magnitude/severity (The North Slope Borough, 2015). There are three recorded events with limited extent in the City of Barrow in the Borough's HMP. Damage from an ivu event was determined to be an acceptable risk for the current study, so only a depth-limited wave height was used to size the armor rock. To capture some of the uncertainty in the proposed armor rock size, due to RSLC not being incorporated in the 2004 modeling and the currently proposed TSP, a sensitivity analysis was also performed to bound the armor rock size (Section 14 Volume Sensitivity Analysis). To calculate the new armor rock size, the three RSLC curves at the 50-year life cycle of the structure were linearly added to the water depth originally used to calculate the design wave height. The new water depth was then used to calculate the armor rock size using the Hudson Equation (Eq. VI-5-67, EM 1110-2-1100) with a K_d value of 2.0, as was used in the original design. The three W_{50} armor rock sizes used for the sensitivity analysis were 2.7 ton, 3.8 ton, and 5.25 ton. The 2.7 ton armor rock was used for the analysis of the lowest crest height associated with the berm, revetted raised road, and revetment, the 3.8 ton armor rock was used for the intermediate crest height associated with the three sections, and the 5.25 ton armor rock was used for the highest crest height associated with the three sections.

PAGE INTENTIONALLY LEFT BLANK

HYDRAULICS AND HYDROLOGY APPENDIX

1.	Introduction	1
1.1.	Project Purpose	1
1.2.	Description of Project Area	1
1.3.	Background	7
1.3.1.	Previous Storm Damage Reduction Measures	13
2.	Study Constraints	18
3.	Climatology, Meteorology, and Hydrology	18
3.1.	Temperature	18
3.2.	Ice Conditions	19
3.3.	Tides	24
3.4.	Wind	25
4.	Wave Climate	27
4.1.	Wind Hindcast	28
4.1.1.	Wind Field Description	28
4.2.	Ice Field Specifications	30
4.2.1.	Ice Field Methodology	30
4.3.	Deepwater Hindcast	32
4.3.1.	Verification of Deepwater Wave Model	33
4.3.2.	Wave Climate Analysis	37
4.3.3.	Extreme and Average Wave Climate	52
4.4.	Shallow Water Wave Transformation	56
4.4.1.	Bathymetry	56
4.4.2.	Water Level and Wind	57
4.4.3.	Sample Output	57
4.4.4.	Field Data	59
4.4.5.	Model Validation	62
4.4.6.	Summary of Results	65
5.	Currents and Water Levels	65
5.1.	Water Surface Modeling with ADCIRC	66
5.1.1.	Inverted Barometric Correction	66
5.1.2.	Ice Coverage Effect	67

5.1.3.	Total Surge.....	68
5.2.	Currents	70
6.	Sea Level Change	72
7.	Sediment Transport.....	78
7.1.	Cross Shore Sediment Transport.....	78
7.2.	Longshore Sediment Transport.....	80
8.	Coastal Erosion.....	82
8.1.	Shoreline Mining History.....	90
9.	Coastal Flooding.....	97
9.1.	Model Verification.....	110
10.	Storm Damage Reduction Options	111
10.1.	Erosion Risk Reduction	111
10.1.1.	Non-structural Measure	111
10.1.2.	Revetment.....	111
10.1.3.	Beach Nourishment	112
10.1.4.	Seawalls.....	115
10.1.5.	Offshore Breakwaters.....	115
10.1.6.	Groins	116
10.2.	Flood Risk Reduction.....	118
10.2.1.	Non-structural Measures.....	118
10.2.2.	Revetted Berm Structure	118
10.2.3.	Beach Nourishment	118
10.2.4.	Seawall	119
10.3.	Selected Features.....	119
10.3.1.	Bluff Erosion Risk Reduction - Revetment	119
10.3.2.	Flood Risk Reduction - Revetment.....	120
10.3.3.	Alternative Constraints	120
10.3.4.	Maintenance.....	120
10.4.	Design Parameters.....	121
10.4.1.	Total Water Level.....	121
10.4.2.	Run-up for Low Lying Area Structure	123
10.4.3.	Run-up for Bluff Revetment.....	123
10.4.4.	Design Wave.....	124

10.4.5.	Revetment Design – Armor Rock.....	124
10.4.5.1.	Armor Rock Sized to Withstand Ivu Events.....	124
10.5.	Structure Design.....	128
10.5.1.	Bluff Erosion Risk Reduction Governed by Waves - Revetment.....	128
10.5.2.	Low Lying Coastal Flooding Risk Reduction Governed by Waves.....	129
10.5.2.1.	Revetted Berm Structure.....	129
10.5.2.2.	Raised and Revetted Stevenson Street.....	130
10.5.3.	Design Considerations for Relative Sea Level Change.....	130
10.5.4.	Beach Access.....	131
10.5.5.	Potential Temporary Barge Landings and Staging Areas.....	132
10.5.6.	Middle Salt Lagoon Discharge.....	136
11.	Alternatives Considered in Detail.....	136
11.1.	General.....	136
11.2.	No Action.....	146
11.3.	Alternative A: Barrow and Lagoon.....	146
11.4.	Alternative B: Barrow, Lagoon, and Bluff.....	146
11.5.	Alternative C: Barrow, Lagoon, Bluff, and Browerville.....	146
11.6.	Alternative D: Barrow, Lagoon, and South and Middle Salt.....	146
11.7.	Alternative E: Barrow, Lagoon, Bluff, and South and Middle Salt.....	147
11.8.	Alternative F: Barrow, Lagoon, Bluff, Browerville, and South and Middle Salt.....	147
11.9.	Alternative G: Barrow, Lagoon, Bluff, South and Middle Salt, and NARL.....	147
11.10.	Alternative H: Barrow, Lagoon, Bluff, Browerville, South and Middle Salt, and NARL	147
12.	Construction Considerations.....	147
13.	Risk and Uncertainty.....	148
14.	Volume Sensitivity Analysis.....	148
15.	Future Work to be Completed in PED.....	149
16.	References.....	150

PAGE INTENTIONALLY LEFT BLANK

1. INTRODUCTION

This hydraulics and hydrology appendix describes the technical aspects of the Barrow, Alaska Coastal Erosion Feasibility Study. It provides the background for determining the Federal interest in construction of a project that would reduce the risk of damages to the Barrow coastline from storms impacting the north coast of Alaska.

The North Slope Borough (NSB) currently provides temporary flooding and erosion control measures for storm events. The NSB requested that the United States Army Corps of Engineers (USACE) determine the feasibility of Federal participation in a coastal storm risk management project.

To determine the feasibility of a project, numerical model studies were conducted to better define the winds, waves, currents, and sediment movement along the coastline at Barrow. A physical model study was performed to design a risk reduction measure that could withstand an ivu event, when the shorefast ice is pushed onto the beach and the leading edge digs into the beach and buckle up into piles of ice blocks as high as 30 ft (Section 3.2 Ice Conditions

This report is an update to the 2010 Barrow, Alaska Coastal Storm Damage Reduction Technical Report that investigated the Federal interest in a design to reduce damage from flooding and coastal erosion in an environmentally and economically sound manner. No National Economic Development (NED) or locally preferred plan was identified in that study.

1.1. Project Purpose

The authorized project purpose is coastal storm risk management. The purpose of the study is to determine whether there is a Federal interest in developing a solution to the flooding and erosion problems being experienced at Barrow.

This feasibility study is intended to identify a safe and functional method of coastal storm damage risk reduction with the following objectives:

- Reduce risk to public health, life, and safety
- Reduce damage caused by flooding and shoreline erosion to residential and commercial structures and critical public infrastructure
- Reduce or mitigate damage to tangible cultural heritage

1.2. Description of Project Area

Barrow, the northernmost community in the United States, is located on the Chukchi Sea coast. It is located 725 air miles from Anchorage at 71° 18' N, 156° 47' W. (Sec. 06, T022N, R018W, Umiat Meridian). It is approximately 6 miles south of Point Barrow, which divides the Chukchi and Beaufort Seas. The shoreline runs northeast to southwest, with the town facing the Chukchi Sea (Figure 1 and Figure 2). The Wiley Post-Will Rogers Memorial Airport is at the southern end of town. Isatkoak Lagoon and Tasigarook Lagoon separate the community of Barrow from the community of Browerville, which are collectively called Barrow. Further to the northeast are the South and Middle Salt Lagoons and the former Naval Arctic Research Lab (NARL) (Figure 3).

The sun does not set between May 10th and August 2nd, and does not rise between November 18th and January 24th.

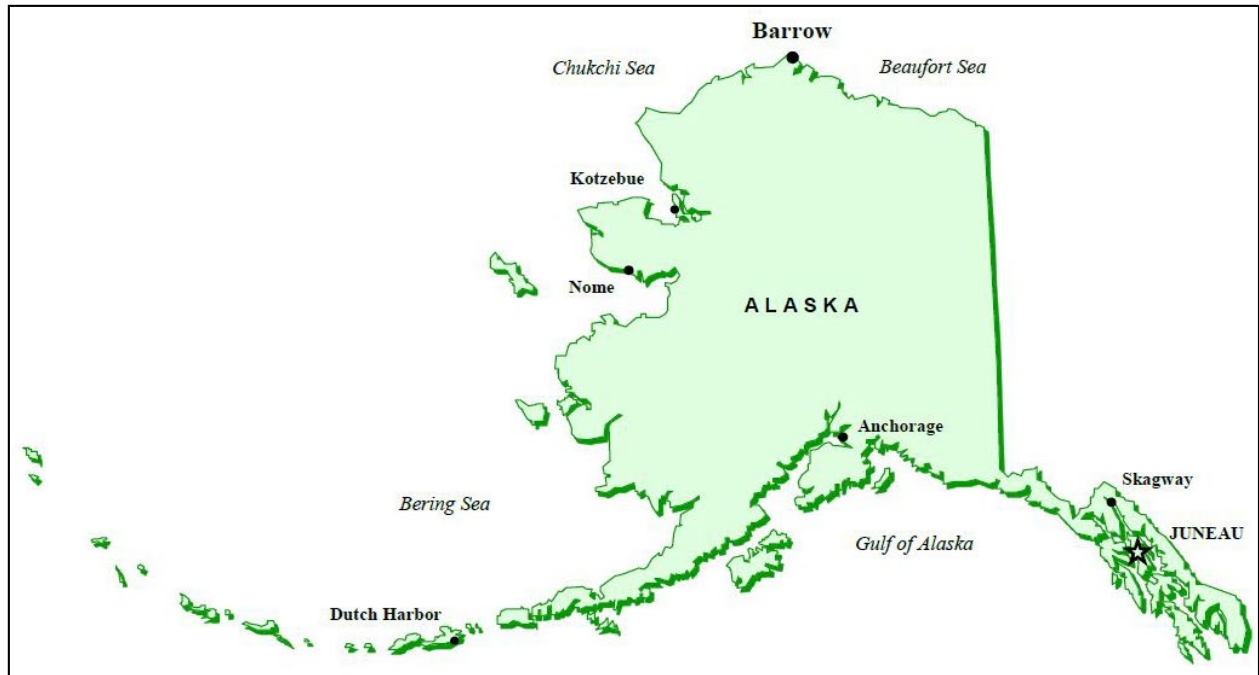


Figure 1. State of Alaska Location Map

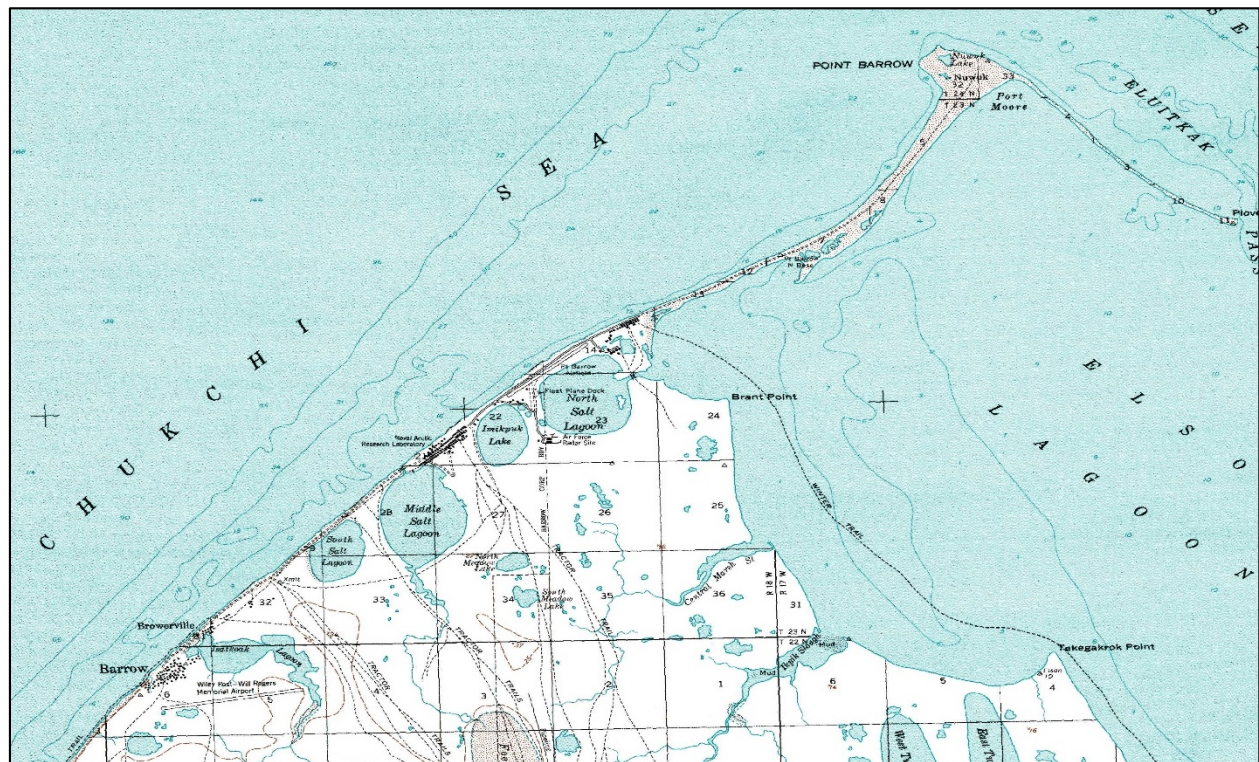


Figure 2. Barrow and Surrounding Area

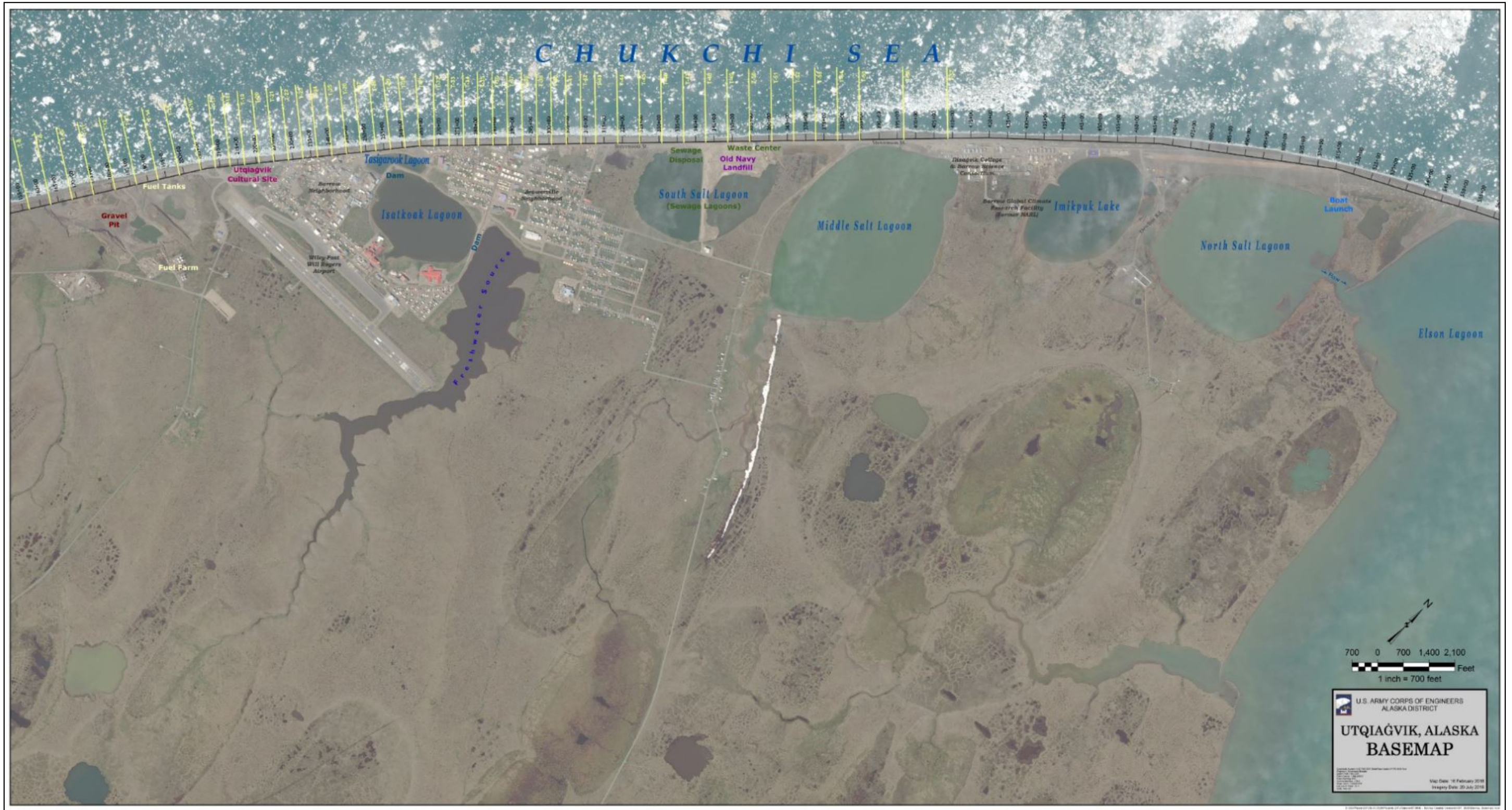


Figure 3. Barrow and Local Features

PAGE INTENTIONALLY LEFT BLANK

Bluffs, up to 30 ft high, occur along the beach in the southwestern portion of Barrow (Figure 4). These bluffs decrease in height until they disappear between the Wiley Post-Will Rogers Memorial Airport and Tasigarook Lagoon (Figure 5). North of this, the back edge of the beach rises to an elevation of approximately 8 ft, where it grades into fairly level tundra (Figure 6).



Figure 4. Bluffs at the South End of Barrow



Figure 5. Decreasing Bluff Height in Front of the Community of Barrow



Figure 6. Beach and Level Tundra North of the Community of Browerville

The beach fronting Barrow and extending out to Point Barrow is comprised of sand and gravel with an average median diameter of 3.0 mm. The beach material is poorly sorted with significant size fractions between 0.3 and 20 mm. Figure 7 shows an example of the beach sediment; the scale is in inches.



Figure 7. Example of Beach Sediment taken at the Water Line, SW Barrow, 10/28/2004

1.3. Background

Barrow is situated on a coastline that runs in a northeast and southwest direction. This orientation leaves Barrow most vulnerable to storms from the north and west. The shoreline is most susceptible to storm activity in the months of August through October (late summer to fall), when there is open water and the permanent ice pack stays a few hundred miles offshore. From November through July, there is generally enough ice present to restrict wave development. The location of the ice edge plays an important role in limiting the fetch for the development of storm waves, which have their greatest impact on the beach during the open water season.

The two coastal problems of greatest concern to the local residents are erosion of the bluffs and storm induced flooding. Bluff erosion has endangered several of the ocean-front homes (Figure 8), and has destroyed archeological evidence found in the bluffs, Figure 9. Flooding has occurred several times when summer and fall storms arrive from the west accompanied by large waves and elevated total water levels. The October 1963 storm is remembered as being particularly severe and it caught many residents unprepared (Figure 10 through Figure 12). Figure 13 shows more recent flooding due to a storm event in 2002.



Figure 8. Undermining of Structure from Erosion

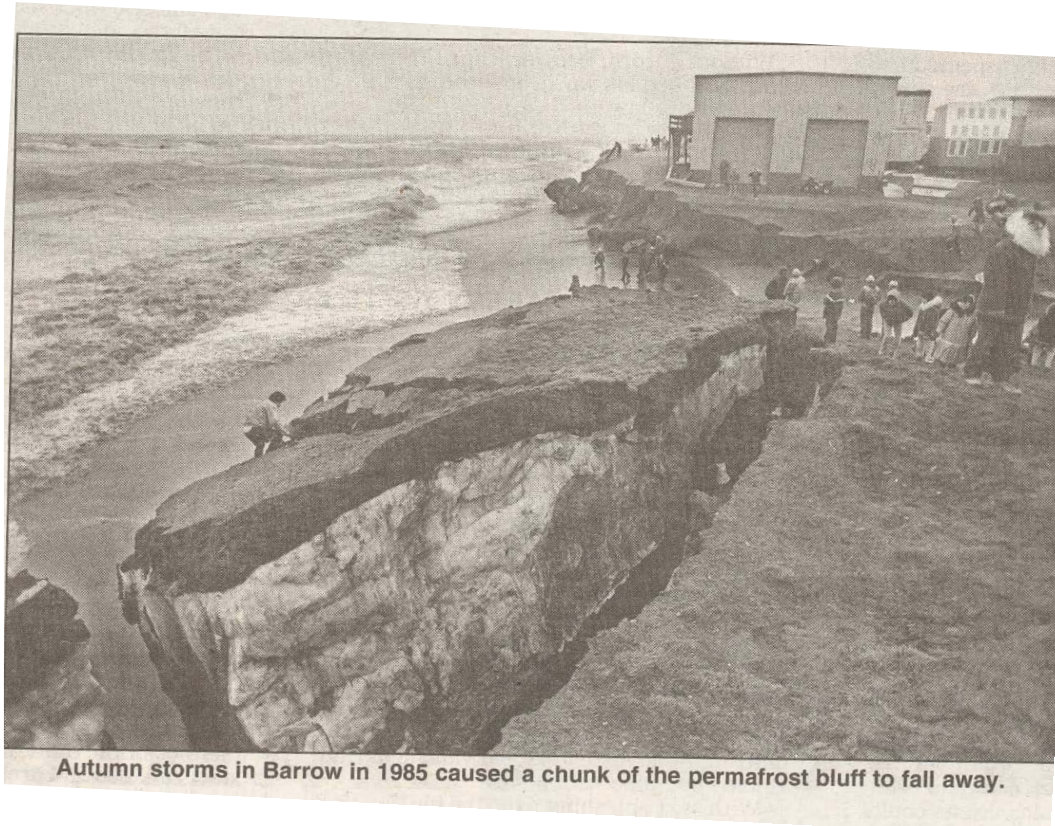


Figure 9. Massive Bluff Failure Located near the Site of a 16th Century House Mound During the 1985 Storm Exposed a Man's Foot. Before the Foot could be Excavated, a Storm Washed his Remains Away.





Figure 11. Flooding at Barrow, 1963



Figure 12. Flooding at NARL



Figure 13. Flooding the Coastal Road (2002)

The three most recent storms events in Barrow were the August 2015, September 2017, and August 2018 events. The August 2015 (Figure 14) and the September 2017 (Figure 15 and Figure 16) events caused flooding in low lying areas and erosion along the bluffs, prompting Federal disaster declarations (DR-4244 and DR-4351, respectively). In August 2018 (Figure 17), the gabion baskets in front of Barrow failed due to storm surge.



Barrow Sea Ice Cam 2015-08-27 10:35:00-0800

Figure 14. Storm Inundation near Tasigarook Lagoon in August 2015 (Sea Ice Group at the Geophysical Institute, 2019)



Figure 15. Flooding of Middle Salt Lagoon Outfall and Erosion along Stevenson Street (Sept 2017)



Figure 16. Erosion along Bluff Threatening Egasak Street in Barrow (Sept 2017)



Figure 17. High Total Water and Run-up that Failed the Gabion Baskets along the Bluff in Barrow (Aug 2018)

1.3.1. Previous Storm Damage Reduction Measures

The NSB has made numerous attempts to curb the erosion and flooding that impacts the coastline fronting Barrow. Coastal erosion and flooding mitigation measures that have been, or are currently being used include:

- Pushing the beach material into berms during storm events (Figure 18 and Figure 19)
- Placing sacrificial berms along the road (Figure 20)
- Offshore dredging and beach nourishment (Figure 21)
- Geotextile sack revetment (Figure 22)
- Filled Utilidor seawall (Figure 23)
- Laid back tar barrels (Figure 24)
- Geotextile tubes (Figure 25)



Figure 18. Bulldozer Working on the Beach Building Berms



Figure 19. Bulldozer Pushing Beach Material During Heavy Surf



Figure 20. Sacrificial Berms Placed along Road



Figure 21. Remains of Beach Nourishment after Storm. The dredge Program was never Completed. The North Slope Borough's Dredge Grounded During a Storm in 2000.



Figure 22. Supersack Revetment



Figure 23. Wooden Utilidors Backfilled with Local Material



Figure 24. Tar Barrels Laid on Beach at an Angle



Figure 25. Geotextile Tube Risk Reduction

The community installed a seawall type structure using geotextile fabric encased in a wire basket in the summer of 2004. The HESCO baskets failed during an event in August 2018 (Figure 26).



Figure 26. HESCO Baskets in front of Barrow near The Fur Shop from September 2017 (Left) and after the August 2018 Event (Right)

2. STUDY CONSTRAINTS

During the feasibility study, a number of study constraints were identified, including:

- Any in water work would need to be coordinated to not interfere with subsistence hunting of marine mammals.
- Work in the beach area is governed by ice formation.
- The coast is the site of numerous archaeological sites.
- Gravel sized material that is locally available for construction is limited.
- Ice constrains the shipping season for the importation of construction materials and there are no offloading facilities other than the beach.

3. CLIMATOLOGY, METEROROLOGY, AND HYDROLOGY

3.1. Temperature

Barrow is in an arctic environment. Total average annual precipitation (rain and melted snow water) is light, averaging 4.5 inches. The average annual snowfall is 34 inches. Temperature extremes range from -55 to 79°F, with average summer temperatures ranging around 38°F (Figure 27). The daily minimum temperature is below freezing 300 days of the year. Prevailing

winds are easterly and average 12 mph. The Chukchi Sea is typically ice-free from mid-June through October.

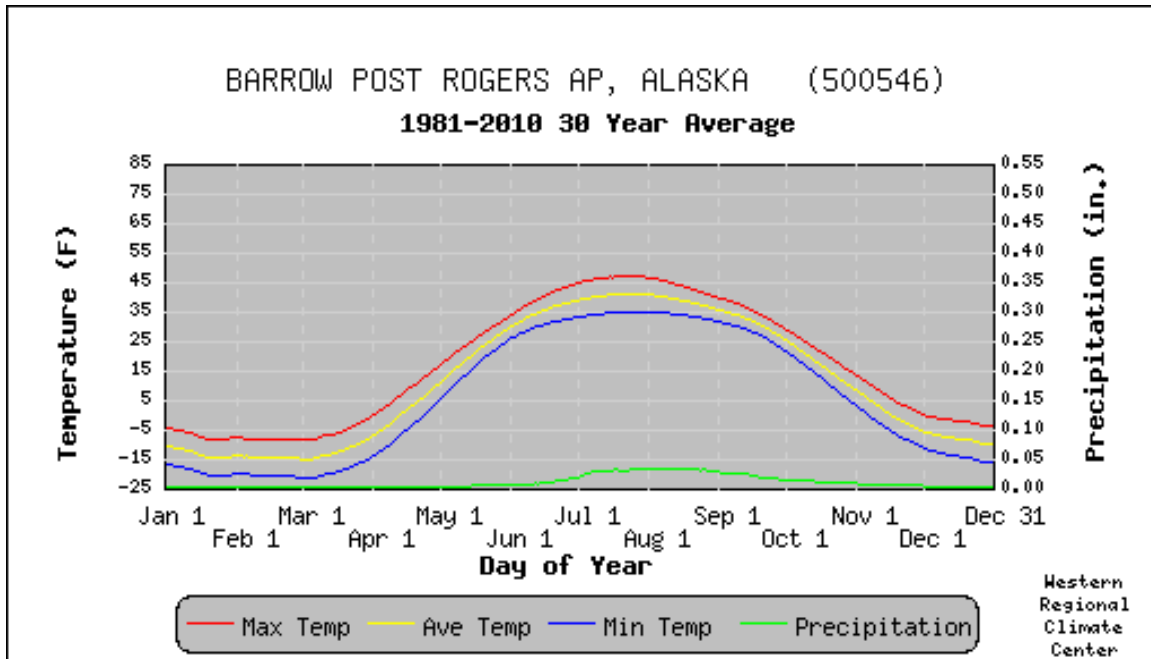


Figure 27. Temperature and Precipitation at Barrow (Western Regional Climate Center)

3.2. Ice Conditions

At Barrow, freeze up typically occurs in November, but the formation of stable shorefast ice may be delayed. Stability is achieved after one or more significant pack ice “shoves” deform and ground the ice. Grounding can take place as late as January, or not at all. Thin ungrounded, maturing ice in the nearshore area is vulnerable. A strong offshore wind can tear away young ice all the way to the beach, leaving open water even when winter temperatures are low. In “cold years,” the ice tends to stabilize by November, but recently ice has been (more) unstable, with episodes of shorefast ice breaking off at the beach as late as January or February. Once grounded and stabilized, the shorefast ice cover remains in place until the start of breakup in July. General ice features are illustrated in Figure 28.

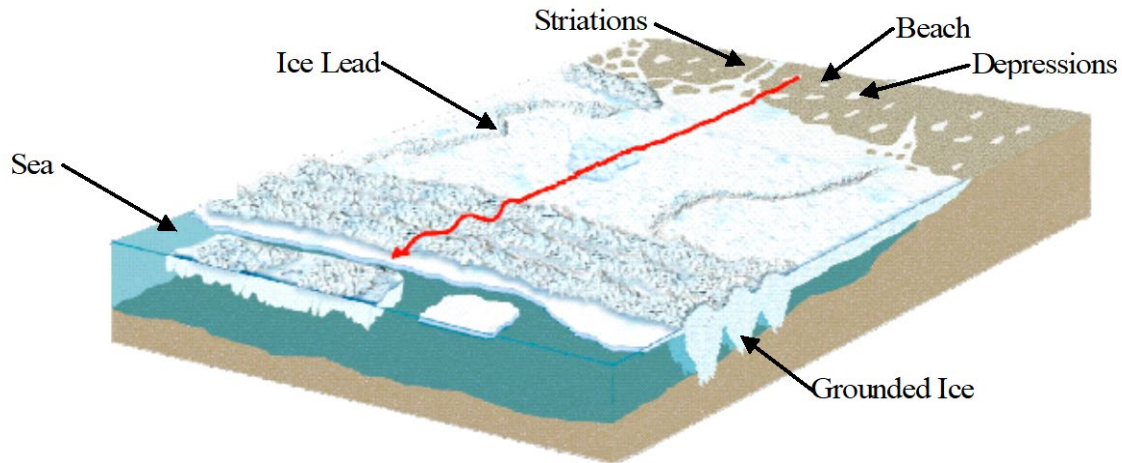


Figure 28. Illustration of Nearshore ice Processes

Point Barrow extends northward and is a major barrier to ice movement. As a result, the beaches near Barrow are subjected to the pushing action of ice more than most regions. There are several possibilities when ice moves on to a beach. The ice sheet may glide over the beach, striating it much like a miniature glacier, and pushing a small pile of debris ahead of it (Figure 29). After the ice melts, the striations show the passage of the ice and the ridge-like, pile of debris marks the terminus of flow much like an end moraine. This is very evident in the early summer after the ice is gone from the beach (Figure 30). As the beach experiences wave action during the summer it is smoothed and resembles the beach profile of a beach shaped by waves (Figure 31). At times, instead of gliding over the beach, the ice may dig its leading edge into the beach and buckle up into piles of ice blocks as high as 30 ft. This ice shove event is known locally as an “ivu” event (Figure 32). When this ice melts, it leaves a depression where it pushed into the beach, but any depression will be obliterated eventually by wave action. However, when the ice buckles, may also push gravel ahead of it in a mound several feet in height. Sometimes the ice carries additional sediment, which was frozen to its base when in shallow water or washed or blown onto its surface. After melting, a mound is left on the beach until storm waves smooth it beyond recognition (Hume and Schalk, 1976). The effect of sediment transport by ice was not considered in this feasibility study.



Figure 29. Ice on the Beach



Figure 30. Beach after the Ice goes out Appears Heavily Worked



Figure 31. Beach after a Season of Wave Action is Smooth and Typical of Beaches in Temperate Regions



Figure 32. Ivu Event in Front of Barrow in January 2006. (Sea Ice Group at the Geophysical Institute, 2019)

A search of ice data collected from the Barrow area was performed to determine ice strength and thickness. Results of the search are presented in Figure 33 and Figure 34. Representative ice covers are on the order of 4.9 ft thick (1.5 m) and have a flexural strength of 90 psi (600 kPa). This information was used in a physical model study at the Cold Regions Research and Engineering Laboratory (CRREL) in Hanover, New Hampshire, described in Section 10.4.5.1 (Armor Rock Sized to Withstand).



Figure 33. Location of Ice Measurements

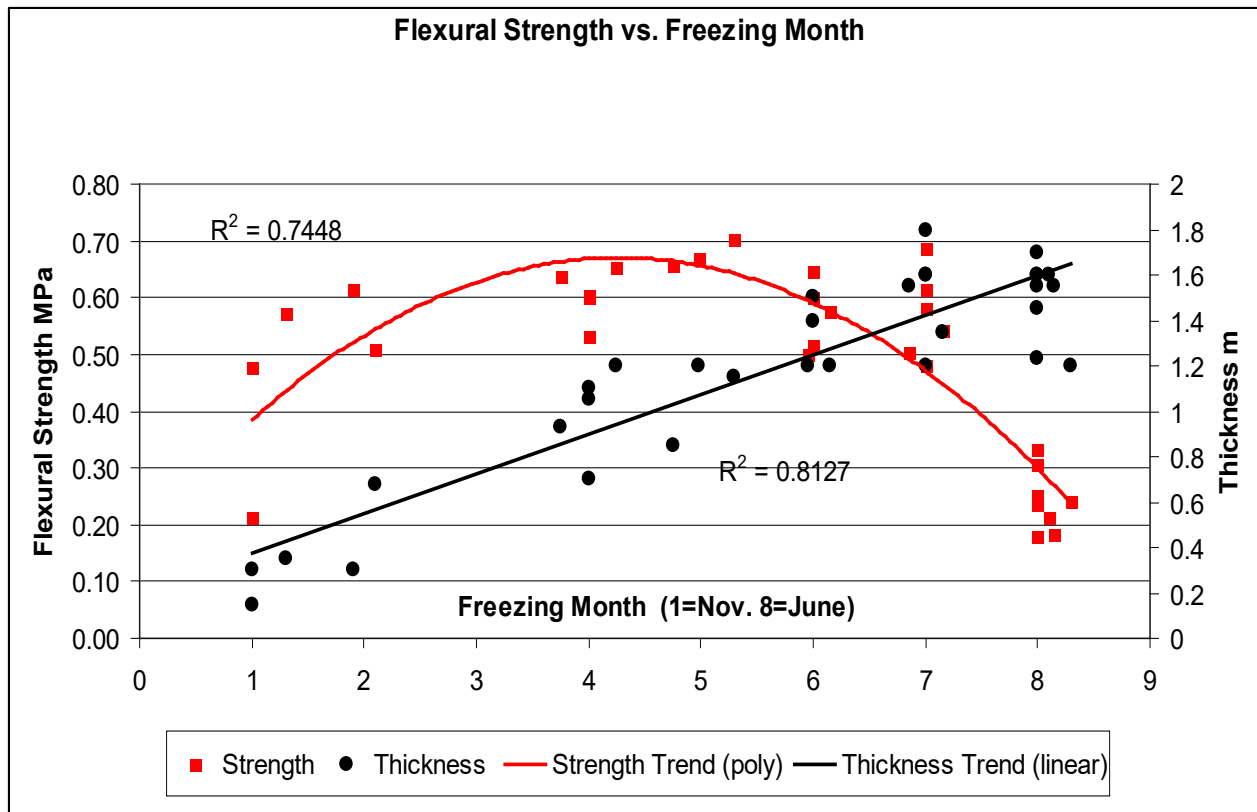


Figure 34. Summary of Ice Measurements

The National Oceanic and Atmospheric Administration (NOAA) began publishing an annual, peer-reviewed Arctic Report Card in 2006. The Report Card is a “source for clear, reliable, and concise environmental information on the current state of different components of the Arctic environmental system relative to historical records” (Osborne, Richter-Menge, and Jeffries, 2018). The 2018 Report Card states that the Arctic sea ice cover is continuing to decline in the summer maximum extent and winter minimum extent (Perovich, et al., 2018). The minimum sea ice extent usually occurs in late September. In 2018, the ice cover was 26 percent lower in later September than the average coverage between 1981 and 2010 and was tied for the 6th lowest ice cover since 1979 (Perovich, et al., 2018). With a decreased sea ice extent there is a larger fetch for wave development. As with sea ice extent, the extent of shorefast ice can affect the vulnerability of a community (Mahoney, 2018). The extent of shorefast ice is closely dependent on local bathymetry, but between 1976 and 2007 the extent of shorefast ice in the Arctic decreased by approximately 0.7 percent per year (Yu, et al., 2013 in Mahoney, 2018). “Pan-Arctic observations suggest a long-term decline in coastal [shorefast] sea ice since measurements began in the 1970s, affecting this important platform for hunting, traveling, and coastal protection for local communities” (Osborne, Richter-Menge, and Jeffries, 2018).

3.3. Tides

Barrow is in an area of semi-diurnal tides with two high waters and two low waters each lunar day. Tidal parameters at Barrow are similar to those predicted for Barrow Offshore (approximately 2.3 miles offshore of NARL). The tidal parameters in Table 1 were determined using the NOAA Tidal

Benchmarks at Barrow Offshore (Station ID 9494935). The tidal datum was determined over a 1-year period from September 2008 to August 2009 based off of the 1983-2001 tidal epoch. There was a highest observed water level recorded on December 14, 2008, of 2.92 ft and a lowest observed water level recorded on January 29, 2010, of -2.57 ft. The highest and lowest observed water levels, which are much higher and lower than the determined Mean Higher High Water (MHHW) and Mean Lower Low Water (MLLW), could be due to storm surge, isostatic (inverted barometer) effect, and/or ice affect.

Table 1. Tidal Datum Elevations Relative to Mean Lower Low Water – Barrow Offshore

Parameter	Elevation [ft]
Highest Observed Water Level	2.92
Mean Higher High Water (MHHW)	0.66
Mean Sea Level (MSL)	0.31
Mean Tide Level (MTL)	0.30
Mean Lower Low Water (MLLW)	0.00
Lowest Observed Water Level	-2.57

The tidal determination was performed post storm surge modeling presented in Section 5 (Currents and Water Levels). Therefore, only an estimated MHHW of +0.5ft MLLW was used in the analysis. The estimated tide was established based on engineering judgment and modeler’s prior experience with ocean circulation modeling in the Arctic.

3.4. Wind

The Alaska Climate Research Center at the Geophysical Institute, University of Alaska Fairbanks, compiled wind data from 1971 to 2000 for Barrow. There is an average wind speed of 10 mph (Figure 35). The predominant wind direction is out of the east and north east with the majority of the wind coming out of the east northeast (Table 2).

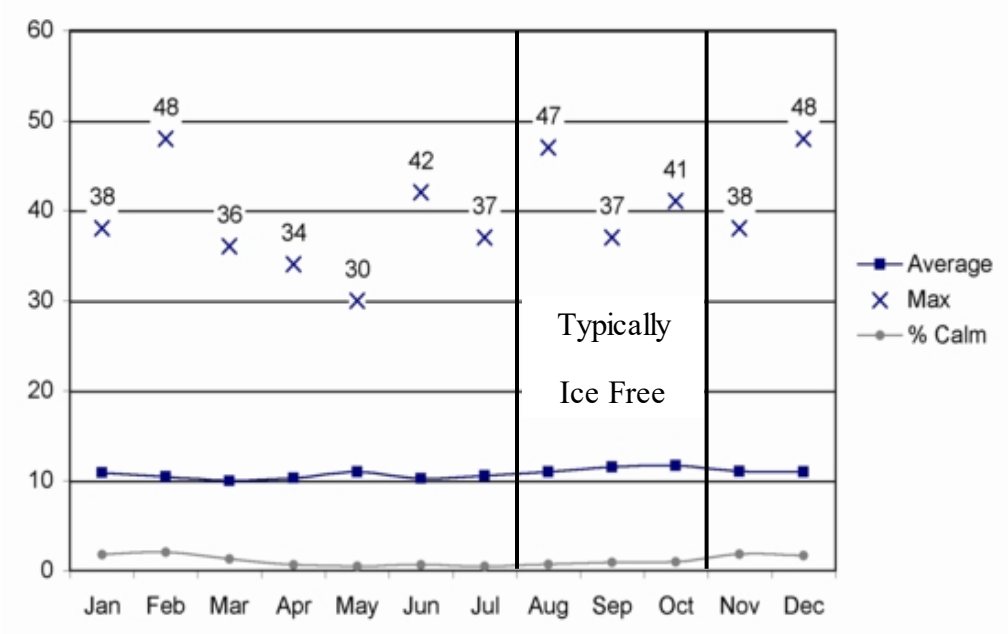


Figure 35. Barrow, AK (71° 17'N / 156° 46' W, 30.5ft above sea level) Mean and Maximum Monthly Wind Speed (mph) and Percent Calm Observation. Barrow, AK is Typically Ice Free from August through October.

Table 2. Monthly and Annual Wind Frequency Distribution (%) by Direction (1971 – 2000). Barrow, AK is Typically Ice from August through October

<i>Direction</i>	<i>Typically Ice Free</i>												
	JAN	FEB	MAR	APR	MAY	JUN	JUL	AUG	SEP	OCT	NOV	DEC	ANNUAL
N	2.8	4.1	3.9	3.4	2.4	4.8	4.9	4.6	3.8	4.0	3.0	2.6	3.7
NNE	2.9	3.0	5.4	4.1	2.6	4.7	4.4	3.7	3.0	3.2	2.7	2.8	3.5
NE	12.6	10.9	12.9	14.6	9.5	8.9	7.7	6.3	9.5	9.5	12.4	13.3	10.6
ENE	22.2	18.1	19.4	22.0	23.0	15.8	14.7	10.5	17.0	17.6	23.0	27.1	19.2
E	10.7	11.1	10.9	13.7	19.7	18.5	18.5	14.7	13.3	12.8	15.5	13.6	14.4
ESE	5.5	7.3	5.4	7.3	11.7	9.0	7.7	7.9	7.6	9.0	8.3	6.6	7.8
SE	3.7	4.1	3.2	3.4	4.8	3.7	2.9	3.7	4.8	6.8	5.2	3.5	4.2
SSE	3.0	2.6	2.5	2.8	3.0	2.9	2.2	2.9	4.1	5.6	4.4	2.4	3.2
S	3.4	3.5	2.7	3.2	2.8	2.1	2.1	3.0	4.3	6.3	4.7	2.9	3.4
SSW	4.7	4.7	4.0	3.2	2.5	1.5	2.1	3.4	3.9	4.7	4.4	3.5	3.5
SW	4.2	4.9	4.3	4.2	3.5	3.8	5.0	5.3	4.2	2.3	1.9	3.2	3.9
WSW	4.8	5.8	6.1	4.1	4.1	5.4	8.4	9.1	5.2	2.2	2.1	3.8	5.1
W	5.5	6.4	5.7	3.4	3.2	5.1	6.7	8.2	5.5	2.5	2.1	4.7	4.9
WNW	5.7	5.4	5.3	3.5	2.3	4.8	4.9	6.3	5.0	3.8	3.6	4.3	4.6
NW	5.0	4.5	4.1	3.5	2.4	4.2	3.8	5.9	4.7	5.2	3.3	3.2	4.2
NNW	3.5	3.8	4.3	3.4	2.4	4.7	3.9	4.5	4.0	4.7	3.6	2.6	3.8

4. WAVE CLIMATE

Specification of a long-term wave climate along a coastal reach is dictated by principal forcing functions: the winds and site-specific oceanographic or geographical constraints. In the case of Barrow, the complexities increase because of its location and the ever-changing offshore ice coverage opening up the area for wind-wave development, or preventing it as the ice builds in the fall. Because of its location, Barrow remains relatively protected from growing wave conditions in the Beaufort Sea to the east, and swells south of Cape Lisburne in the Chukchi Sea. Barrow is unique and its wave climate is dictated by storms in the Arctic Ocean, limited in extent by the pack ice.

The Coastal and Hydraulics Laboratory (CHL) of the Engineer Research and Development Center (ERDC) developed a deepwater wave hindcast for the years 1982-2003 using hindcast generated wind data, supplemented with 27 pre-1982 storms (Jensen, R. E., 2009), and then transformed the waves from a deepwater wave hindcast boundary output point to the nearshore (Smith and Sherlock, 2009) for the 2010 Technical Report.

The deepwater wind hindcast data was used to determine deepwater wave hindcast data using Wave prediction Model (WAM). NOAA, National Environmental Satellite Data Information Services (NESDIS) ice grid data was used to determine times when the ice coverage would be too heavy to generate waves. The deepwater wave hindcast data was used to estimate extreme and average wave climate offshore to establish the 51 typical wave events and 28 storm events to transform into the nearshore using the STeady-State Spectral WAVE (STWAVE) model. The

nearshore waves were then used as a boundary forcing for Storm-induced BEach CHange Model (SBEACH), which in turn was used to determine the total water level along the project extents along with the depth-limited wave height impacting any proposed alternatives.

4.1. Wind Hindcast

The specification of the wind fields is critical to the generation of an accurate wave climate. A 10 percent uncertainty in the wind speed estimate will lead to an approximate 20 percent uncertainty in the wave height. To accurately characterize the forcing mechanisms for the wave and current modeling, a hindcast was performed for the years 1982-2003 by Oceanweather Inc. (OWI), under contract to the CHL. The hindcast was supplemented with 27 storms for the years 1954 to 1982.

4.1.1. Wind Field Description

The Interactive Optimum Kinematic Analysis (IOKA) System was used to construct the Barrow wind fields. All wind field estimates were restricted to the target domain shown in Figure 36. Five critical elements are required for the IOKA system:

- Background wind fields
- Point source measurements (airport anemometer records, buoy data)
- Ship records (archived wind speed and direction)
- Scatterometer estimates of the wind speed
- Kinematic control points (KCPs)

These data sets (excluding the KCPs) must be adjusted for stability and brought to a common reference level. Stability accounts for the changes in the boundary layer due to differences between air and water temperatures. Considerations to the differences in boundary layer effects over the pack ice were neglected.

The background wind fields selected for the Barrow project were derived from the National Center for Environmental Prediction/National Center for Atmospheric Research (NCEP/NCAR) Reanalysis Project. These wind fields were spatially interpolated to a fixed spherical grid.

Point source measurements such as buoy data and airport records reflect wind speeds and directions based on short time burst averaging. These short-term averages (1 to 10 minute averages) are temporally interpolated to hourly data. Land based wind measurements were also adjusted for boundary layer effects. Every land based, point source measured, data set was individually investigated, and adjustments were made as needed. These adjustments depended not only on the wind direction, but also on the wind magnitude.

Scatterometer wind fields derived from satellites are not true wind speed measurements. They are derived from inversion techniques and are extremely useful because of the spatial coverage obtained during one satellite pass. The repeat cycle is 35 days (on a 12 hour orbit); therefore, temporally continuous data are not available as in the case of point source measurements. In addition, data from all satellite-based scatterometers do not span the entire hindcast period, or any of the pre-1982 extreme storms that were considered in the study. Including these data may produce a series of discontinuities in the development of the wind field climatology; however,

use of these data adds considerable value to the final wind products, and outweighs concerns regarding the consistency of the climatological wind products.

Once all data sets were transformed to equivalently neutral, stable 33.3 ft (10 m) winds, the IOKA system is used. Each input wind data product carries a specified weight which can be overridden by an OWI analyst at any time. Background wind fields are ingested into OWI's Graphical Wind Work Station, displaying all the available data sets (point source measurements, scatterometer data). The NCEP/NCAR Reanalysis wind fields are at a 6-hour time step, so all 1-hour point source wind measurements are repositioned via "moving centers relocation." This assures continuity between successive wind fields.

The most powerful tool of the IOKA system is the use of KCPs by the analyst. This tool can input and define ultra-fine scale features such as frontal passages, maintain jet streaks, and control orographic effects near coastal boundaries. The analyst can use the KCPs to define data sparse areas using continuity analysis, satellite interpretation, climatology of developing systems, and other analysis tools. The IOKA system contains a looping mechanism that will continually update the new wind field based on revisions performed by the analyst.

The final step in the construction of the OWI regional wind fields was to spatially interpolate the winds to a target domain and resolution. The final wind fields were spatially interpolated to the target domain at a longitudinal resolution of 0.50° , a latitudinal resolution of 0.25° at a time step of 6-hours. This was done because the NCEP/NCAR Reanalysis wind fields are resolved at 6-hour time steps.

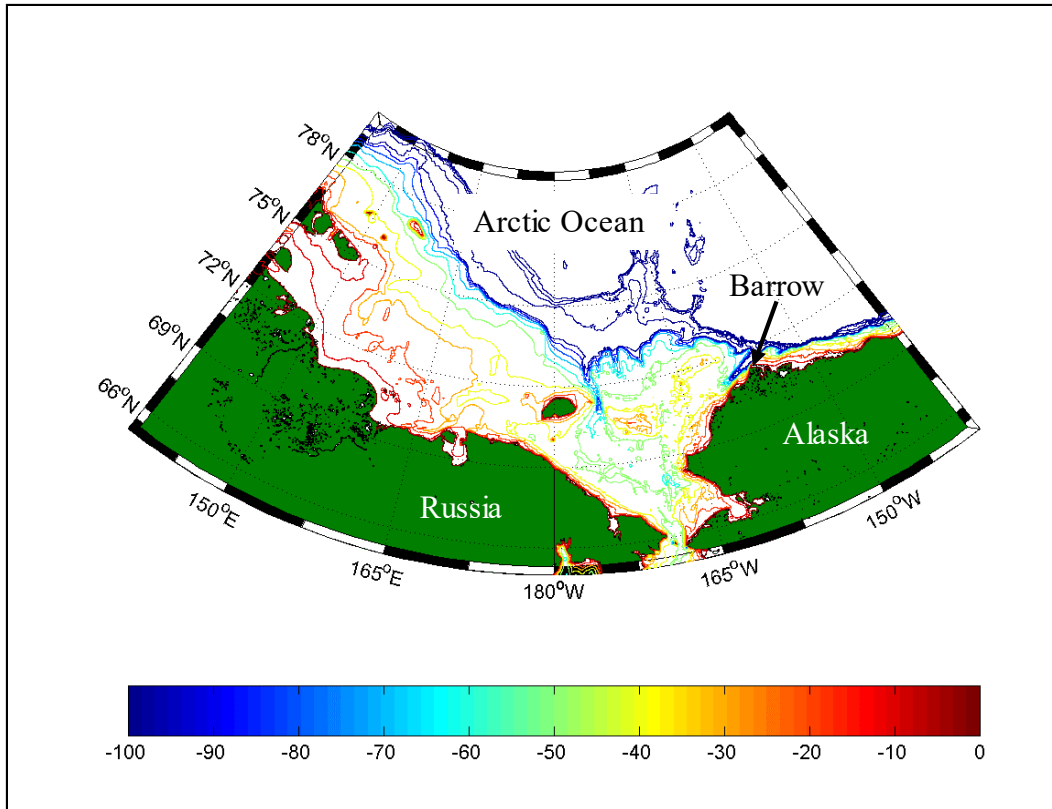


Figure 36. The Barrow Deep Water Wind, Ice, and Wave Model Target Domain. Water Depths are Contoured in Meters (1 m ~ 3.3 ft)

4.2. Ice Field Specifications

The specification of the ice edge quantifying the open water capable of wind-wave growth is one of the major controlling variables in the specification of the wave climatology. Barrow is adjacent to the Chukchi Sea and the Arctic Ocean where changes in the pack ice cover occurs more or less on a weekly basis.

4.2.1. Ice Field Methodology

Mean weekly ice maps were used for the modeling effort because of the rapid changes in the neighboring Chukchi Sea. An example of the final ice map for week 31 (30 July through 5 August) in 1998 is presented in Figure 37. Digital ice field maps are derived from remote sensing techniques using visible and infrared imagery from the polar orbiting satellites that have been used since 1972. Algorithms have been built to estimate the sea ice concentration and more recently sea ice thickness. Once established, these images are then translated to gridded information, and archived at NOAA, National Environmental Satellite Data Information Services (NESDIS). The approximate resolution is 25 km. Weekly estimates of the ice concentration were generated for this project (140° E to 140° W Longitude and 65° to 80° N Latitude) at 0.5° longitude/latitude resolution, and at 0.25° for the area defined by 167° to 142° W Longitude and 68° to 73° N Latitude (under contract to University of Alaska Anchorage). Ice maps for selected storm events prior to the 1972 digital database were constructed by OWI.

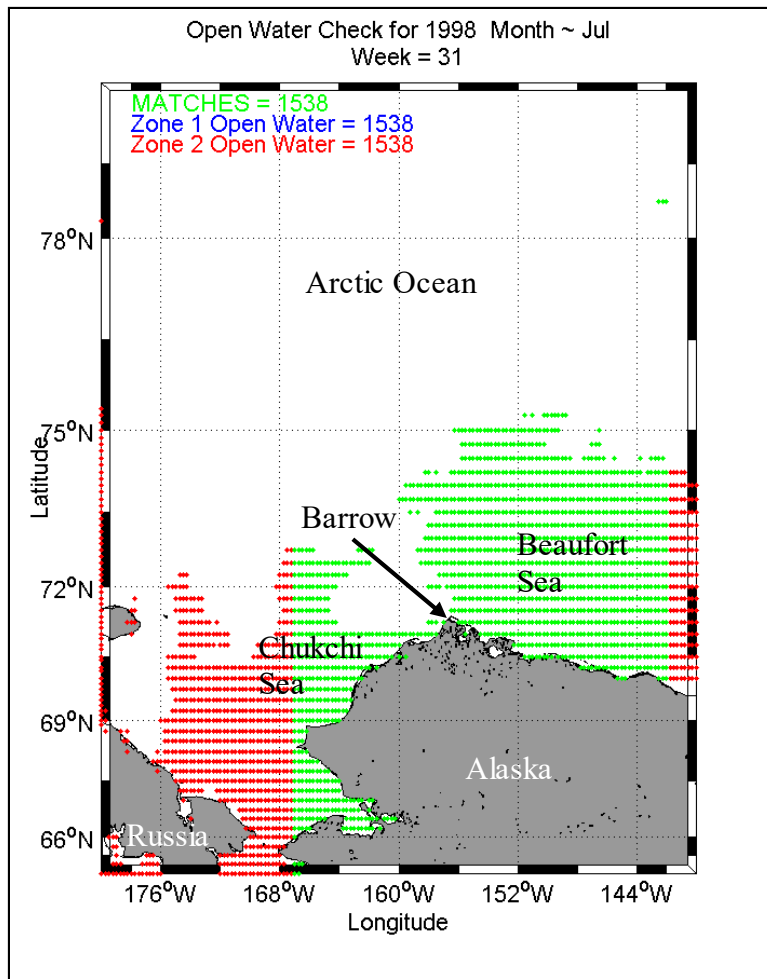


Figure 37. Example of the Final Ice Map used in Wave Model Simulation. Note: the Symbols Identify the Open Water Area

The construction of the final wave model ice field resident on a 0.25° longitude/latitude grid system used both of the two zonal fields generated by the University of Alaska Anchorage. The coarse ice field concentration was spatially interpolated from 0.5° to the 0.25° grid, and masked to the land-water grid assuring consistency across the land/water boundary. The fine scale ice field replaced the area in close proximity to the Barrow site. The concentration level (from 0 to 100 percent where the higher levels of concentration indicate increased ice compared to water) was interpolated rather than the designation of land/water mask. A predetermined concentration level of the ice field must be set to either open water or land. This study used a concentration level of 70-percent or greater to switch the water point to land. This concentration was chosen based on previous wave hindcast experience for the USACE Navigation Improvements Draft Interim Feasibility Report, Delong Mountain Terminal (United States Army Corps of Engineers, Alaska District, 2005). Examples of sea ice differences are shown in Figure 38 and are derived from NOAA's Observers Guide to Sea Ice (prepared by Dr. O. Smith, University of Alaska, Anchorage, <http://response.restoration.noaa.gov>).



5 - 6 tenths "open drift"



7 - 8 tenths "close pack"

Figure 38. Example of Sea Ice Concentrations. Left 50-60% , Right 70-80% Concentration

4.3. Deepwater Hindcast

The deepwater waves were analyzed using the Wave prediction Model (WAM). WAM is a third generation wave model which predicts directional spectra as well as wave properties such as significant wave height, mean wave direction and frequency, swell wave height and mean direction. All source terms (wind input, wave-wave interaction, white capping, wave bottom effects, and wave breaking) are specified with the same degree of freedom in WAM with which the resulting directional wave spectra are specified. There is no a priori assumption governing the shape of the frequency or directional wave spectrum. WAM has been used extensively at weather prediction centers with the option to include ice coverage.

Model Assumptions for WAM are:

- Time dependent wave action balance equation.
- Wave growth based on sea surface roughness and wind characteristics.
- Nonlinear wave and wave interaction by Discrete Interaction Approximation.
- Free form of spectral shape.
- High dissipation rate to short waves.

The domains describing the wind, ice and wave model are found in Table 3 and were shown in Figure 36. For the Barrow study only the *open water season* (June through the end of December) of each year are simulated. Each year's simulation is started from fetch-limited calculations based on the 0000-hour wind field on 1 June.

Table 3. Wind, Ice, and Wave Model Domain Specifications

Field Specification	Longitude		Latitude		Resolution	
	West	East	South	North	Δ Lon / Δ Lat	Δ t
Wind Field	140.0 E	140.0 W	65.0	80.0	0.50° / 0.25°	6-hr
Ice Field Zone 2	140.0 E	140.0 W	65.0	80.0	0.50° / 0.50°	Weekly
Ice Field Zone 1	167.0	142.0 W	68.0	73.0	0.25° / 0.25°	Weekly
Ice Field Final	140.0 E	140.0 W	65.0	80.0	0.25° / 0.25°	weekly
WAM Waves	140.0 E	140.0 W	65.0	80.0	0.25° / 0.25°	120 / 600 s

4.3.1. Verification of Deepwater Wave Model

There is not a regularly maintained wave buoy in the Chukchi Sea against which the model could be compared. In the absence of long-term continuous data, point source measurements were obtained from Shell Oil Company, for two non-directional wave buoys deployed in 1983 and 1984. The general location of these sites is shown in Figure 39 and despite their distance from the Barrow Project Site, can strongly suggest the overall quality in the wave model's performance. All data representing the measurements were hand-digitized from time plot records. These results should not be construed as ground-truth as in the case of digital wave records. Note: The direction convention for all time plots of the θ_{mean} wave, and the wind direction are in a meteorological coordinate system (e.g. 0° from the north, 90° from the east).

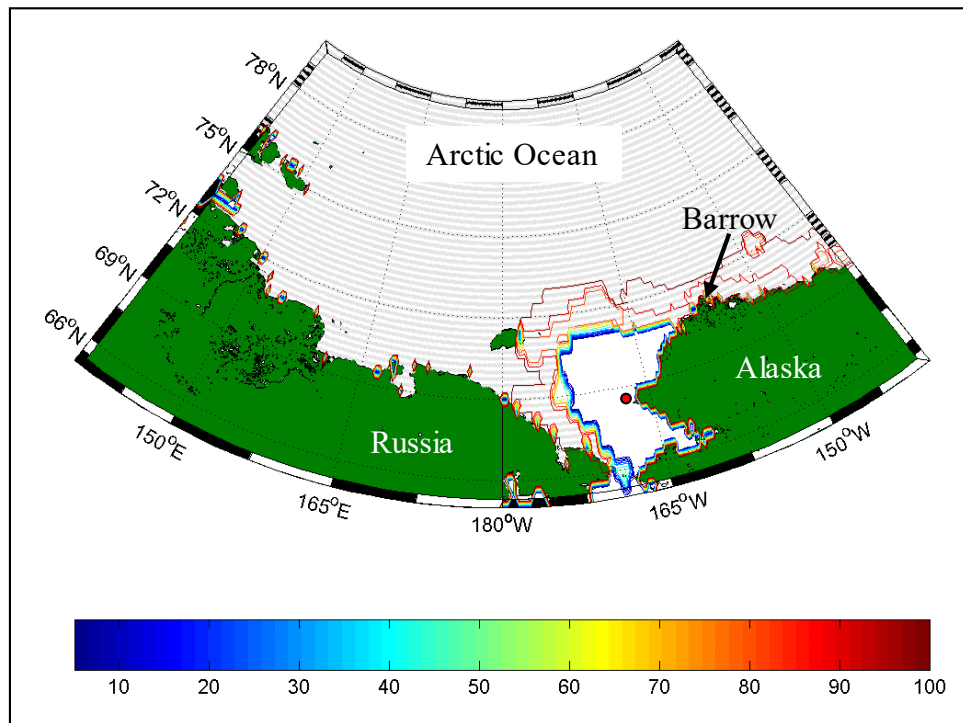


Figure 39. Location (Red Symbol) of the Shell Oil Wave Measurements for Station A and B during Two Deployment Cycles of 1983 and 1984. Ice Concentrations are Color Contoured; the Grey Area Signified the Ice Pack.

All verification WAM runs were made with wind and ice fields identical to that of the climatology simulations. These tests were made to assure quality in the overall performance of the winds, ice coverage, and ultimately the wave model. Time and scatter plots as well as statistical tests were generated, however because of the paucity of data, the statistical results will be biased and regarded as an approximation to the true performance of the wave model. Estimates of the significant wave height (H_{mo}), and mean wave period, (T_{m}) for 1983 are presented in Figure 40 and Figure 41 for Site A and B. The WAM H_{mo} , and T_{m} estimates for the first deployment period shows remarkable similarity to the measurements. The storm peaks are well represented in all but one case (21 September), and are slightly low. There is one storm, occurring at about 30 September, that is completely missed in the model results. The maximum wave height measured during this missed event was on the order of 1 m (3.3 ft). The winds are in

a decaying mode, and the wind directions are rapidly turning from a northeasterly direction to a southerly direction. The winds for this case may be slightly low for this case or the direction slightly off. It could also be the wave model, its grid and/or spectral directional resolutions. If the errors found at Site A, under similar meteorological conditions persist, then it would be reasonable to conclude the wave model is in error. However, in general the model emulates the measurements quite well in height and mean wave period.

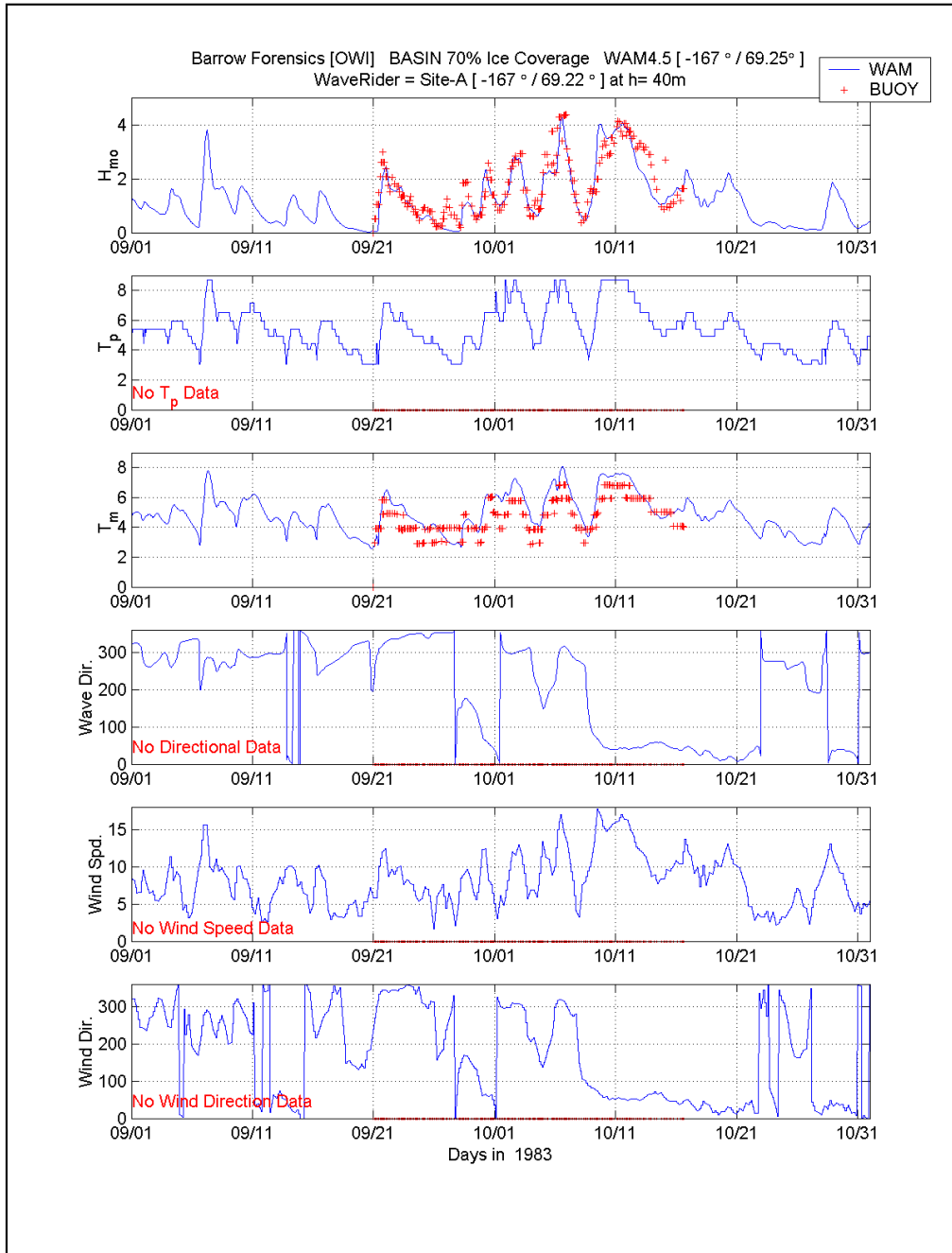


Figure 40. Comparison of WAM Cycle 4.5 (solid blue line) to Shell Oil Co. Buoy Data during Deployment 1, at Site A. Note: Wind and Wave Directions are in the Convention of "from which."

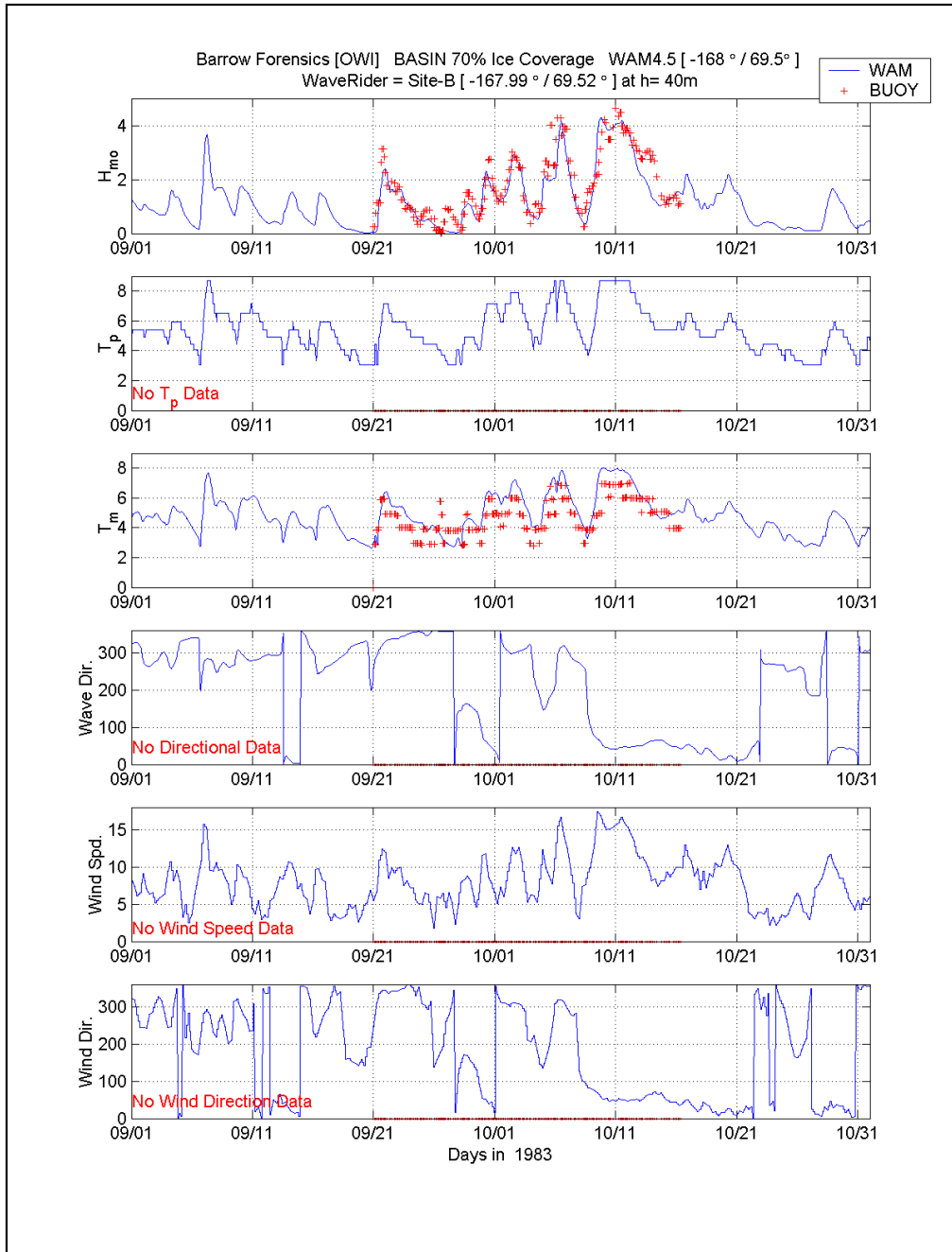


Figure 41. Comparison of WAM Cycle 4.5 (solid blue line) to Shell Oil Co. Buoy Data during Deployment 1, at Site B. Note: Wind and Wave Directions are in the Convention of "from which."

The results of WAM during the second deployment (found in Figure 42 and Figure 43 for Site A and B respectively) emulate the measurements, with exception to a slight over-estimation during the storms of 5-7 September and 5-8 October at Site A. At the same time, the mean wave period results are elevated by roughly 2 sec. In general, the storm peaks are captured and the rapid growth of all storms are maintained. For the decay cycles, either rapid in the case of 21 September at Site A, or much slower cycle after the 6 October storm peak, trends are emulated in the model results. The mean wave periods though seem to grow correctly, then reach higher

values at the most intense portion of the storm, and fail to decay as rapidly as in the measurements. It does not seem appropriate at this time to infer what the cause of these differences is. It could be elevated wind speeds, potentially blowing at an incorrect angle. It could also be the definition of the ice coverage, neglecting the fast-ice component at the shoreline, using the condition for land defined as ice concentration levels above 70 percent.

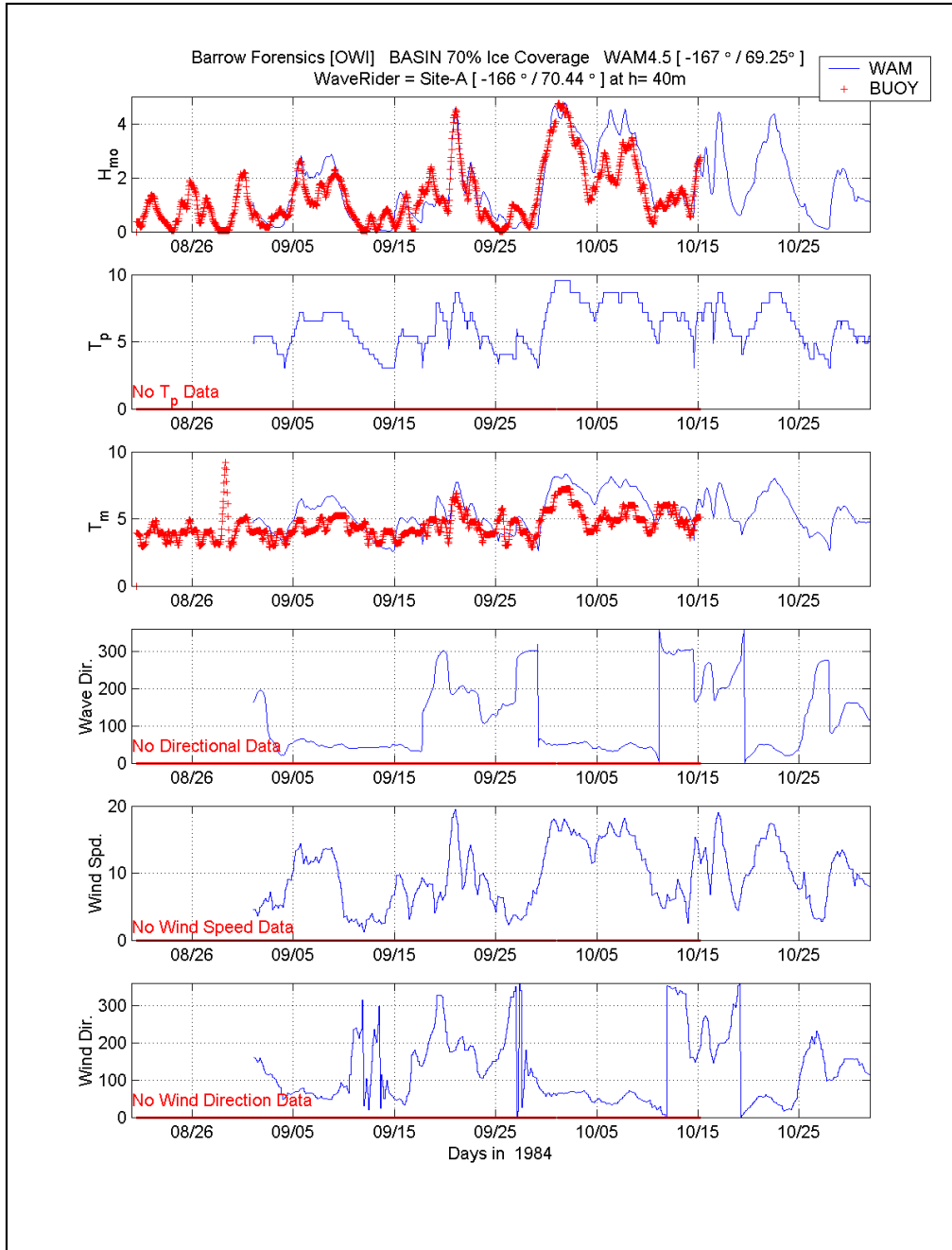


Figure 42. Comparison of WAM Cycle 4.5 (solid blue line) to Shell Oil Co. Buoy Data during Deployment 2, at Site A. Note: Wind and Wave Directions are in the Convention of “from which.”

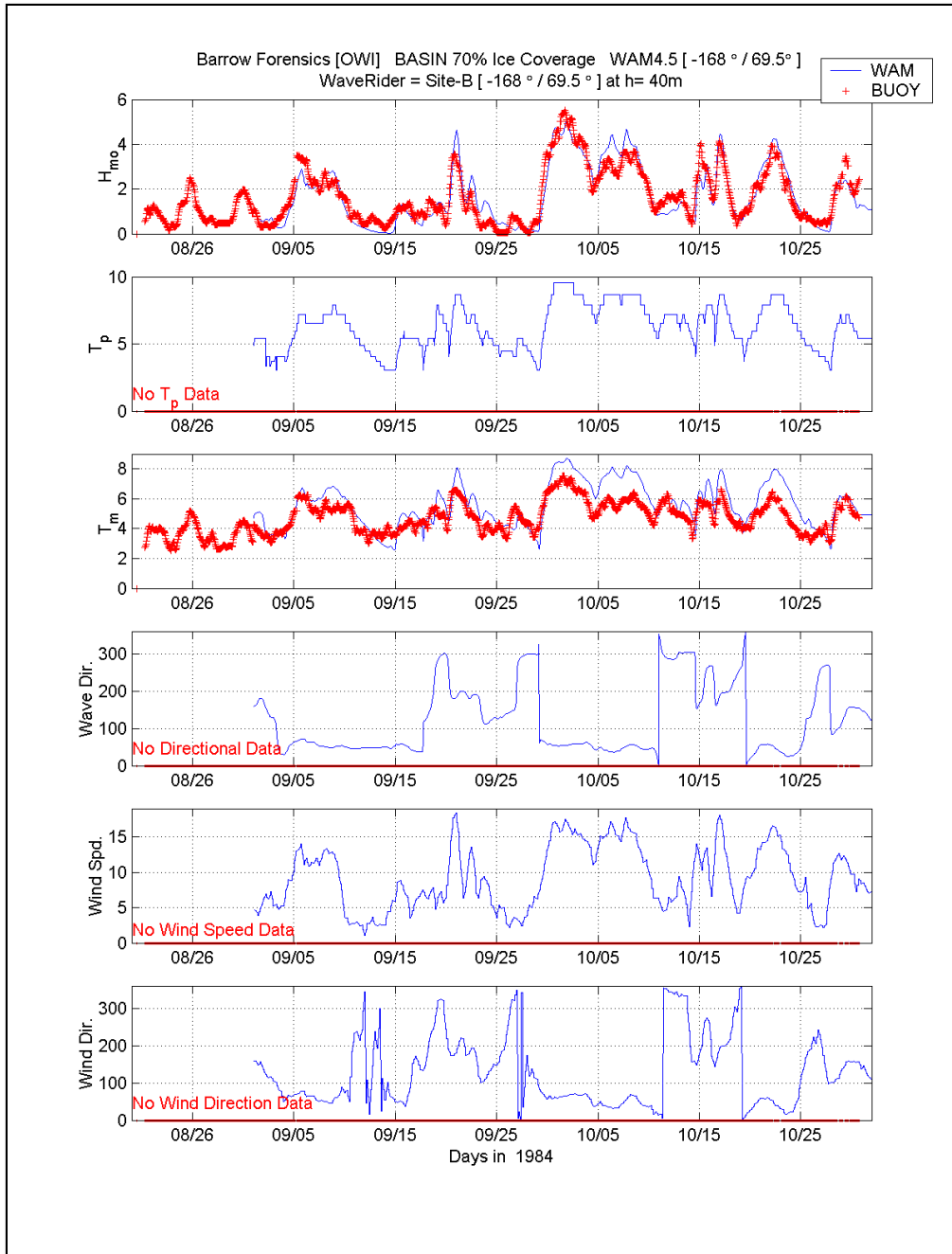


Figure 43. Comparison of WAM Cycle 4.5 (solid blue line) to Shell Oil Co. Buoy Data during Deployment 2, at Site B. Note: Wind and Wave Directions are in the Convention of “from which.”

4.3.2. Wave Climate Analysis

There are two distinct and separate parts in the development of the Barrow offshore wave climate. A continuous portion was run and encompassed the years 1982 through 2003 starting on 1 June and ending on 1 January of the subsequent year. The length of each simulation period varied because of the weekly changes in the ice maps, and the monthly changes in the wind fields. However, to retain continuity between each simulation period, a RESTART (or warm start) file was retrieved from the previous simulation. Hence, consistency was maintained

throughout each year that was processed. For each year WAM Cycle 4.5 was started from a cold start, preconditioning the wave field with fetch-limited wave estimates derived from the input wind fields, operating on the open water dictated by the ice coverage. Wave data output for the subsequent nearshore wave transformation is shown in Figure 44.

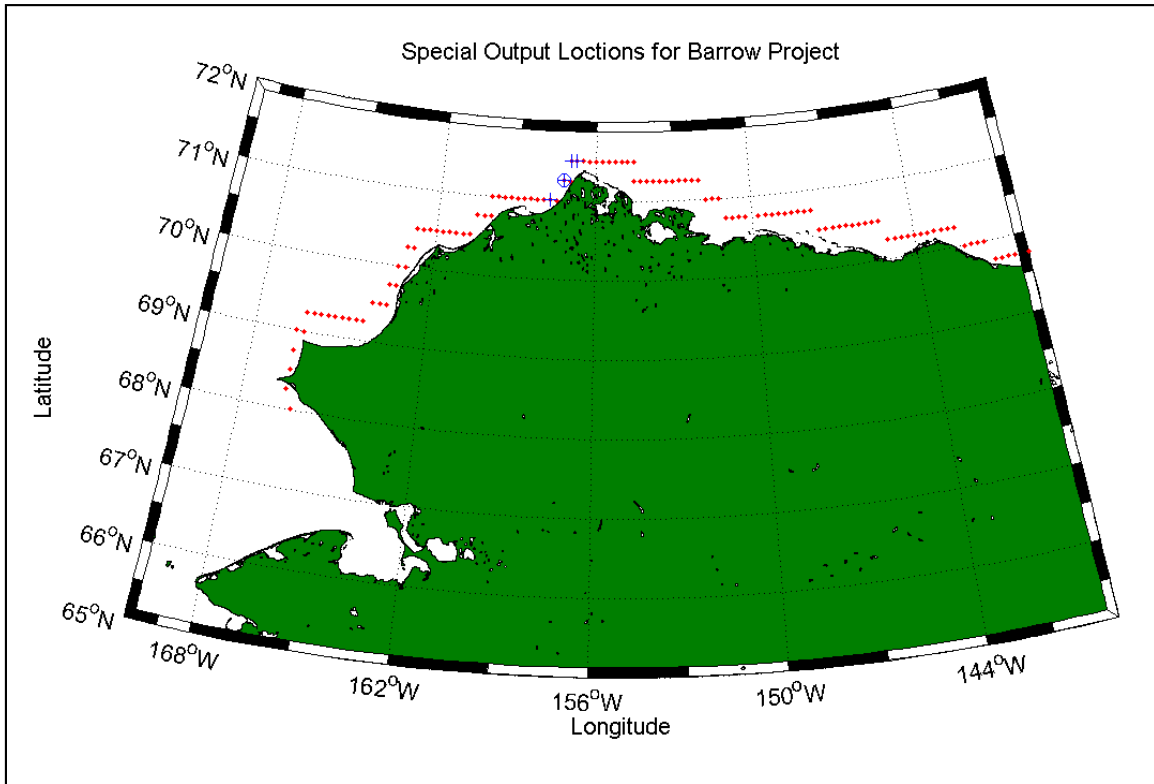


Figure 44. Special Output Locations (red) and Stations 47, 51, and 52 (blue +), and the STWAVE Input Site Station 49 (blue⊕).

The second set of hindcasts were developed from a series of individual storm simulations that had documented evidence producing large water levels and/or elevated wave conditions along the Barrow Project Study site. Some of these storms were selected from a historical database used for design wave estimates for the North Slope and the USACE Alaska District provided a selected number. The last set was derived from storm analysis procedures used by OWI. The 27 storms are summarized in Table 4. These storms were of short duration so that a mean monthly ice field was used for all storm simulations. This was dictated by the availability of high quality digital ice maps only provided on a monthly basis for the earlier storms on record. Consistency in the procedures throughout the time span was deemed more important for reducing any added false discontinuity.

A series of special output locations (119 total) were saved along the land/water boundary defined in the Barrow grid. These output locations are shown in Figure 44, where Stations 47, 49, 51 and 52 focus in the area just offshore of the Barrow Site. Station 49 is the location where the deep water wave spectra were used as input for Nearshore Wave Transformation. Figure 45 shows Station 49 and its associated bathymetry. Figure 46 presents the integral wave parameters in height, peak spectral wave period, and vector mean wave direction. Note: The direction

convention for all distribution plots of the wind and wave direction are in the convention of “towards which’ (0° toward the north, 90° toward the east).

Table 4. Extreme Storms Pre-1982.

Storm No.	Date	Type	Simulation Period
1	5409	NW	54091601-54091900
2	5410	NW	54100300-54100512
3	5507A	SW	55071706-55072006
4	5507B	SW	55071912-55072212
5	5707	SW	57071500-57071800
6	5709	NE	57091200-57091500
7	6009	SW	60092500-60092812
8	6106	SW	61061618-61061918
9	6209	SW	62090312-62090518
10	6308	SW	63082118-63082400
11	6310A	NW	63100306-63100506
12	6310B	NE	63100600-63100900
13	6410	SW	64101800-64102100
14	6509	NE	65090500-65090800
15	6709	NE	67091700-67092000
16	6809	NW	68092112-68092312
17	7210	NE	72101500-72101800
18	7307	SW	73073112-73080312
19	7310	SW	73101500-73101712
20	7410A	NE	74100512-74100812
21	7410B	NE	74102212-74102512
22	7508	NW	75082512-75082718
23	7710A	NE	77101000-77101300
24	7710B	NE	77101812-77102200
25	7810	NE	78100700-78101000
26	7910	NE	79100312-79100612
27	8009	NE	80092612-80100100

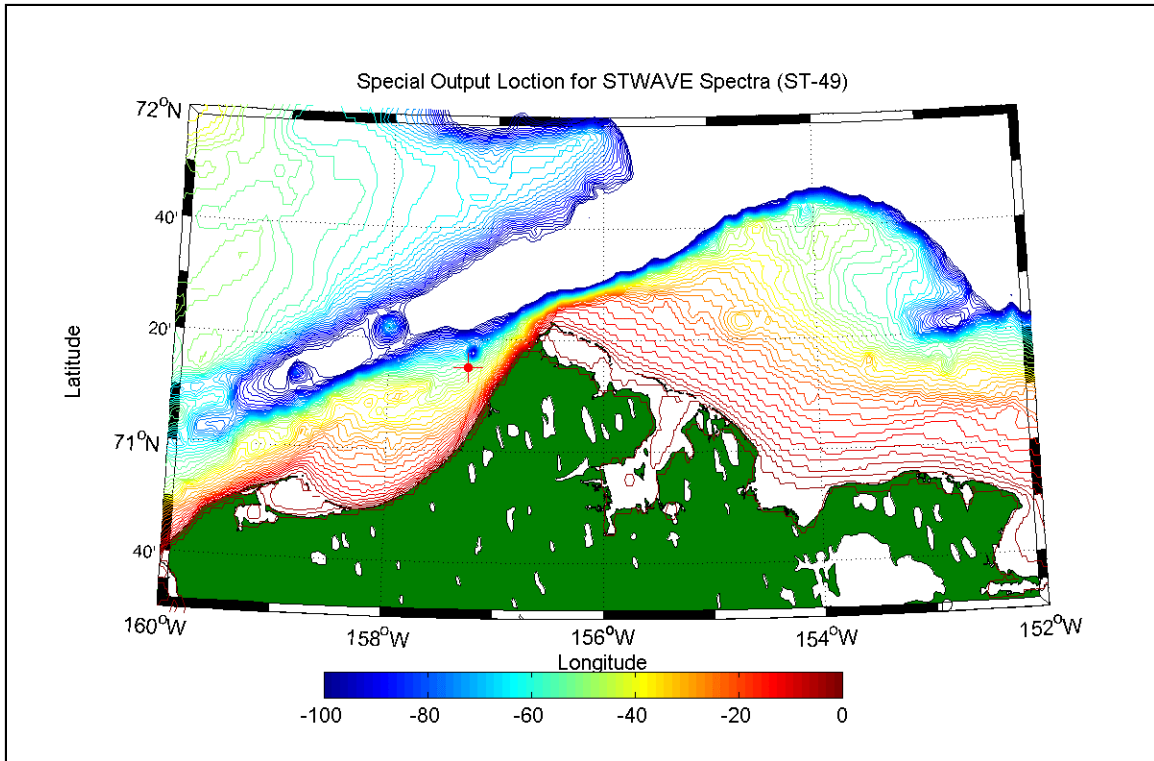


Figure 45. Zoomed View of the Barrow Site and Station 49 (red cross). Note: Only Water Depths less than 100-m are Color contoured to Emphasize the Local Bathymetry. Water Depths Greater than 100-m Exist and are Identified by the White area Outside the Blue 100-m Contour Interval.

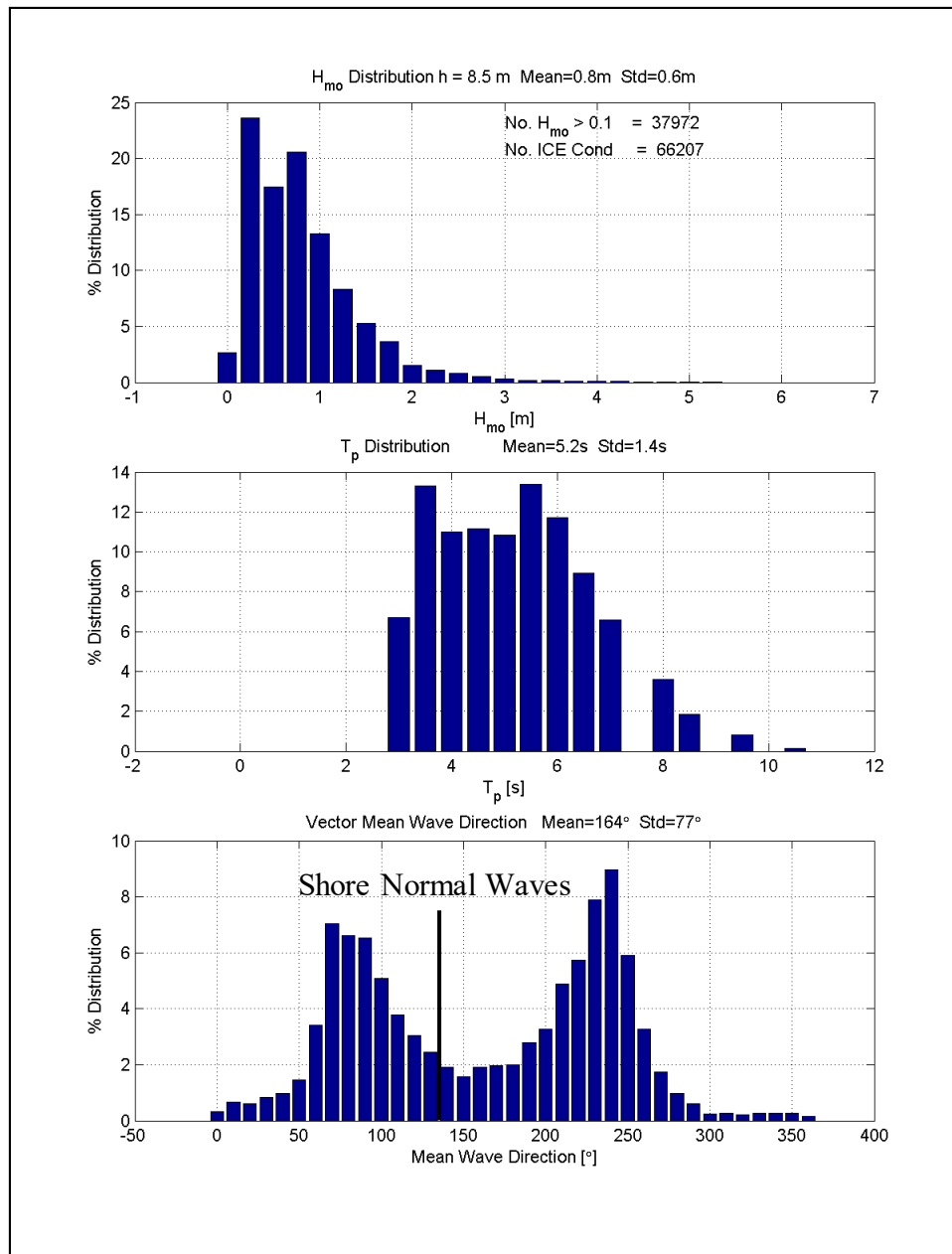


Figure 46. Height, Peak Wave Period and Vector Mean Wave Direction Distributions for the 1982-2003 (June through November) at Station 49. Note: Waves directions are in the convention of “towards which”. Onshore waves have a wave direction of 135°. Wave direction that effect the project area are wave toward 45° to 225°.

The H_{mo} and T_p distributions support a general trend for local wind-sea dominance. Very limited long period (generally greater than 10 sec) waves are contained in the entire wave record. The absolute maximum wave height estimated is slightly over 16.4 ft with a peak spectral wave period of 10.2 sec. What is interesting to note is the mean wave directional distribution. Noting the direction convention is waves propagating towards shore normal at about 135° and waves going towards the east at 90°. Virtually all the waves contained in the left-hand lobe consist of waves coming into the coast, and most likely derived from northwesterly storms. The right-hand lobe in the vector mean wave direction consists of waves derived from the northeast, traveling in

the offshore direction. Point Barrow causes a sheltering effects for waves propagating towards 315° and further north rapidly dropping off in occurrence.

The wind speed and directional distributions are provided in Figure 47. There is a dominant trend in the winds at Station 49. For the coastal area, wind speeds in excess of 22.4 mph are limited to about 15 percent. The bulk of the winds range from 11.2 to 20.1 mph. Two lobes exist in the wind directional distribution, however the magnitudes compared to the wave direction are quite different, where there is clearly visible persistence for easterly directions which are offshore and cause a set-down at the shoreline.

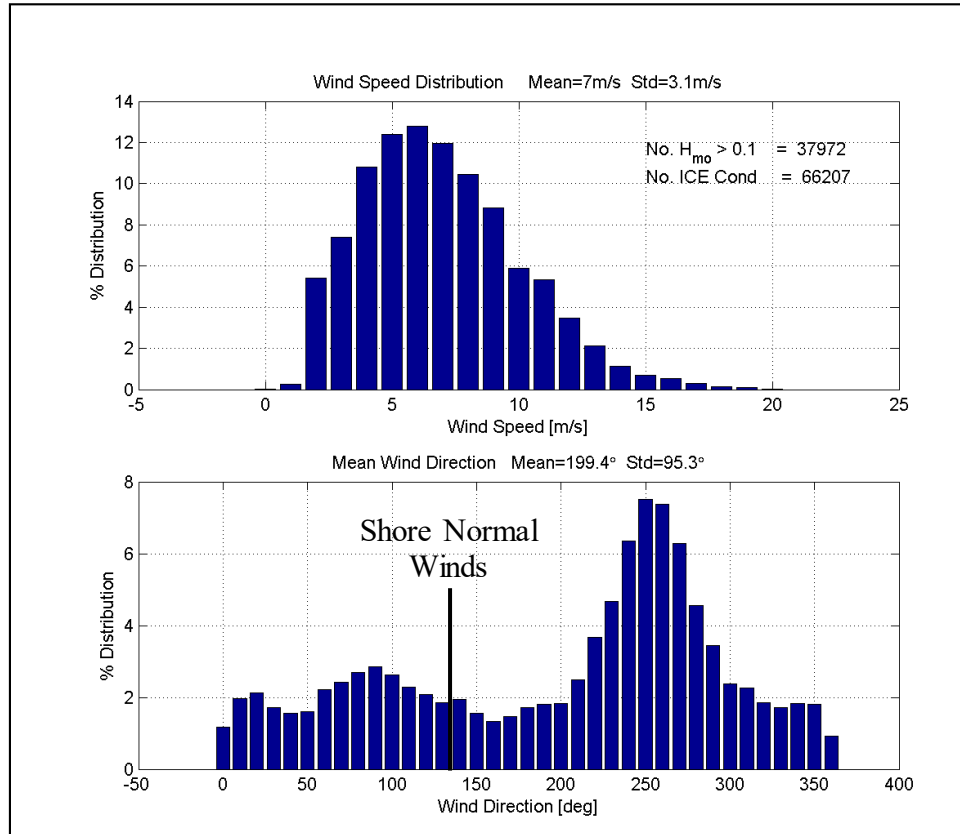


Figure 47. WindSpeed and Direction Distribution for the 1982-2003 (June through November) at Station 49.
Note: Waves directions are in the convention of “toward which”. Onshore winds have a wind direction of 135°. Wind directions that are traveling toward the project area are wind toward 45° to 225°.

The analysis thus far removes the time domain focusing on only the distribution of wind and wave characteristics for the entire climate simulation. Found in Figure 48 are bar plots of the number of observations, the mean and maximum conditions occurring for the June through December months from 1983 through 2003. The values used for plotting purposes are also summarized in

Table 5. There are variations from year to year, increasing in the latter 1990s through the end of the simulation period.

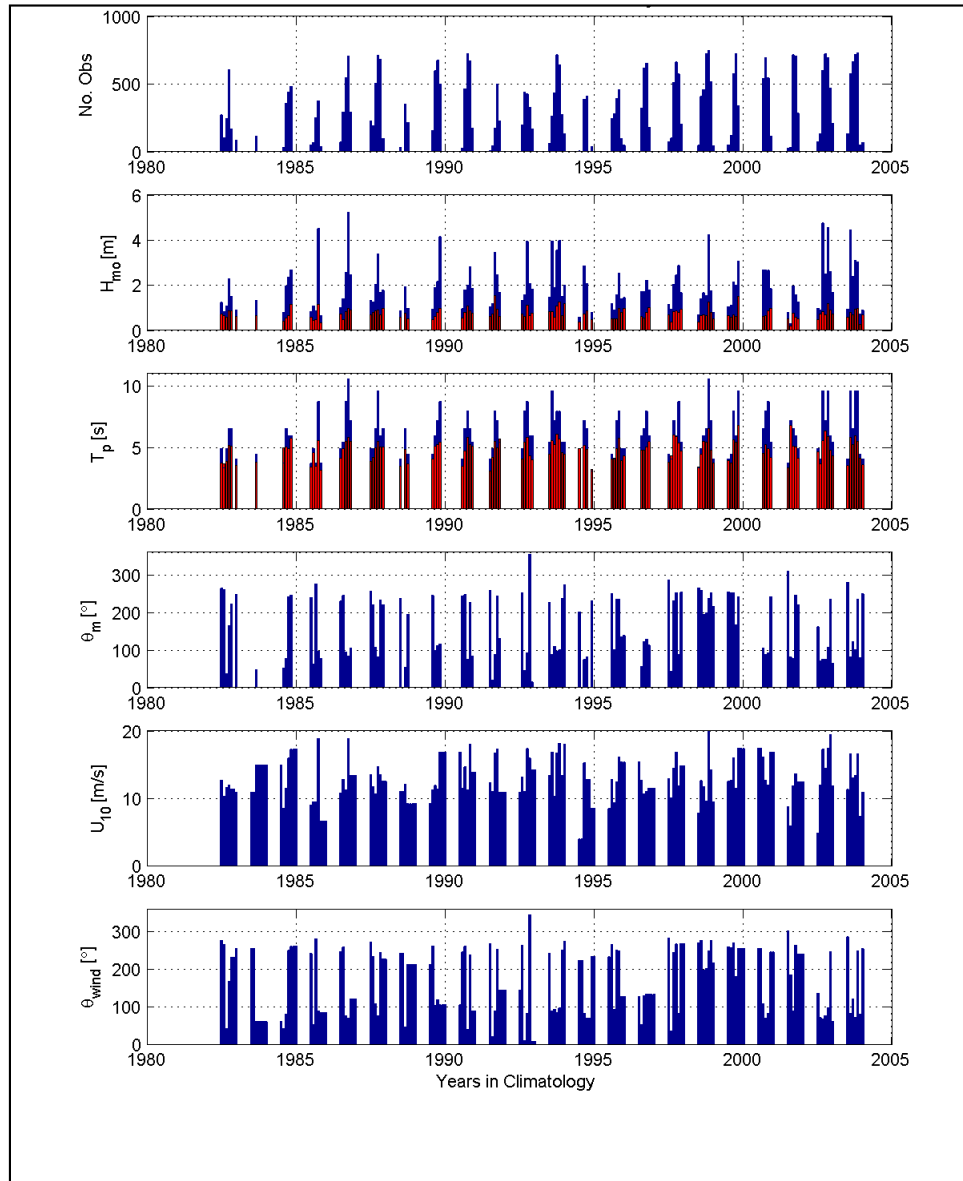


Figure 48. Climate Summary at Station 49 Where Various Panels Define the Variation of Parameter Over Time (Monthly Information); Red Indicates the Mean, Blue the Maximum. Note: Wind and wave directions are in the convention of “toward which” where onshore winds and waves have a direction of 135°.

There are three dependent variables dictating the wave height maximums. First, meteorological systems with winds in excess of 22 mph (10 m/s); secondly these winds need to be directed toward the Barrow Project Site; third, the amount of open water is sufficiently large to build the waves. The shoreline faces NW (315°). The wind directions generally are traveling more or less down the coastline. The vector-mean wave direction is nearly identical to the wind direction at the H_{m0} maximums, indicating a dominant local wind-sea environment, which is further supported by the T_p results in the range of 8 to over 10 sec during the maximum wave height

events. The shore normal direction is towards approximately 135° , with a landward attack angles between 45° and 225° . Figure 49 shows the Barrow shoreline for reference. The predominant storm generated waves come from the north, to northeasterly directions. These would be very oblique approach angles, relative to the shoreline orientation. Hence, the wave climate produced in this portion of the study area reflects the offshore environment, and not the environment close to the coast.

PAGE INTENTIONALLY LEFT BLANK

In summary, there are only modest variations in the local deepwater wave climate dictated by the intensity and duration of meso-scale meteorological events. For the Barrow deepwater conditions, the dependency in a sustainable wind speed is far more pronounced than the fetch it blows over. Extreme events quantified by the maximum H_{mo} , for wave heights in excess of 13.1 ft, may be on the rise due to potential increase in open water periods, specifically for the years of 2003 and 2004.

Table 5. Wave Characteristics for 1983 through 2003 Climate Simulations. Note: Wind and wave directions are in the convention of “toward which” where onshore winds and waves have a direction of 135°

Wave Characteristics for 1983 through 2003 Climate Simulations

Year Month	No. Obs	Mean		Maximum at Height Max				
		H _{mo} [m]	T _p [s]	H _{mo} [m]	T _p [s]	Wave Dir	Wind Speed	Wind Dir
198206	271	0.718	3.710	1.24	4.91	263	12.7	277
198207	105	0.642	3.680	0.82	3.35	260	10.3	266
198208	245	0.587	3.878	1.09	4.91	36	11.6	44
198209	603	0.853	5.173	2.26	6.53	164	12	169
198210	169	0.854	5.062	1.49	6.53	222	11.3	232
198211	1	ICE	ICE	ICE	ICE	ICE	ICE	ICE
198212	86	0.629	3.528	0.91	4.05	246	10.9	255
198306	1	ICE	ICE	ICE	ICE	ICE	ICE	ICE
198307	1	ICE	ICE	ICE	ICE	ICE	ICE	ICE
198308	115	0.656	3.790	1.31	4.46	48	14.9	62
198309	1	ICE	ICE	ICE	ICE	ICE	ICE	ICE
198310	1	ICE	ICE	ICE	ICE	ICE	ICE	ICE
198311	1	ICE	ICE	ICE	ICE	ICE	ICE	ICE
198312	1	ICE	ICE	ICE	ICE	ICE	ICE	ICE
198406	1	ICE	ICE	ICE	ICE	ICE	ICE	ICE
198407	35	0.402	4.922	0.8	3.69	52	8.5	44
198408	355	0.554	5.010	1.95	6.53	78	11.5	82
198409	438	0.658	4.887	2.34	5.94	241	15.9	250
198410	481	1.142	5.699	2.68	5.94	245	17.2	261
198411	1	ICE	ICE	ICE	ICE	ICE	ICE	ICE
198412	1	ICE	ICE	ICE	ICE	ICE	ICE	ICE
198506	48	0.583	3.411	0.83	3.69	239	9	242
198507	66	0.454	4.529	1.09	4.91	63	9.5	55
198508	252	0.478	3.464	0.87	3.69	275	9.5	281
198509	374	1.162	5.540	4.49	8.69	97	18.8	91
198510	36	0.348	3.147	0.64	3.69	78	6.6	85
198511	1	ICE	ICE	ICE	ICE	ICE	ICE	ICE
198512	1	ICE	ICE	ICE	ICE	ICE	ICE	ICE
198606	72	0.727	4.107	1.02	4.91	229	10.8	247
198607	293	0.468	4.875	1.41	5.4	244	12.8	259
198608	547	0.817	5.473	2.55	8.69	95	11.2	77
198609	704	0.970	5.817	5.22	10.51	84	18.8	71

Wave Characteristics for 1983 through 2003 Climate Simulations

Year Month	No. Obs	Mean		Maximum at Height Max				
		H _{mo} [m]	T _p [s]	H _{mo} [m]	T _p [s]	Wave Dir	Wind Speed	Wind Dir
198610	289	0.896	5.486	2.45	7.18	105	13.4	121
198611	1	ICE	ICE	ICE	ICE	ICE	ICE	ICE
198612	1	ICE	ICE	ICE	ICE	ICE	ICE	ICE
198706	225	0.683	3.878	1.32	4.91	256	13.5	272
198707	192	0.803	4.191	1.26	4.91	220	11.7	234
198708	503	0.851	4.958	2.02	6.53	107	10.7	110
198709	710	0.883	5.496	3.37	9.56	81	14.7	77
198710	680	0.673	5.010	1.69	5.94	232	13.5	244
198711	97	0.982	5.028	1.77	6.53	220	12.5	227
198712	1	ICE	ICE	ICE	ICE	ICE	ICE	ICE
198806	34	0.585	3.463	0.88	4.05	237	11	242
198807	1	ICE	ICE	ICE	ICE	ICE	ICE	ICE
198808	352	0.757	4.800	1.93	6.53	53	12.1	48
198809	216	0.515	3.647	0.97	4.46	194	9.2	213
198810	1	ICE	ICE	ICE	ICE	ICE	ICE	ICE
198811	1	ICE	ICE	ICE	ICE	ICE	ICE	ICE
198812	1	ICE	ICE	ICE	ICE	ICE	ICE	ICE
198906	1	ICE	ICE	ICE	ICE	ICE	ICE	ICE
198907	156	0.477	4.024	0.95	4.46	244	11.2	262
198908	595	0.627	5.055	1.9	5.94	99	11.9	105
198909	672	0.800	5.235	2.16	7.18	112	11.3	120
198910	498	0.981	5.426	4.13	8.69	116	16.8	106
198911	1	ICE	ICE	ICE	ICE	ICE	ICE	ICE
199006	1	ICE	ICE	ICE	ICE	ICE	ICE	ICE
199007	27	0.564	3.452	0.96	4.05	243	11.5	246
199008	463	0.808	4.711	1.8	6.53	246	14.6	261
199009	720	1.071	5.777	2.01	7.9	75	11.2	42
199010	667	0.866	5.229	2.79	6.53	225	17.9	239
199011	174	0.759	5.088	1.85	5.4	84	13.8	90
199012	1	ICE	ICE	ICE	ICE	ICE	ICE	ICE
199106	8	0.606	3.043	1.05	4.05	258	12.3	267
199107	46	0.721	4.182	1.19	4.91	20	11	23
199108	172	1.548	5.478	3.43	7.9	87	16.7	89

Wave Characteristics for 1983 through 2003 Climate Simulations

Year Month	No. Obs	Mean		Maximum at Height Max				
		H _{mo} [m]	T _p [s]	H _{mo} [m]	T _p [s]	Wave Dir	Wind Speed	Wind Dir
199109	498	0.950	4.921	2.45	7.18	242	17.2	254
199110	226	0.610	5.687	1.68	5.4	130	10.9	146
199111	1	ICE	ICE	ICE	ICE	ICE	ICE	ICE
199112	1	ICE	ICE	ICE	ICE	ICE	ICE	ICE
199206	1	ICE	ICE	ICE	ICE	ICE	10.9	146
199207	199	0.709	4.032	1.33	4.91	251	13.1	264
199208	437	0.618	5.396	1.56	7.9	45	11	11
199209	424	1.118	5.812	3.93	8.69	93	17.3	83
199210	326	0.650	4.306	2.08	5.94	353	15.9	344
199211	169	0.769	3.987	1.83	5.94	15	14.2	10
199212	1	ICE	ICE	ICE	ICE	ICE	ICE	ICE
199306	60	0.839	4.456	1.47	5.4	226	13.4	243
199307	260	0.841	5.507	3.94	9.56	88	16.8	91
199308	431	0.571	5.198	1.9	7.18	109	10.3	95
199309	712	1.071	6.039	3.54	7.9	97	16.7	86
199310	639	1.257	5.632	3.96	7.9	100	18.1	98
199311	276	0.659	4.567	1.49	5.4	237	13.4	251
199312	132	1.172	4.405	2.01	5.4	272	17.9	275
199406	7	0.380	4.91	0.58	4.91	200	4	223
199407	1	ICE	ICE	ICE	ICE	ICE	ICE	ICE
199408	385	0.729	5.125	2.84	7.18	75	15.2	84
199409	406	0.865	4.813	2.07	6.53	82	12.8	71
199410	1	ICE	ICE	ICE	ICE	ICE	ICE	ICE
199411	37	0.475	3.225	0.78	3.05	229	8.5	233
199412	1	ICE	ICE	ICE	ICE	ICE	ICE	ICE
199506	1	ICE	ICE	ICE	ICE	ICE	ICE	ICE
199507	246	0.499	4.062	1.18	4.46	249	12.8	266
199508	280	0.508	4.092	0.9	4.05	101	9.3	95
199509	394	0.500	4.915	1.56	7.18	235	12.4	250
199510	457	0.971	5.74	2.53	7.9	234	16.1	248
199511	95	0.811	3.909	1.38	4.91	134	15.3	129
199512	49	0.983	4.291	1.45	4.91	138	15.3	129
199606	1	ICE	ICE	ICE	ICE	ICE	ICE	ICE
199607	320	0.625	4.727	1.71	5.94	56	12.6	53
199608	612	0.563	4.754	1.71	6.53	121	10.6	131

Wave Characteristics for 1983 through 2003 Climate Simulations

Year Month	No. Obs	Mean		Maximum at Height Max				
		H _{mo} [m]	T _p [s]	H _{mo} [m]	T _p [s]	Wave Dir	Wind Speed	Wind Dir
199609	652	0.787	4.995	2.22	7.9	129	11	134
199610	181	1.020	5.438	1.78	5.94	113	11.5	134
199611	1	ICE	ICE	ICE	ICE	ICE	ICE	ICE
199612	1	ICE	ICE	ICE	ICE	ICE	ICE	ICE
199706	73	0.695	3.809	1.13	4.46	284	12.9	282
199707	100	0.356	4.312	0.93	4.05	44	10.1	38
199708	511	0.836	5.996	2.02	7.18	230	14.4	244
199709	659	0.854	5.848	2.44	5.94	251	16.8	267
199710	571	0.804	5.319	2.86	8.69	87	11.8	84
199711	202	0.923	4.720	1.66	5.4	253	14.8	268
199712	1	ICE	ICE	ICE	ICE	ICE	ICE	ICE
199806	48	0.360	3.378	0.7	3.35	264	7.8	271
199807	407	0.662	4.402	1.41	4.91	257	12.6	276
199808	458	0.694	5.494	1.66	5.94	194	11.7	199
199809	720	0.667	5.416	1.52	6.53	197	9.6	203
199810	744	1.239	6.533	4.21	10.51	237	19.8	249
199811	517	0.788	4.731	1.76	7.18	252	14.2	276
199812	44	0.514	3.703	0.79	4.05	215	9.5	217
199906	52	0.659	3.912	1.05	4.05	254	12.5	260
199907	121	0.592	3.749	1.11	4.46	252	12.7	258
199908	576	0.697	5.628	2.13	7.9	250	16	271
199909	720	0.628	5.372	1.98	5.94	166	11.5	182
199910	337	1.505	6.751	3.06	9.56	241	17.3	256
199911	1	ICE	ICE	ICE	ICE	ICE	ICE	ICE
199912	1	ICE	ICE	ICE	ICE	ICE	ICE	ICE
200006	1	ICE	ICE	ICE	ICE	ICE	ICE	ICE
200007	1	ICE	ICE	ICE	ICE	ICE	ICE	ICE
200008	537	0.604	4.501	2.65	6.53	105	16.1	109
200009	691	0.656	5.217	2.68	7.9	87	12.7	71
200010	542	0.857	4.875	2.65	8.69	93	12	83
200011	117	0.980	4.161	1.84	5.4	241	16.8	246
200012	1	ICE	ICE	ICE	ICE	ICE	ICE	ICE
200106	29	0.50828	3.328	0.8	3.69	308	8.8	301
200107	35	0.21114	6.749	0.31	7.18	81	6	186
200108	712	0.77621	5.098	1.97	6.53	77	11.8	90

Wave Characteristics for 1983 through 2003 Climate Simulations

Year Month	No. Obs	Mean		Maximum at Height Max				
		H _{mo} [m]	T _p [s]	H _{mo} [m]	T _p [s]	Wave Dir	Wind Speed	Wind Dir
200109	705	0.58187	5.008	1.57	5.94	245	13.6	264
200110	283	0.52643	4.113	1.26	4.91	219	12.4	240
200111	1	ICE	ICE	ICE	ICE	ICE	ICE	ICE
200112	1	ICE	ICE	ICE	ICE	ICE	ICE	ICE

4.3.3. Extreme and Average Wave Climate

Severe, historic storms dating back to 1954, which were thought to have a significant influence on wave conditions at Barrow, were included in the hindcast. Inclusion of the additional storms provided higher confidence in the extreme wave estimates (those representing 50-year return-period events) that are critical for design of any coastal storm risk management project.

The percent of occurrence for the range of wave heights and periods is shown in Table 6. The largest storm of record in the extremal wave analysis occurred in September 1986. The peak significant wave height was 17 ft with a 10.5 sec period. The return period predicted for this storm by the extremal analysis is 30.3 years. A plot of the deep-water significant wave height and return period is shown in Figure 50. Significant wave heights for the selected storms from 1954 to 2003 are shown in Table 7, along with their rankings.

Table 6. Percent Occurrence (x1000) 1983-2003 from WAM of Wave Height and Period for all Directions at Station 71.25 N, 157.25 W.

H [ft]	Peak Period [sec]										Total
	<5.0	5.0-5.9	6.0-6.9	7.0-7.9	8.0-8.9	9.0-9.9	10.0-11.9	12.0-12.9	14.0-15.9	16.0+	
0.0-0.3	68838
0.4-1.6	6623	3158	827	643	34	1	11286
1.7-3.2	8022	1624	808	525	41	4	1	.	.	.	11025
3.3-4.8	2061	1819	627	683	75	18	5283
4.9-6.5	74	966	496	556	75	21	2188
6.6-8.1	.	74	139	356	99	53	1	.	.	.	722
8.2-9.8	.	8	26	161	80	77	5	.	.	.	357
9.9-11.4	.	.	1	88	35	16	3	.	.	.	143
11.5-13.0	.	.	.	25	40	11	9	.	.	.	85
13.1-14.7	18	5	9	.	.	.	32
14.8-16.3	1	3	4
16.4-18.0	3	10	.	.	.	13
18.1+	0
TOTAL	16780	7649	2924	3037	498	212	38	0	0	0	

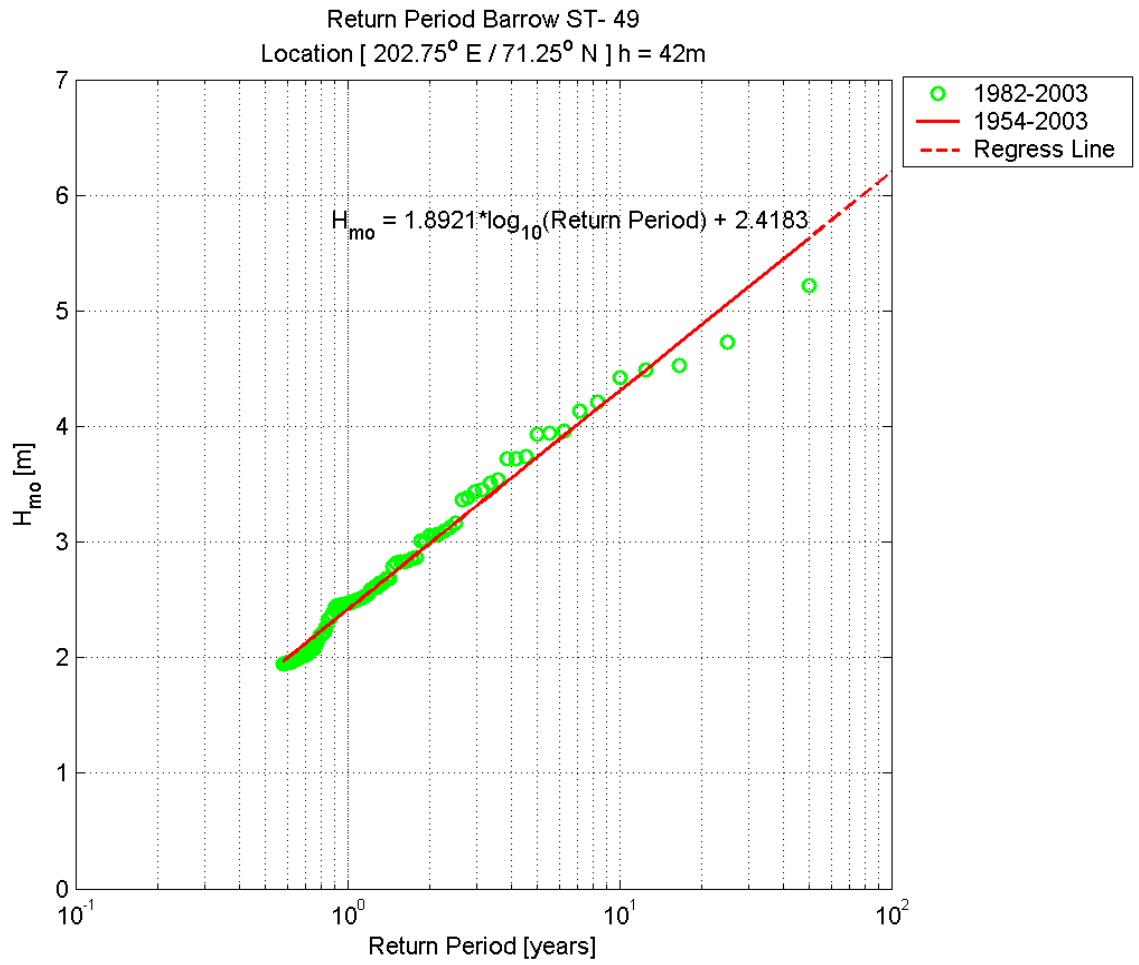


Figure 50. Deep Water Wave Height Return Period

Table 7. Storm Ranking. Note: Wind and wave directions are in the convention of “toward which” where onshore winds and waves have a direction of 135°.

Storm ranking.

Rank	Return Interval	Year	Month	Date	Time	Hmo [m]	Hmo [ft]	Tp	DIR (TWD WCH)	Wsp [m/s]	Wdir
1	30.3	1986	9	21	12	5.22	17.1	10.51	84	18.8	71
2	16.7	2002	8	15	09	4.73	15.5	9.56	76	17.2	69
3	13.1	2002	10	06	07	4.53	14.9	9.56	106	17.4	99
4	12.4	1985	9	16	13	4.49	14.7	8.69	97	18.8	91
5	11.4	2003	7	29	19	4.42	14.5	9.56	81	16.5	83
6	8.8	1998	10	25	01	4.21	13.8	10.51	237	19.8	249
7	8.0	1989	10	09	07	4.13	13.5	8.69	116	16.8	106
8	6.5	1993	10	12	01	3.96	13.0	7.9	100	18.1	98
9	6.4	1993	7	30	07	3.94	12.9	9.56	88	16.8	91
10	6.3	1992	9	10	01	3.93	12.9	8.69	93	17.3	83
11	5.0	2002	10	09	07	3.74	12.3	9.56	122	14.1	136
12	4.9	1986	9	12	13	3.72	12.2	8.69	79	16.5	74
13	4.9	1954	9	18	10	3.72	12.2	7.9	123	16.1	112
14	3.9	1993	9	19	01	3.54	11.6	7.9	97	16.7	86
15	3.8	1993	9	27	01	3.51	11.5	8.69	108	14.6	104
16	3.5	1968	9	22	19	3.45	11.3	8.69	112	14.1	107
17	3.4	1991	8	06	19	3.43	11.3	7.9	87	16.7	89
18	3.2	1993	10	01	13	3.38	11.1	8.69	241	19.2	255
19	3.2	1987	9	14	01	3.37	11.1	9.56	81	14.7	77
20	2.5	1962	9	05	05	3.16	10.4	8.69	72	14	60
21	2.4	1954	10	05	01	3.13	10.3	7.9	98	13.8	94
22	2.3	2003	9	11	07	3.1	10.2	9.56	101	13.4	73
23	2.2	1963	10	04	01	3.07	10.1	6.53	107	20.1	107
24	2.2	1993	10	30	13	3.06	10.0	7.9	224	17.2	238
25	2.2	1999	10	07	01	3.06	10.0	9.56	241	17.3	256
26	2.1	1998	10	17	01	3.01	9.9	9.56	233	15.7	250
27	2.1	2003	10	07	07	3.01	9.9	9.56	235	16.5	248
28	1.7	1985	9	21	01	2.87	9.4	7.18	72	15	62
29	1.7	1997	10	09	04	2.86	9.4	8.69	88	11.8	84
30	1.7	1994	8	15	01	2.84	9.3	7.18	75	15.2	84
31	1.7	2002	8	17	09	2.83	9.3	8.69	109	12.7	107
32	1.7	1993	10	04	03	2.83	9.3	7.18	103	14.6	108
33	1.6	1986	9	24	13	2.82	9.2	7.9	134	13.7	131
34	1.6	1990	10	24	13	2.79	9.2	6.53	225	17.9	239
35	1.4	2000	9	19	16	2.68	8.8	7.9	87	12.7	71

Storm ranking.

Rank	Return Interval	Year	Month	Date	Time	Hmo [m]	Hmo [ft]	Tp	DIR (TWD WCH)	Wsp [m/s]	Wdir
36	1.4	1984	10	01	08	2.68	8.8	5.94	245	16.5	259
37	1.3	2000	8	11	10	2.65	8.7	6.53	105	16.1	109
38	1.3	2000	10	05	13	2.65	8.7	8.69	93	12	83
39	1.3	2003	9	09	07	2.61	8.6	8.69	94	11.8	60
40	1.3	1993	10	08	19	2.61	8.6	7.18	70	14.5	69
41	1.2	2002	11	06	01	2.59	8.5	5.94	234	19.4	247
42	1.2	1986	8	19	16	2.55	8.4	8.69	95	11.2	77
43	1.1	1995	10	09	13	2.53	8.3	7.9	234	16.1	248
44	1.1	1994	8	19	16	2.52	8.3	7.18	79	13.5	82
45	1.1	1973	8	01	20	2.51	8.2	7.18	45	14.2	37
46	1.1	2002	9	03	01	2.5	8.2	7.18	75	14.4	78
47	1.1	1984	10	17	13	2.49	8.2	7.18	52	12.8	22
48	1.1	1957	9	13	07	2.48	8.1	7.18	236	17	250
49	1.1	1993	9	07	01	2.47	8.1	7.18	229	16.4	241
50	1.1	1980	9	28	01	2.47	8.1	7.18	239	17.5	251
51	1.1	1973	10	16	09	2.46	8.1	7.9	42	13.9	8
52	1.0	1992	9	16	05	2.45	8.0	7.18	112	11.9	114
53	1.0	1986	10	11	13	2.45	8.0	7.18	105	13.4	121
54	1.0	1991	9	06	02	2.45	8.0	7.18	241	16.5	253
55	1.0	1997	9	18	07	2.44	8.0	5.94	251	16.8	267
56	1.0	1978	9	27	20	2.42	7.9	7.18	90	13.1	92
57	1.0	2003	8	05	13	2.38	7.8	6.53	122	13	122
58	0.9	1984	9	30	23	2.34	7.7	5.94	241	15.9	250
59	0.9	1998	10	14	07	2.33	7.6	9.56	239	14.2	267
60	0.8	1982	9	17	04	2.26	7.4	6.53	163	12	169
61	0.8	1996	9	09	13	2.22	7.3	7.9	129	11	134
62	0.8	1986	8	22	07	2.2	7.2	6.53	130	12.7	140
63	0.8	1987	9	24	01	2.19	7.2	7.18	246	16.5	263
64	0.7	1989	9	14	01	2.16	7.1	7.18	112	11.3	120
65	0.7	1999	8	20	13	2.13	7.0	7.9	250	16	271
66	0.7	1984	9	21	13	2.08	6.8	6.53	29	13.5	4
67	0.7	1992	10	07	01	2.08	6.8	5.94	353	15.9	344
68	0.7	1960	9	27	07	2.08	6.8	5.94	9	15.7	352
69	0.7	1994	9	06	01	2.07	6.8	6.53	82	12.8	71
70	0.6	1967	9	19	01	2.03	6.7	6.53	235	15.3	240
71	0.6	1987	8	30	13	2.02	6.6	6.53	107	10.7	110
72	0.6	1997	8	26	01	2.02	6.6	7.18	230	14.4	244

Storm ranking.

Rank	Return Interval	Year	Month	Date	Time	Hmo [m]	Hmo [ft]	Tp	DIR (TWD WCH)	Wsp [m/s]	Wdir
73	0.6	1993	12	30	16	2.01	6.6	5.4	272	17.9	275
74	0.6	1990	9	18	01	2.01	6.6	5.94	237	15.3	250
75	0.6	1990	9	13	01	2.01	6.6	7.9	75	11.2	42
76	0.6	1997	10	04	22	1.99	6.5	7.9	221	11.9	228
77	0.6	1999	9	27	08	1.98	6.5	5.94	166	9.9	171
78	0.6	1989	10	20	16	1.98	6.5	6.53	171	11.2	169
79	0.6	2001	8	13	07	1.97	6.5	6.53	77	11.8	90
80	0.6	1990	9	27	13	1.96	6.4	5.94	101	12.7	104
81	0.6	1992	9	08	01	1.96	6.4	5.94	103	13.1	99
82	0.6	2000	10	02	23	1.96	6.4	7.18	79	11	71
83	0.6	2002	11	30	07	1.95	6.4	5.94	241	15.6	259
84	0.6	2003	10	30	01	1.95	6.4	6.53	52	11.9	25
85	0.6	1984	8	15	01	1.95	6.4	6.53	78	11.5	82
86	0.6	1989	10	12	09	1.94	6.4	6.53	102	10.9	100

4.4. Shallow Water Wave Transformation

The shallow water wave analysis consisted of numerically modeling the deep water wave transformation (Smith and Sherlock, 2009). The deep-water waves were transformed to nearshore waves using STWAVE.

STWAVE is a steady state finite difference model based on the wave action balance equation. It simulates depth-induced wave refraction and shoaling, current-induced refraction and shoaling, depth- and steepness-induced wave breaking, wind-wave growth, and wave-wave interaction and white capping that redistribute and dissipate energy in a growing wave field.

The numerical model was used to simulate historical storms that were forced by offshore wave conditions. These wave model results were used as input to the sediment transport calculations and in the development of the coastal risk reduction design alternatives.

4.4.1. Bathymetry

Figure 51 shows a contour plot of the bathymetry for the Barrow STWAVE grid. The grid was developed by merging digit bathymetry from NSIDC and beach profiles provide by the Alaska District. The grid origin is $x = 1,740,000$ ft and $y = 6,310,000$ ft (Alaska State Plane, Zone 6). The grid has 280 rows (south to north, alongshore) and 94 columns (cross-shore), and grid spacing is 300 ft. The grid orientation is 315° meaning that the x-axis points toward land in the cross-shore direction. Depths are relative to Mean Lower Low Water (MLLW). The offshore boundary of the grid is in a water depth of approximately 150 ft.

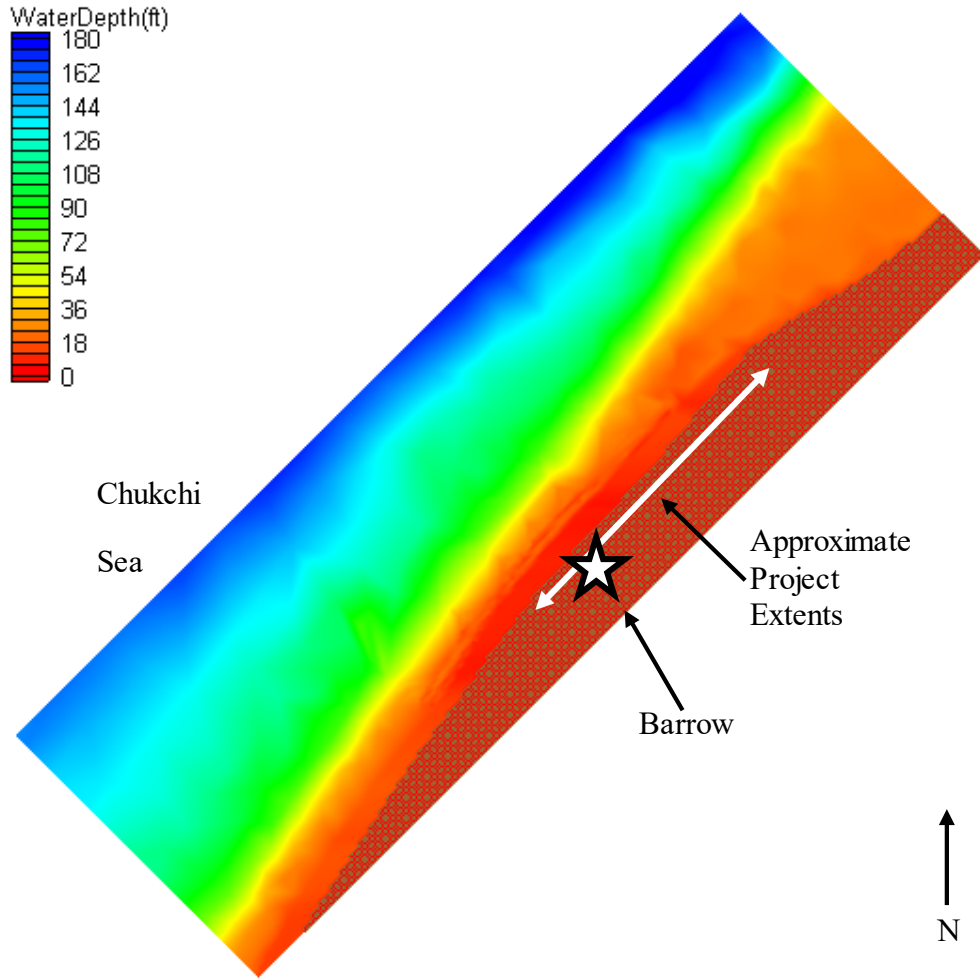


Figure 51. STWAVE Bathymetry Grid for Barrow, AK (depths in ft). Land Area is Shown in Brown.

4.4.2. Water Level and Wind

Water level variations used in the STWAVE model were based on the ADCIRC wind surge simulations (Section 5.1 Water Surface Modeling with ADCIRC) and maximum tide (+0.5 ft MLLW). Water level is applied in STWAVE as constant water depth increase, relative to MLLW, over the entire grid. Water levels for typical wave condition simulations were specified as mean tide level.

Wind input in STWAVE simulates wave growth across the grid domain. Local wind input was not included for the typical wave simulations. Wind speed and direction for the storm simulations were taken from the WAM output station at 71.25° N and 157.25° W and applied to the entire STWAVE grid.

4.4.3. Sample Output

Figure 52 shows example output from STWAVE. The color contours represent wave height. The red contours are areas of local focusing and the yellow are areas of defocusing caused by the nearshore bathymetry. The blue and green represent areas where the waves have dissipated due

to depth-limited wave breaking. The incident wave condition for this case is a wave height of 8.9 ft, peak period of 8.7 sec, and a direction of 275° applied at the offshore boundary and did not include a tide or wind surge in the water depth. The offshore water depth is shown in Figure 51 (average of approximately 150 ft).

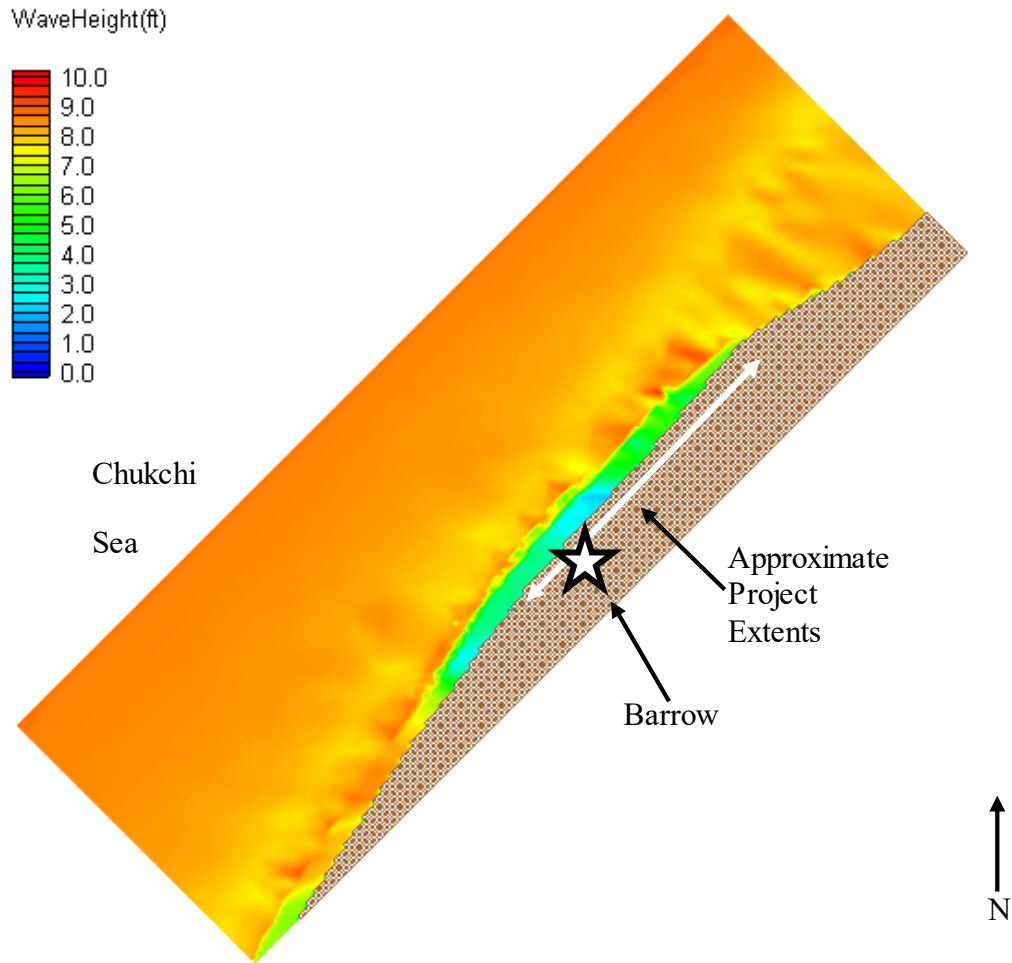


Figure 52. Sample STWAVE Transformed Wave Height Field

4.4.4. Field Data

The model was validated using nearshore wave measurements acquired during the summer and fall of 2003 at depths of 33 and 16 ft. The wave gages used for this study were RD Instruments Sentinel 1200 kHz Acoustic Doppler Current Profilers (ADCP). The gages were deployed 12 September-4 November 2003, with a short gap for servicing on 1-2 October 2003. The gages were deployed at 71.296341° N, 156.812040° W in a depth of approximately 33 ft and at 71.294176° N, 156.799910° W in a depth of approximately 16 ft (Figure 53). Data recovery included a storm event occurring 8-12 September 2003. The peak wave height during the storm was 10 ft with a peak period of 10 sec, observed by the ADCP in 33-ft water depth (Figure 54 and Figure 55). Wave periods of 10 sec and greater cause high run-up and more erosion. Figure 54 through Figure 56 show the wave height, period, and direction, respectively, for both gages throughout the deployment period.

An attempt to collect a second season of data was unsuccessful as one gage was damaged by an ice keel and ice formation made the collection of the second gage impossible at the end of the season. Attempts to retrieve the second gage the following season were unsuccessful.

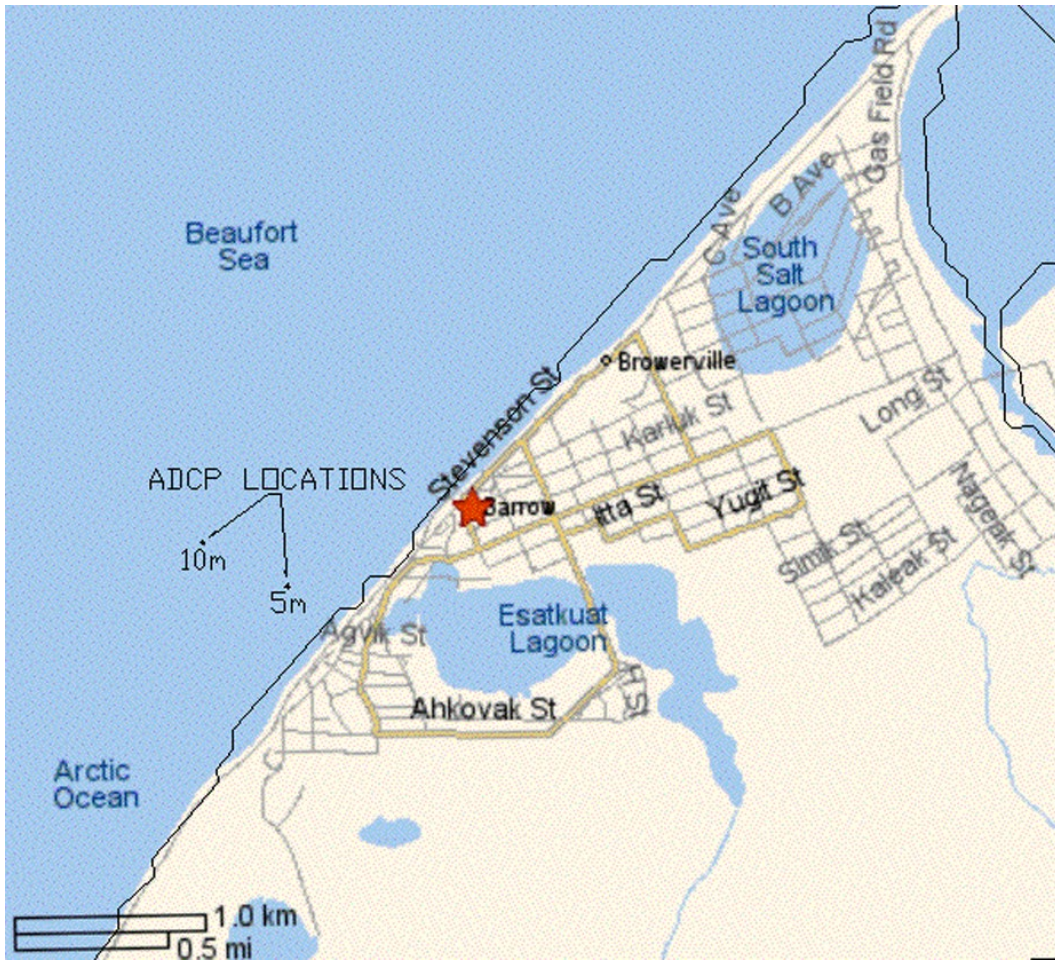


Figure 53. Location of ADCP Instruments

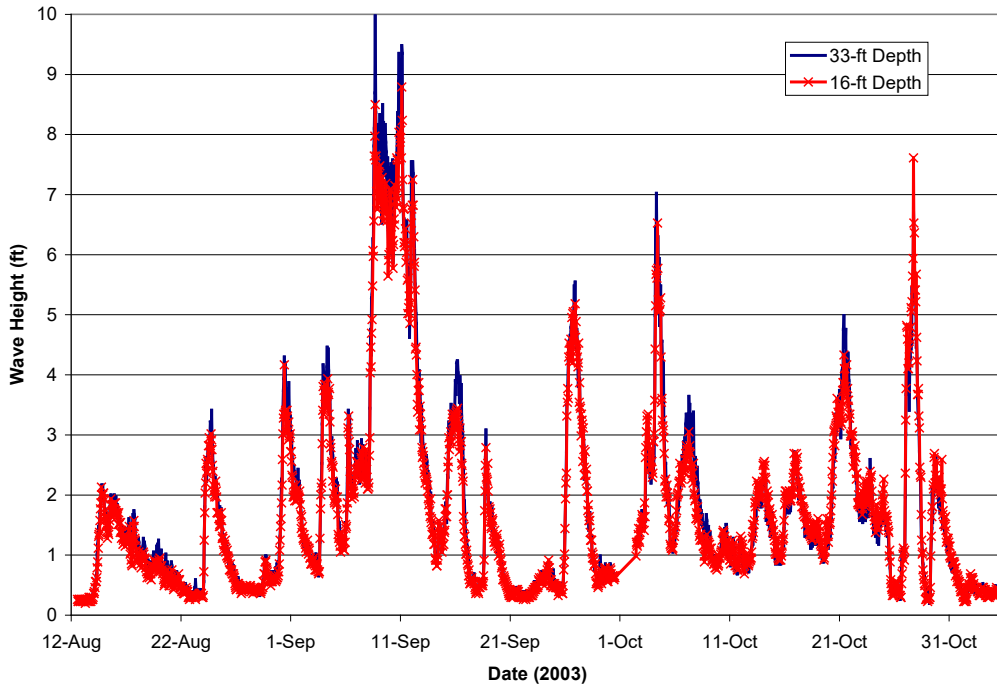


Figure 54. Measured Wave Height at 33 and 16 ft Depths

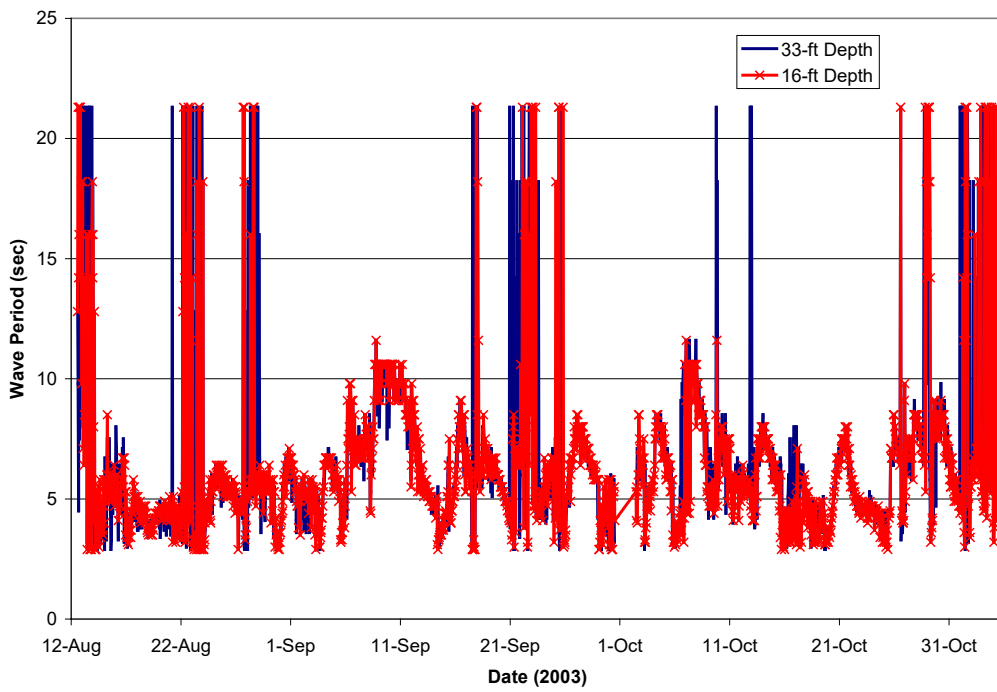


Figure 55. Measured Peak Wave Period at 33 and 16 ft Depths

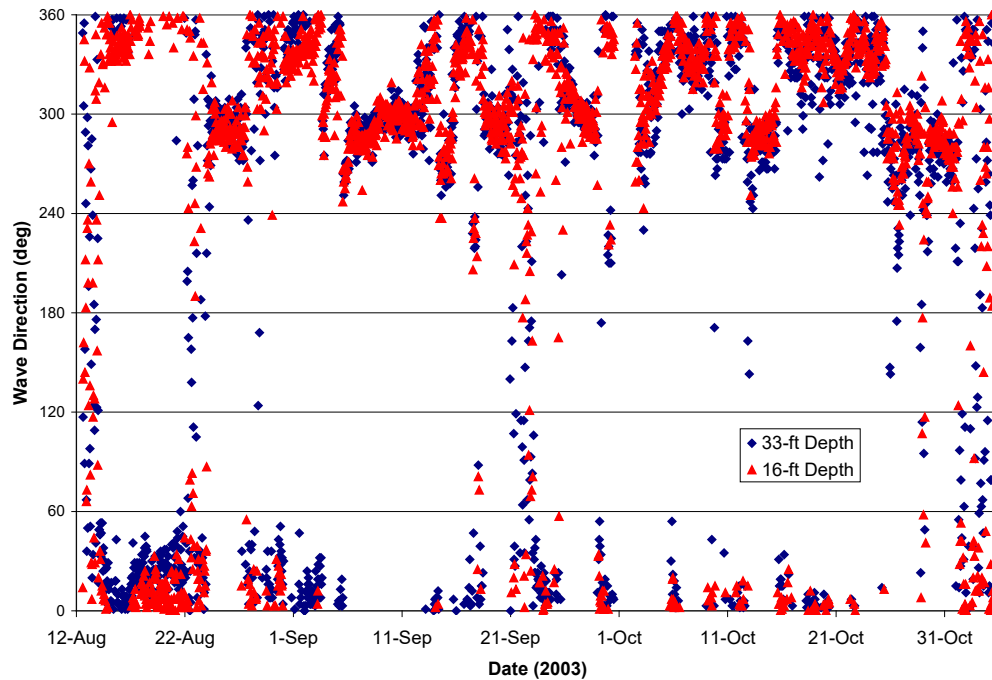


Figure 56. Measured Wave Direction at 33 and 16 ft Depths

4.4.5. Model Validation

STWAVE was validated for Barrow using the wave data collected at water depths of 33 and 16 ft. Within the August through November 2003 wave record, the largest waves occurred during the period 28 August-17 September 2003. The measurements include wave height, peak period, and mean wave direction. Figure 57 presents simulated wave heights and periods compared with the data at the 33 ft gage, and Figure 58 shows the mean direction comparisons. The wave heights show good agreement with a mean error of 0.07 ft and a root-mean-square error of 0.69 ft. A positive mean error indicates an underestimate by the model. The comparison of wave periods show differences in the first few days (as the measured period bounces between sea and swell periods), but then track the measurements quite well. The mean error in peak period is 0.5 sec and the root-mean-square error is 2.4 sec. The mean error in direction is 8.3° and the root-mean-square error is 31°. The model and measurements have a slightly different definition of wave direction; the model provides the overall vector mean and the measurements provide the mean direction at the peak frequency. This difference can lead to significant differences when both sea and swell are present.

As the waves transform to the shallower gage in a depth of 16 ft, the wave height error increases slightly, as the period and directional errors decrease. Comparisons with measurements at the 16 ft depth are shown in Figure 59 for wave height and peak period and Figure 60 for mean direction. The mean wave height error is -0.23 ft and the root-mean-square error is 0.75 ft. The measured periods again jump between sea and swell, but less than at the deeper gage. The mean error in peak period is 0.3 sec and the root-mean-square error is 2.1 sec. The mean error in mean direction is 0.6° and the root-mean-square error is 26°. The validation shows good agreement between the modeling methodology and the measurements.

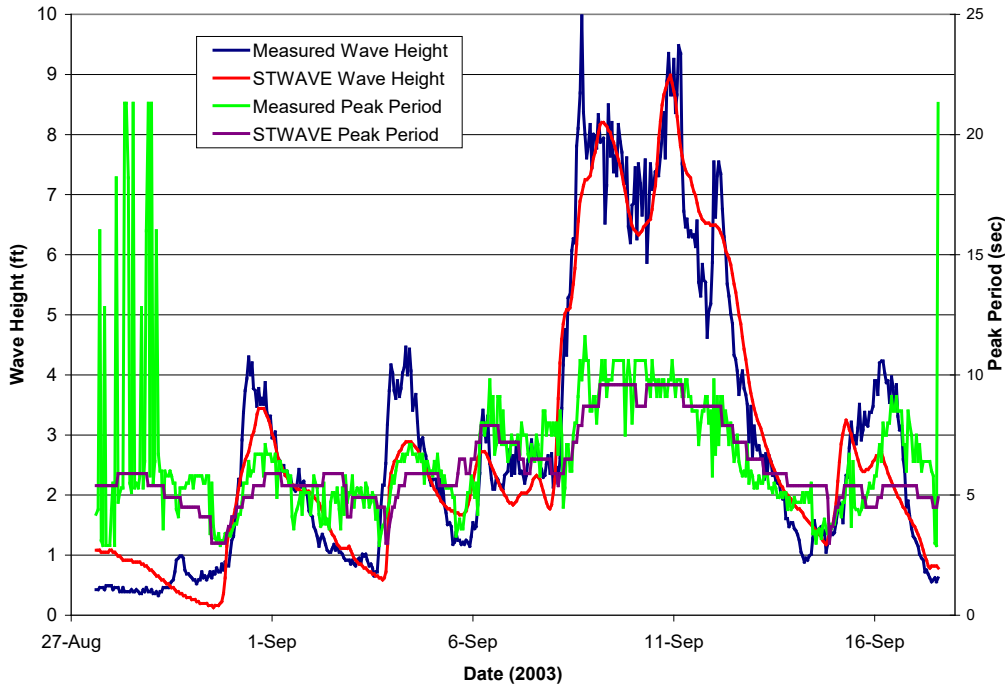


Figure 57. STWAVE Validation of Wave Height and Peak Period with Measurements at 33 ft depth for 27 August - 17 September.

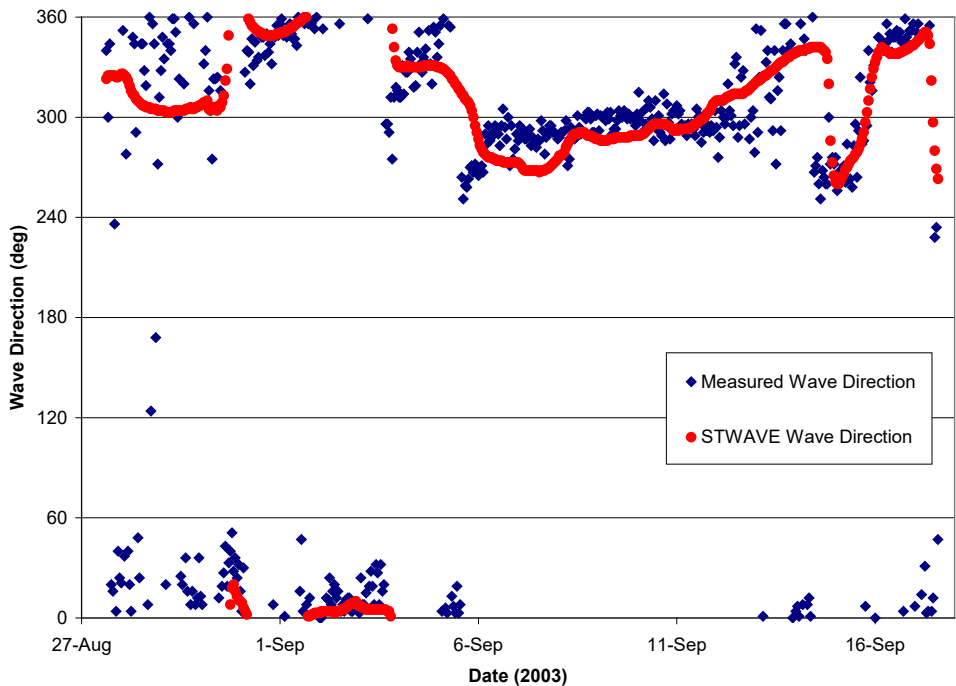


Figure 58. STWAVE Validation of Mean Wave Direction with Measurements at 33 ft depth for 27 August - 17 September.

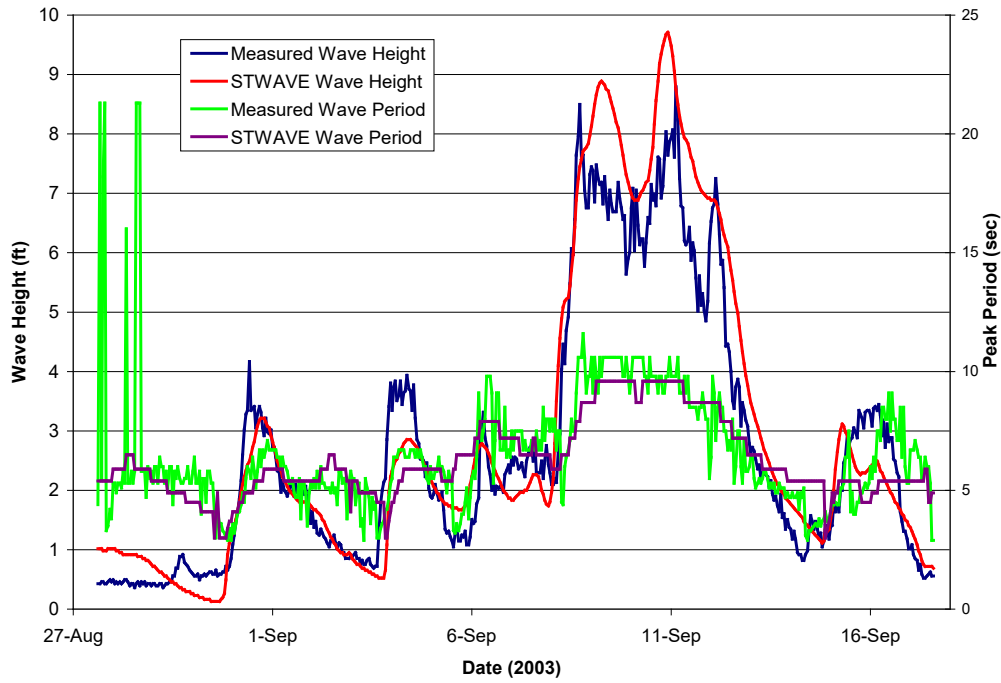


Figure 59. STWAVE Validation of Wave Height and Peak Period with Measurements at 16 ft depth for 27 August – 17 September.

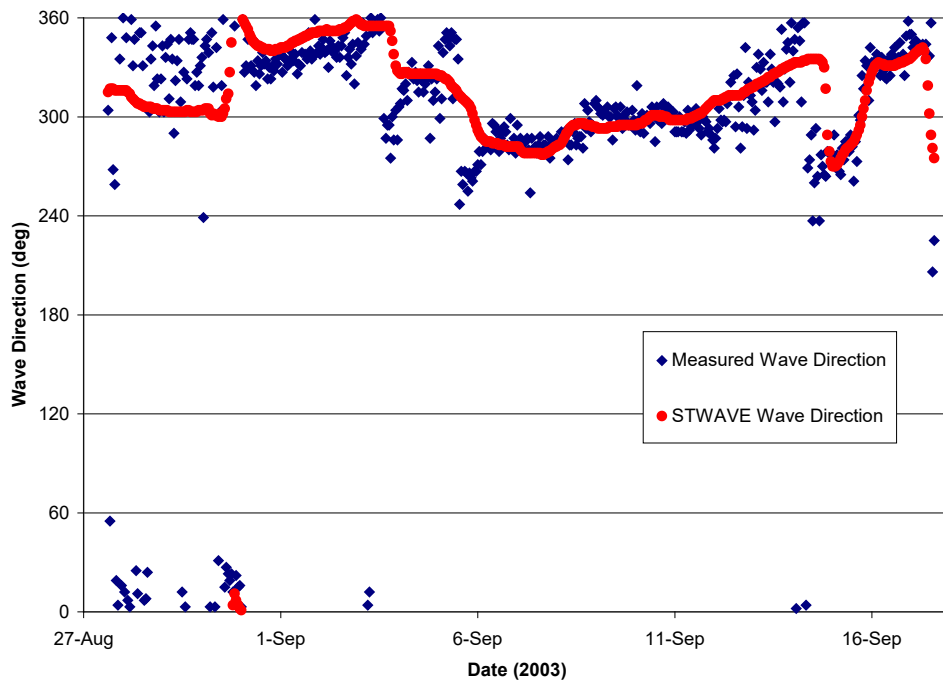


Figure 60. STWAVE Validation of Mean Wave Direction with Measurements at 16 ft depth for 28 August - 17 September.

4.4.6. Summary of Results

The wave transformation model STWAVE was used to transform waves from the deepwater wave hindcast boundary output point to the nearshore at Barrow. The modeling simulations included 51 typical waves and 28 storm events. The model was validated using nearshore wave measurements acquired during the summer and fall of 2003 at depths of 33 and 16 ft. The validation shows good agreement between the model and measurements, indicating the deepwater hindcast and nearshore transformation model methodologies are sufficiently skilled to provide design input. Figure 61 provides the nearshore wave height (in 28.5 ft water depth, directly offshore of Barrow) as a function of return period based on the storms simulated between 1954 and 2003. The STWAVE model results were then used as a forcing function for the run-up model (SBEACH).

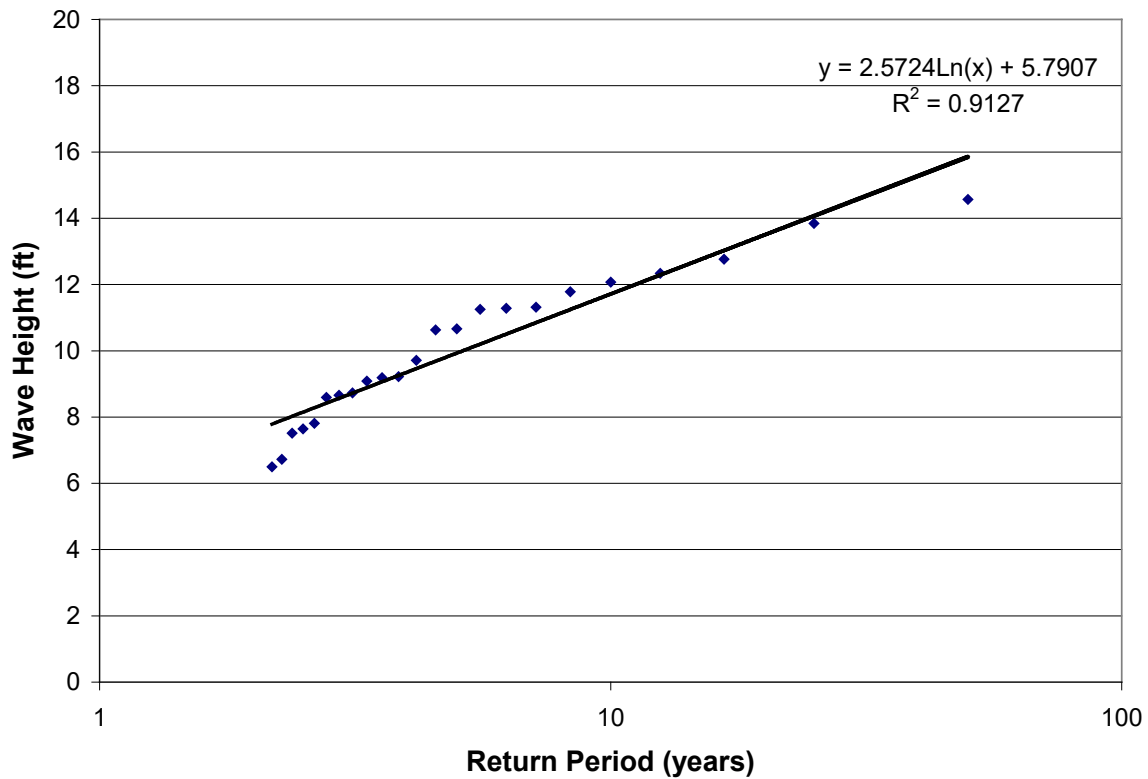


Figure 61. Return Period for Nearshore Storm Wave Heights (1954-2003). Results were Generated from Model Output in 28.5 ft Water Depth directly Offshore of Barrow.

5. CURRENTS AND WATER LEVELS

Information on currents and water levels was needed in order to evaluate sediment transport and flooding. Investigation of the water levels and currents consisted of a literature search for information in the area, deployment of instrumentation in 2003 and 2004, and modeling to characterize currents and water levels in the site vicinity.

Historic water-surface elevations and currents for storm events were computed by the CHL (Chapman, 2009) for the 2010 Technical Report using the ADvanced CIRCulation (ADCIRC)

model, a two-dimensional, depth integrated, barotropic-time dependent long wave, hydrodynamic circulation model. The bathymetry used for the ADCIRC model is shown in Figure 62. The effect of wave set-up and run-up on the total water level was computed by the CHL using the SBEACH model. This model simulates cross-shore beach, berm, and dune erosion produced by storm waves and total water levels.

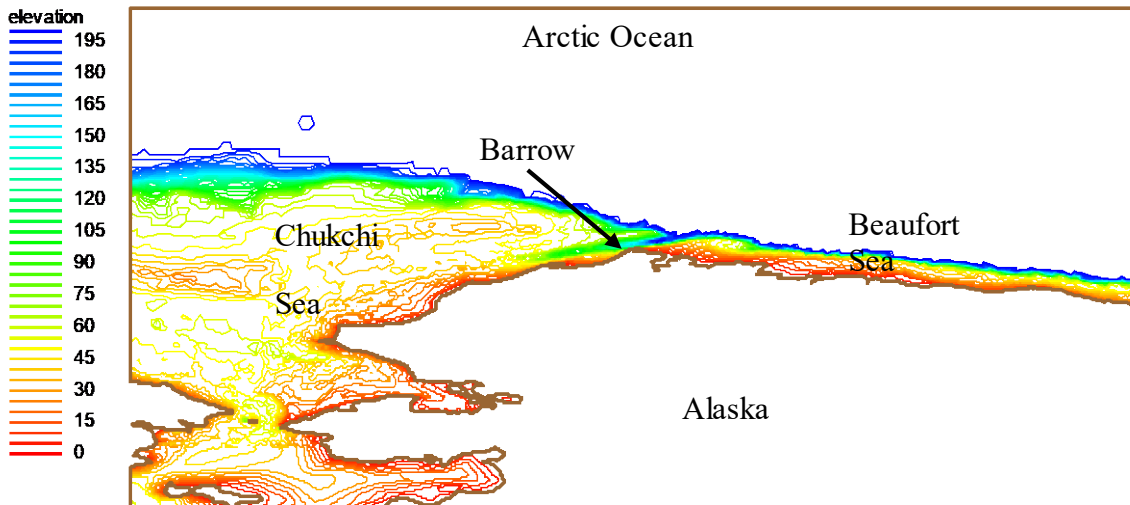


Figure 62. Regional ADCIRC Grid Bathymetry Showing Depths less than 200 m

5.1. Water Surface Modeling with ADCIRC

Water surface elevations for selected storms were measured and modeled to provide a base storm water surface elevation for modeling wave set-up and run-up. The water surface elevation for the storm events included changes in water surface elevation due to tide, wind stress, and atmospheric pressure.

Model calibration and verification of the water surface elevation was performed with the ADCP data collected in 2003. Initial verification simulations showed that the predicted water surface fluctuations tracked the measurements however; the maximum positive and negative surge elevations were under predicted due to the neglect of the effects of atmospheric pressure variation.

5.1.1. Inverted Barometric Correction

Much of the variation of water surface elevation at Barrow can be attributed to what is commonly known as the inverted barometer effects. The water surface elevation will increase or decrease 1 foot for each 30 millibar of negative or positive change in atmospheric pressure, respectively.

The inverted barometer correction method was tested via a simulation of the westerly storm event that occurred in early September 2003. A verification simulation was performed, in which, the contribution of the inverted barometer effect was included on an hourly basis. Specifically, the inverted barometer contribution was computed by taking hourly atmospheric pressure

measurement starting on the first of September and correcting the still water level by 1 foot for every 30 millibar change in the measured atmospheric pressures during the westerly event. The time series of inverted barometer correction was added to the ADCIRC wind driven water levels. Figure 63 presents a comparison of predicted water levels with and without the inverted barometer correction and observations of the Barrow ADCP instrument deployed in -33 ft of water. As shown in Figure 63, the corrected peak water surface elevation tracks well within the observed wind set-up and tidal range (Days 6-10).

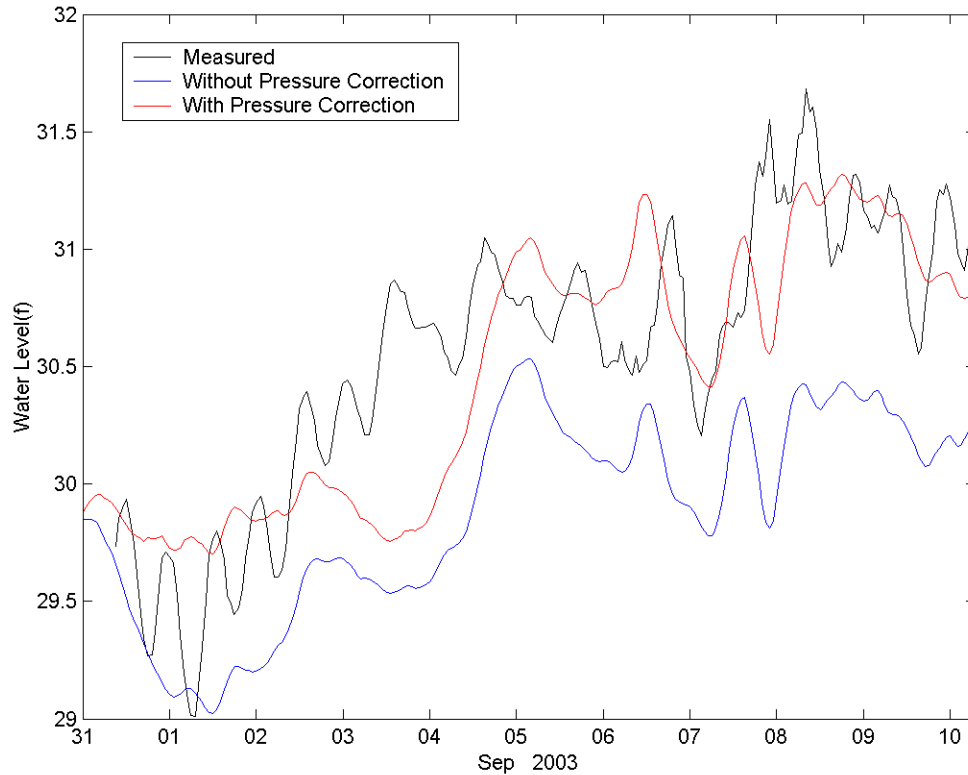


Figure 63. Comparison of Predicted Water Levels with/without the Inverted Barometer Correction and Observations at the Barrow ADCP Instrument Data at the 33 ft Site.

5.1.2. Ice Coverage Effect

The maximum transfer of wind energy into water occurs with 50 percent ice coverage. Figure 64 shows the influence of varying degrees of ice coverage.

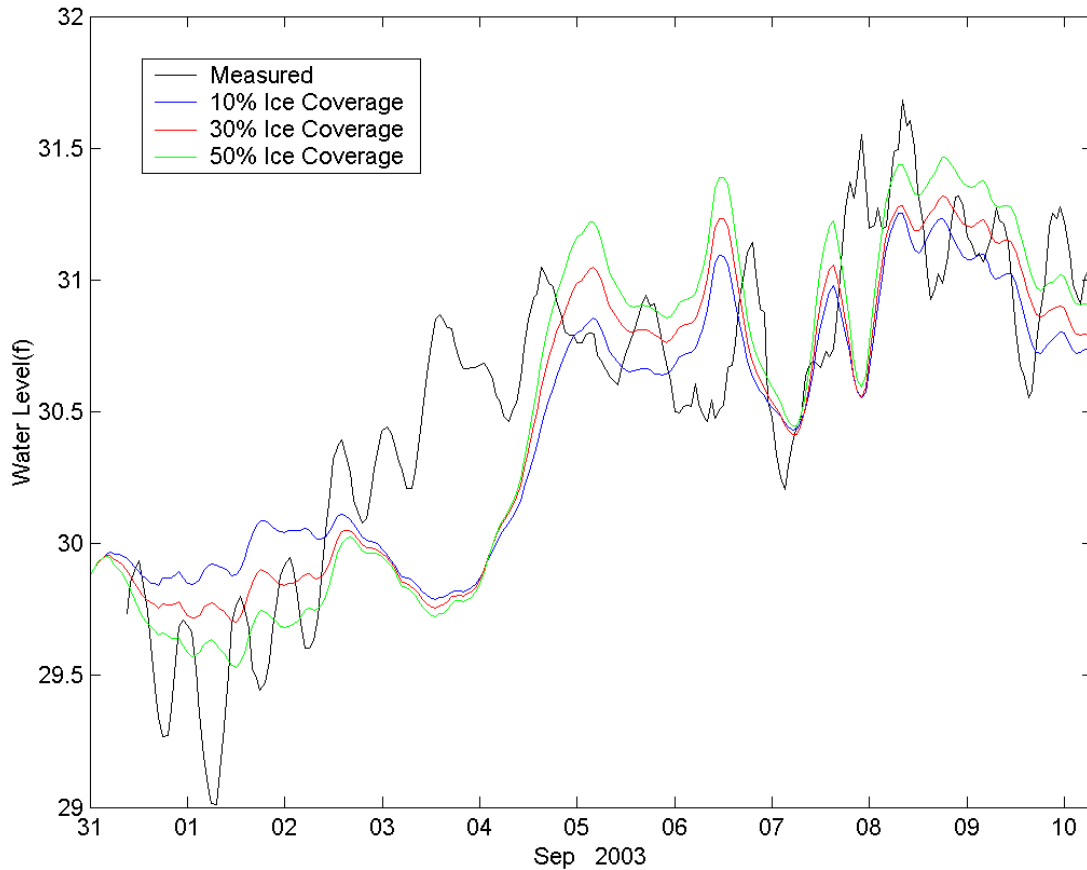


Figure 64. Influence of Varying Degrees of Ice Coverage

5.1.3. Total Surge

The storm events simulated and the date of occurrence are presented in Table 8. In most cases the simulation began when the storm was far to the west of Barrow, and ended after its passage. The influence of the tide and atmospheric pressure (inverted barometer) on the resulting peak water surface elevation are included by linearly adding a tidal range of 0.5 ft and the peak inverted barometer displacement as discussed previously (Equation 1). The tidal determination discussed in Section 3.3 (Tides) was done post ADCIRC modeling. Therefore, actual tidal constituents were not included during the modeling efforts. A tide range of 0.5 ft was determined an appropriate range for the tide based on engineering judgment and the modeler’s prior experience with ocean circulation modeling in the Arctic. Based on the tidal determination performed after the modeling effort (presented in Section 3.3 Tides), the maximum tide of 0.5 ft was determined to be only 0.11 ft lower than the tide range established.

$$\text{Total Surge} = \text{Peak Wind Surge} + \text{Inverted Barometer} + \text{Tide} \quad \text{Equation 1}$$

Peak Wind Surge – ADCRIC Output

Inverted Barometer – Atmospheric Correction (Section 5.1.1 Inverted Barometric Correction)

Tide – +0.5ft MLLW (Section 3.3 Tides)

The results of the storm event simulations, including peak wind surge from ADCIRC output at a still water depth of 33 ft, inverted barometer, and total surge, are presented in Table 8. Total surge is the linearly added peak wind surge, inverted barometer, and 0.5 ft tide contribution. The total surge results were used as a forcing function for the run-up calculations (SBEACH) to determine the water depth at the toe of any proposed structure.

Table 8. Summary of Peak Wind Surge (ADCIRC Output in 33 ft still Water Depth), Inverted Barometer (1 ft per 30 millibar), and Total Surge (Peak Wind Surge + Inverted Barometer + 0.5 ft Tide),

Year	Month	Day	Rank	Peak Wind Surge [ft]	Inverted Barometer [ft]	Total Surge [ft]
1954	September	16	25	0.62	0.69	1.80
1954	October	03	4	1.25	1.38	3.12
1955	July	17	13	1.48	0.39	2.36
1960	September	25	12	0.82	1.08	2.39
1961	June	16	20	1.18	0.49	2.16
1962	September	03	7	1.61	0.89	2.98
1963	August	21	22	0.66	0.92	2.07
1963	October	03	1	2.30	1.02	3.80
1968	September	21	24	0.59	0.79	1.87
1973	July	31	11	1.12	0.85	2.46
1973	October	14	2	1.61	1.31	3.41
1975	August	24	10	0.69	1.31	2.49
1978	September	24	28	0.36	0.82	1.67
1983	August	17	19	1.08	0.66	2.23
1985	September	15	15	1.08	0.69	2.26
1986	September	11	21	0.82	0.79	2.10
1986	September	19	8	1.38	0.92	2.79
1987	September	12	14	1.15	0.62	2.26
1988	September	24	6	1.61	0.92	3.02
1992	September	08	26	0.59	0.66	1.74
1993	September	25	18	0.92	0.82	2.23
1993	October	09	17	1.12	0.62	2.23
2000	July	04	27	0.56	0.62	1.67
2000	August	09	23	0.92	0.62	2.03
2002	August	14	9	1.54	0.56	2.59
2002	October	04	5	1.61	0.98	3.08
2003	July	24	3	2.10	0.75	3.35
2003	September	06	16	0.89	0.85	2.23

The Empirical Simulation Technique (EST) was applied to generate stage-frequency relationships for Barrow. Input to the EST model consisted of the estimated peak wind surge elevations combined with a tidal elevation (0.5 ft) and inverted barometer correction, which results in the “Total Surge” presented in Table 8. In order to increase the population within the

EST sample, half and then all of the tide range was removed to reflect the fact that the storms are of sufficient duration so that the peak wind surge can occur at any level within the tide range. Application of the 84 storm population EST analysis resulted in Table 9, which presents the stage-frequency distribution and standard deviation for 5 to 100 years. The tidal elevation had to be added into the EST after the ADCIRC storm population due to the lack of a tidal determination.

Table 9. Summary of Frequency-of-Occurrence Relationships with Variable Tide Population for Still Water Depth of 33 ft.

Return Period Year	Elevation [ft MLLW]	Standard Deviation [ft]
5	2.30	0.13
10	2.85	0.16
15	3.05	0.16
20	3.18	0.16
25	3.25	0.20
50	3.58	0.36
75	3.87	0.56
100	4.00	0.72

5.2. Currents

The tidal fluctuations at the site are minimal, so the predominant source of currents is wind generation. Current modeling was performed using the ADCIRC model to provide information for the sediment transport. ADCIRC results were output and comparisons to ADCP data were performed at a still water depth of 33 ft. The ADCIRC results were then used as a forcing function for SBEACH and CERC formula (United States Army Corps of Engineers, 2002).

Calibration and verification of ADCIRC was performed using the water surface and current measurements collected during the August-November 2003 ADCP deployment. Calibration of the predicted current speed and direction was performed using the August-September field measurements. The calibrated model was then applied to the October 2003 measurement period for purposes of verifying model calibration. Figure 65 presents a comparison of the predicted depth averaged current with surface, mid-depth and near bottoms ADCP current measurements at the 33 foot depth site.

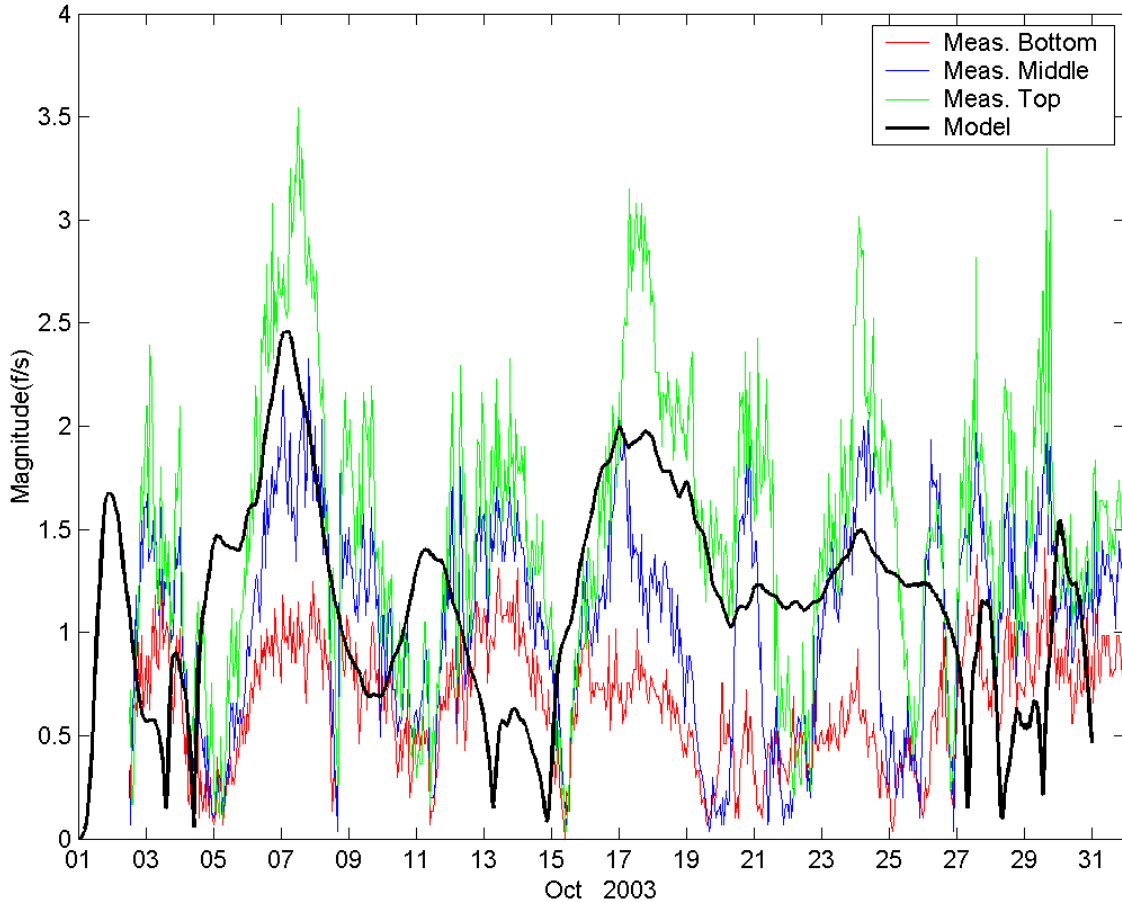


Figure 65. Comparison of Predicted Depth-Averaged Current Speed and Surface, Mid-Depth, and Bottom ADCP Current Measurements at the 33 ft Still Water Depth.

Satisfactory agreement between predicted and measured current magnitudes is achieved during significant wind events. The discrepancies shown in the predicted and observed current magnitudes result from 1) a persistent northeast coastal current that is observed during periods of light winds and 2) the three dimensional nature of the observed currents. A close examination of Figure 65 reveals that there is a factor of three increase in current magnitude from the near bottom to the surface. Furthermore, it is seen in Figure 66 that the change in current direction from the bottom to the surface exhibits a lag of more than two days during periods where changes in wind direction and strength are significant (Days 5-9, 15-19 and 23-26).

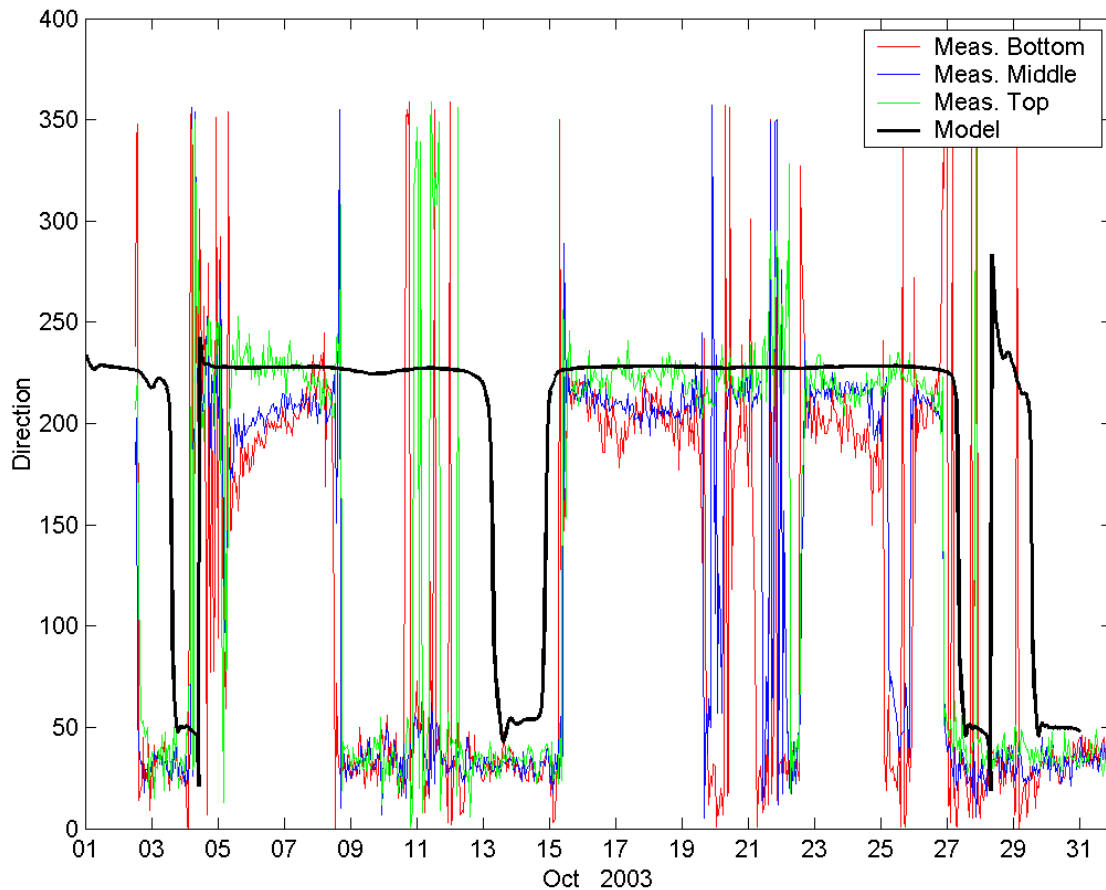


Figure 66. Comparison of Predicted Depth-Averaged Current Direction and Surface, Mid-Depth, and Bottom ADCP Current Direction Measurements at the 33 ft Still Water Depth.

According to model results, depth averaged currents during storm events range between 1 and 1.4 knots. These currents were generally maintained for 12 hours or less. On one occasion these currents were maintained for 24 hours. For the storm events modeled, the currents predominantly flowed in a northeast direction along the coast.

6. SEA LEVEL CHANGE

Evidence suggests that the arctic environment is experiencing a warming trend. The magnitude, duration, and effect of a warming trend is not known; however a shrinking polar ice pack could result in an extended open water season and an increase in frequency of the large storms that could impact the coastline at Barrow.

USACE requires that planning studies and engineering designs over the project life cycle, for both existing and proposed projects, consider alternatives that are formulated and evaluated for the entire range of possible future rates of sea level change (SLC), represented by three scenarios of “low,” “intermediate,” and “high” sea level change. According to Engineering Regulation (ER) 1100-2-8162 (United States Army Corps of Engineers, 2013) and Engineering Technical Letter 1100-2-1 (United States Army Corps of Engineers, 2014), the SLC “low” rate is the historic SLC. The “intermediate” and “high” rates are computed using:

- Estimate the “intermediate” rate of local mean sea level change using the modified National Research Council (NRC) Curve I, the NRC equations, and correcting for the local rate of vertical land movement.
- Estimate the “high” rate of local mean sea level change using the modified NRC Curve III, NRC equations, and correcting for the local rate of vertical land movement. This “high” rate exceeds the upper bounds of Intergovernmental Panel on Climate Change (IPCC) estimates from both 2001 (IPCC, 2001) and 2007 (IPCC, 2007) to accommodate potential rapid loss of ice from Antarctica and Greenland.

The 1987 NRC described these three scenarios using the following equation:

$$E(t) = 0.0012t + bt^2 \quad \text{Equation 2}$$

in which t represents years, starting in 1986, b is a constant, and $E(t)$ is the eustatic sea level change, in meters, as a function of t . The NRC committee recommended “projections be updated approximately every decade to incorporate additional data.” At the time the NRC report was prepared, the estimate of global mean sea-level (GMSL) change was approximately 1.2 mm/year. Using the current estimate of 1.7 mm/year for GMSL change, as presented by the IPCC (IPCC, 2007), results in this equation being modified to be:

$$E(t) = 0.017t + bt^2 \quad \text{Equation 3}$$

The three scenarios proposed by the NRC result in global eustatic sea level rise values, by the year 2100, of 0.5 m, 1.0 m, and 1.5 m. Adjusting the equation to include the historic GMSL change rate of 1.7 mm/year and the start date of 1992 (which corresponds to the midpoint of the current National Tidal Datum Epoch of 1983-2001), results in updated values for the variable b being equal to 2.71E-5 for modified NRC Curve I, 7.00E-5 for modified NRC Curve II, and 1.13E-4 for modified NRC Curve III. The three GMSL rise scenarios are depicted in Figure 67.

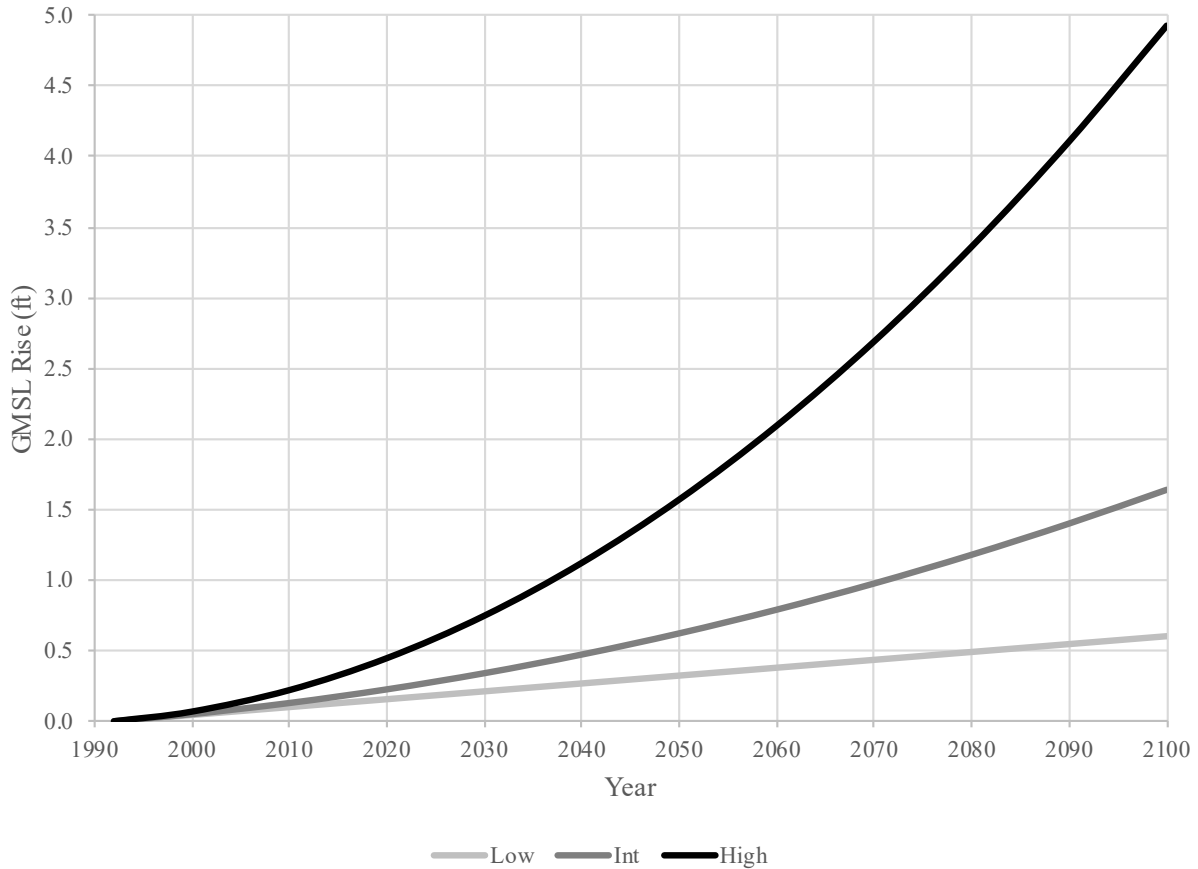


Figure 67. Scenarios for GMSL Rise (Based on Updates to NRC 1987 Equation and Converted to ft).

Manipulating the equation to account for the fact that it was developed for eustatic sea level rise starting in 1992, while projects will actually be constructed at some date after 1992, results in the following equation:

$$E(t_2) - E(t_1) = 0.0017(t_2 - t_1) + b(t_2^2 - t_1^2) \quad \text{Equation 4}$$

where t_1 is the time between the project's construction date and 1992 and t_2 is the time between a future date at which one wants an estimate for sea-level change and 1992 (or $t_2 = t_1 +$ number of years after construction). For the three scenarios proposed by the NRC, b is equal to $2.71\text{E-}5$ for Curve 1, $7.00\text{E-}5$ for Curve 2, and $1.13\text{E-}4$ for Curve 3.

There is no sea level trend data for Barrow or the area around Barrow. Due to Barrow's location along the Arctic Ocean and the lack of data and analysis in this region available for the IPCC estimated GMSL change, the GMSL Rise was deemed an inappropriate base SLC to use to estimate the Relative Sea Level Change (RSLC) in Barrow. Several factors contribute to variations in sea level change across geographic areas, including the distributions of changes in ocean temperature, salinity, winds and ocean circulation (IPCC, 2007). The current estimate for GMSL change, as presented by the IPCC, is based on satellite altimetry, thermosteric data (changes in ocean temperature), and tide gauges (IPCC, 2007). The geographic distribution of

TOPEX/Poseidon satellite altimeter (Chapter 5.5.2 of IPCC, 2007), thermosteric sea level change estimates (Chapter 5.5.4 of IPCC, 2007) and network of tide gauges available for the analysis (Chapter 5.A.4 of IPCC, 2007) did not cover the Arctic Ocean.

Prudhoe Bay, AK is approximately 200 miles northeast of Barrow (Figure 68). It has the closest and longest NOAA-NOS tide gauge record in the Arctic, from 1988 to present (NOAA Station 9497645), which is shorter than the recommended 2 tidal epoch duration of about 40 years. NOAA Center for Operational Oceanographic Products and Services published sea level trend for Prudhoe Bay is +0.00725 ft/yr with a 95 percent confidence interval of ± 0.00577 ft/yr.

The two next closest stations to Barrow are Permanent Service for Mean Sea Level Stations located in Providenia, Russia, approximately 640 miles southwest of Barrow, and Tuktoyaktuk, Canada, approximately 560 miles southeast of Barrow. Due to their distance from Barrow these two stations were not analyzed to estimate a regional sea level change, as recommended in ER 1100-2-8162 (United States Army Corps of Engineers, 2013).



The map above illustrates relative sea level trends , with arrows representing the direction and magnitude of change. Click on an arrow to access additional information about that station.



The Center for Operational Oceanographic Products and Services has been measuring sea level for over 150 years, with tide stations of the [National Water Level Observation Network](#) operating on all U.S. coasts. Changes in RSL, either a rise or fall, have been computed at 142 long-term water level stations using a minimum span of 30 years of observations at each location. These measurements have been averaged by month which removes the effect of higher frequency phenomena in order to compute an accurate linear sea level trend. The trend analysis has also been extended to 240 global tide stations using data from the [Permanent Service for Mean Sea Level \(PSMSL\)](#). This work is funded in partnership with the NOAA OAR [Climate Observation Division](#).

Figure 68. Location of Prudhoe Bay, AK

To estimate RSLC for Barrow, the local rate of vertical land movement (VLM), published by NASA Jet Propulsion Laboratory for Prudhoe Bay, was subtracted from the Prudhoe Bay NOAA sea level trend to estimate a regional sea level trend. The local rate of VLM for Barrow was then added to regional sea level trend. The local rate of VLM for Prudhoe Bay is $0.00859 \text{ ft/yr} \pm 0.00411 \text{ ft/yr}$ (NASA Jet Propulsion Laboratory, 2018) and the local rate of VLM for Barrow is $0.00820 \text{ ft/yr} \pm 0.00143 \text{ ft/yr}$ (NASA Jet Propulsion Laboratory, 2018). This results in an estimated sea level trend of $+0.00686 \text{ ft/yr}$ (Figure 69) for Barrow. For a 50-year project life cycle, a project in Barrow could be exposed to sea level rise as much as $+2.31 \text{ ft}$ (Table 10) after construction, assuming construction in 2020.

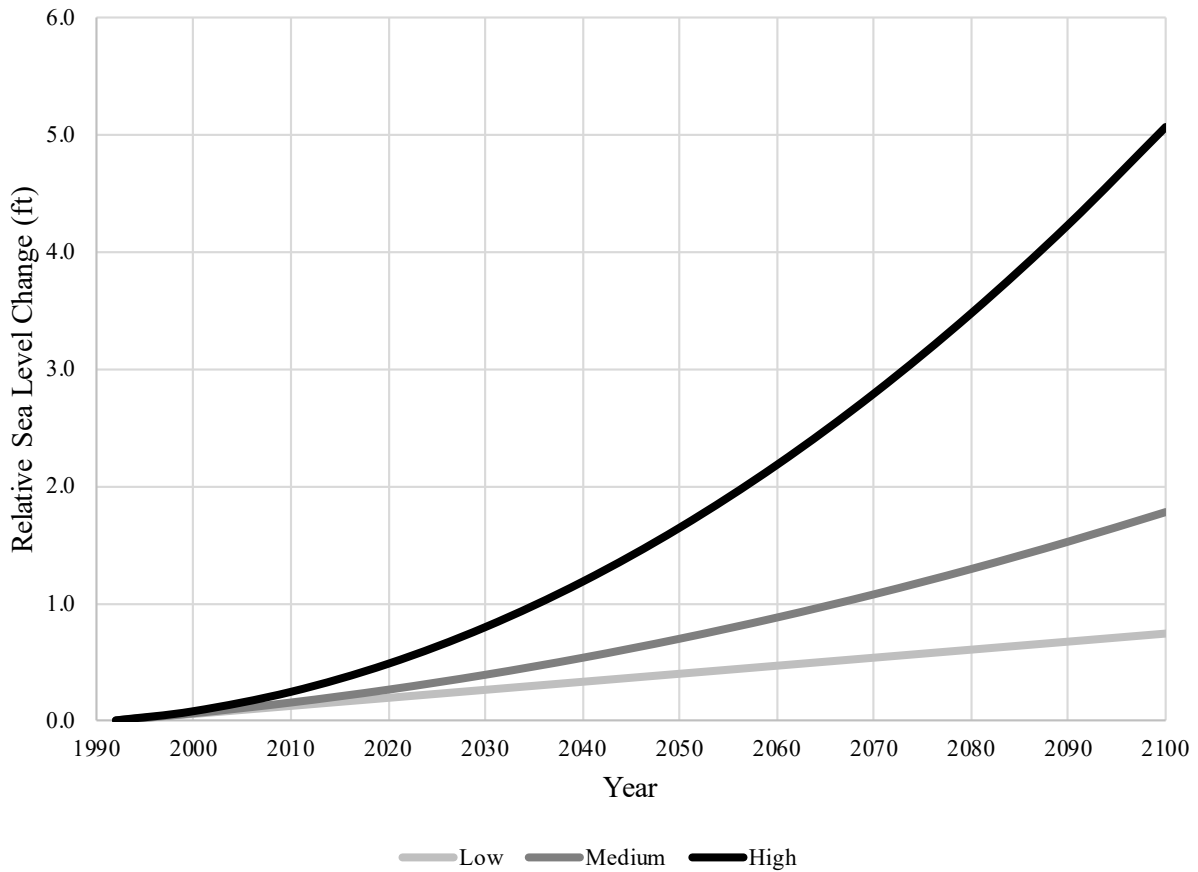


Figure 69. Relative Sea Level Change in Barrow, AK

Table 10. Relative Sea Level Change, in ft, Starting in 1992 for a 50-Year Project Life Cycle Plus 30 Years. Assuming Project Construction in 2020.

Year	Low [ft]	Int [ft]	High [ft]
2020	0.19	0.26	0.48
2030	0.26	0.39	0.80
2040	0.33	0.53	1.18
2050	0.40	0.70	1.65
2060	0.47	0.88	2.18
2070	0.54	1.08	2.79
2080	0.60	1.29	3.47
2090	0.67	1.53	4.23
2100	0.74	1.78	5.07

Though a RSLC analysis was evaluated, it was not included in the wind surge or run-up modeling, and was not taken into account when performing calculations for any of the alternatives proposed. See Section 10.5 (Structure Design) for a discussion on how RSLC would affect the project design, when included in the final design.

7. SEDIMENT TRANSPORT

The development and verification of the sediment transport models are detailed in an unpublished USACE CHL report Longshore Transport and Shoreline Change Modeling performed for the 2010 Technical Report (King, 2009).

7.1. Cross Shore Sediment Transport

Beach profile and shoreline data were obtained and a set of profile ranges were established, as shown in Figure 70. Profiles on most of these lines were obtained in 1987 and 2003. These profiles were the main ones used to analyze long-term shoreline change and as SBEACH input.

Cross shore sediment transport mechanisms were evaluated using the SBEACH program and examining changes in cross shore profiles. Sediment samples were collected for input into the SBEACH model. The D_{50} sediment grain size analyzed for eleven beach samples ranged from 0.3 to 20 mm with an average D_{50} of 3 mm. Model runs with SBEACH indicate that the beach sediments at Barrow generally do not move in the cross shore direction. The threshold sediment size for movement to occur is 0.8 mm, which results in minor changes below the water level only.

Pair wise comparisons of the 1987 and 2003 profiles agree with SBEACH and show the profiles to be remarkably similar in shape and position. The average profile horizontal change of the zero elevation (shoreline) over this 15-year interval is 13.5 ft of accretion, with individual profiles ranging between -62 and +87 ft. Profile 22 is shown as an example in Figure 71, and a blowup of the active portion of this range line is shown in Figure 72.

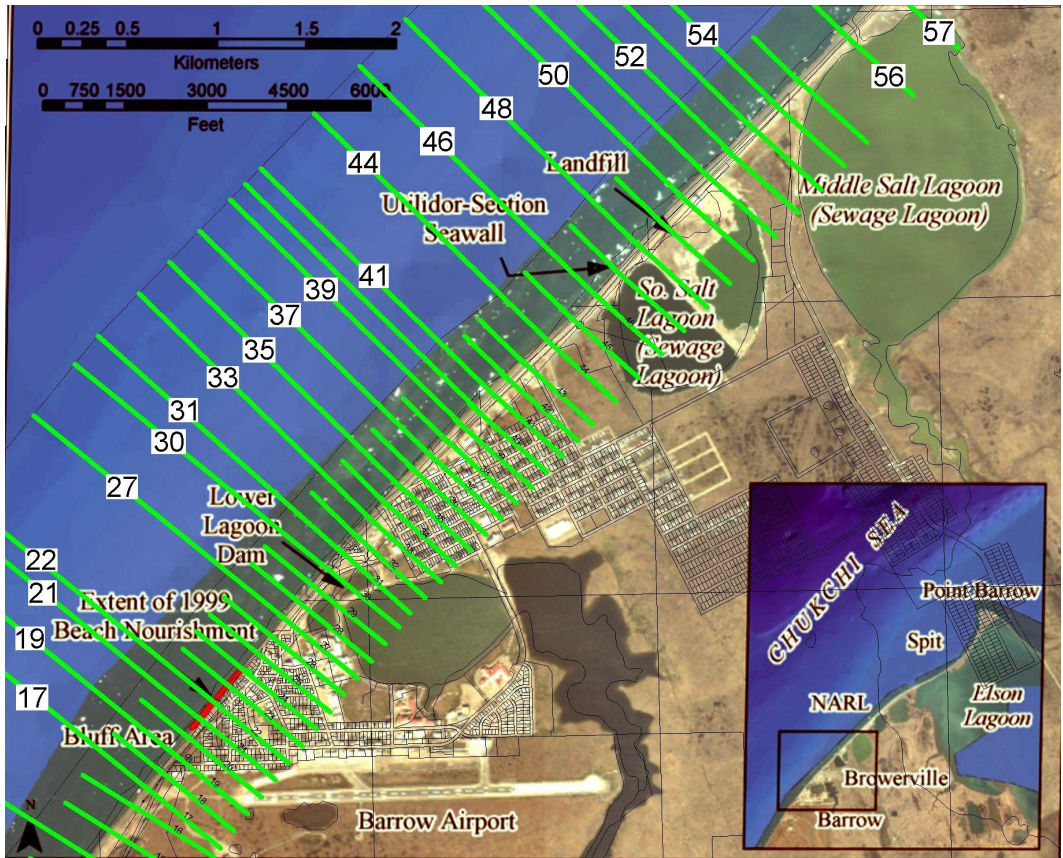


Figure 70. Transect Lines Along the Coast

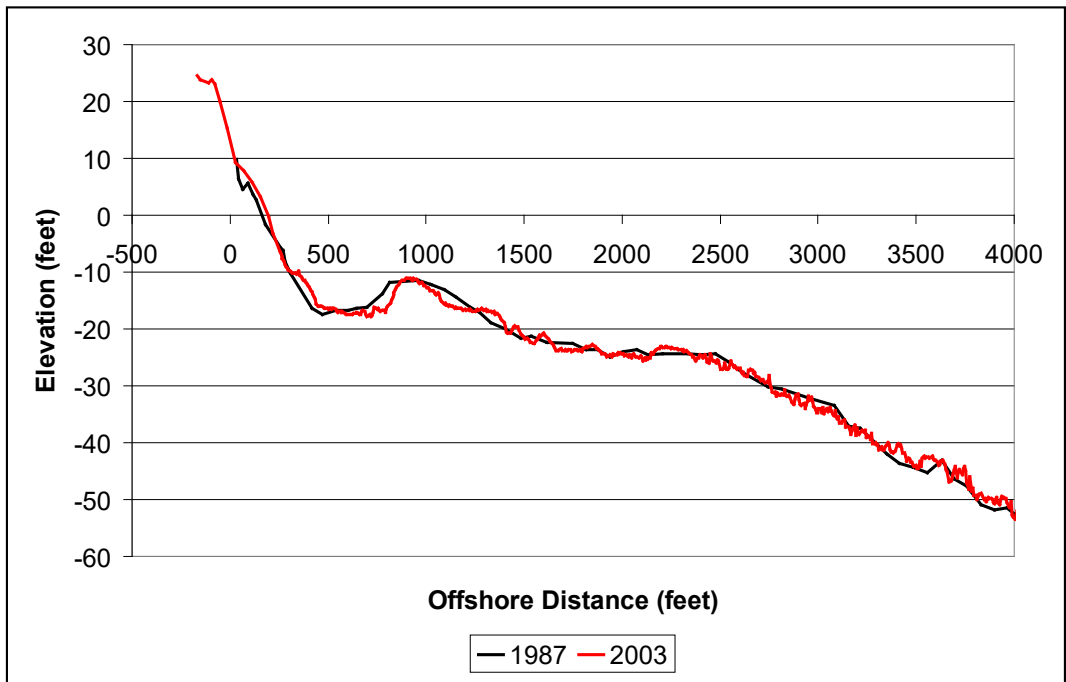


Figure 71. Comparison of 1987 and 2003 Profile-22

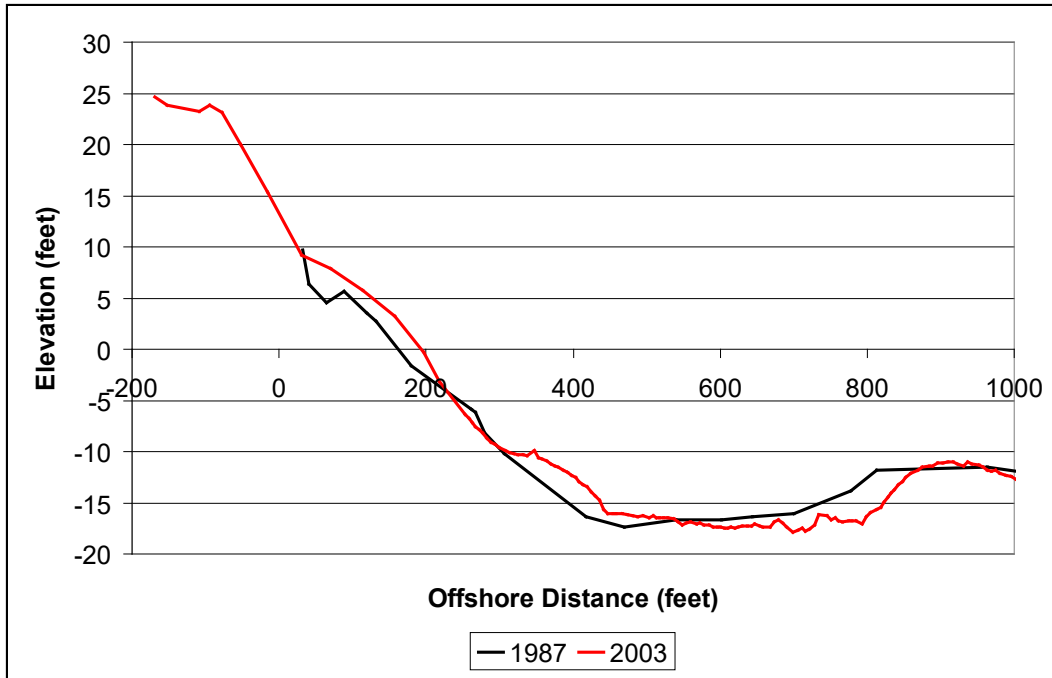


Figure 72. Blowup of Profile-22 Comparison Showing Active Portion of the Profile

7.2. Longshore Sediment Transport

Longshore sediment transport at the site was evaluated using the formula of Soulsby, one of the few which is considered valid for the coarse beach material found at Barrow. Hindcast data from station 49 were used as model input. The Soulsby formula yielded an average annual gross transport rate of 9,800 cubic yards per year and an average annual net transport rate of 7,300 cubic yards per year to the NE, towards Point Barrow. This estimate compares well with previous estimates made by researchers at the NARL of a net transport of 10,000 cubic yards per year.

Calculation of the longshore sediment transport rate using the CERC formula (United States Army Corps of Engineers, 2002) yielded much larger rates unless the value of the calibration coefficient, K , was reduced. Reducing the value by an order of magnitude to $K=0.05$ (all CERC formula calculations used significant wave heights) yielded results that compared very favorably with the Soulsby results, as shown in Figure 73 and Figure 74. Though this is a much smaller value of the CERC K coefficient that is normally used, it is appropriate, considering the grain sizes involved. For beach sediment median diameters in the range of 4 to 8 mm the most appropriate value for the CERC K term was 0.05.

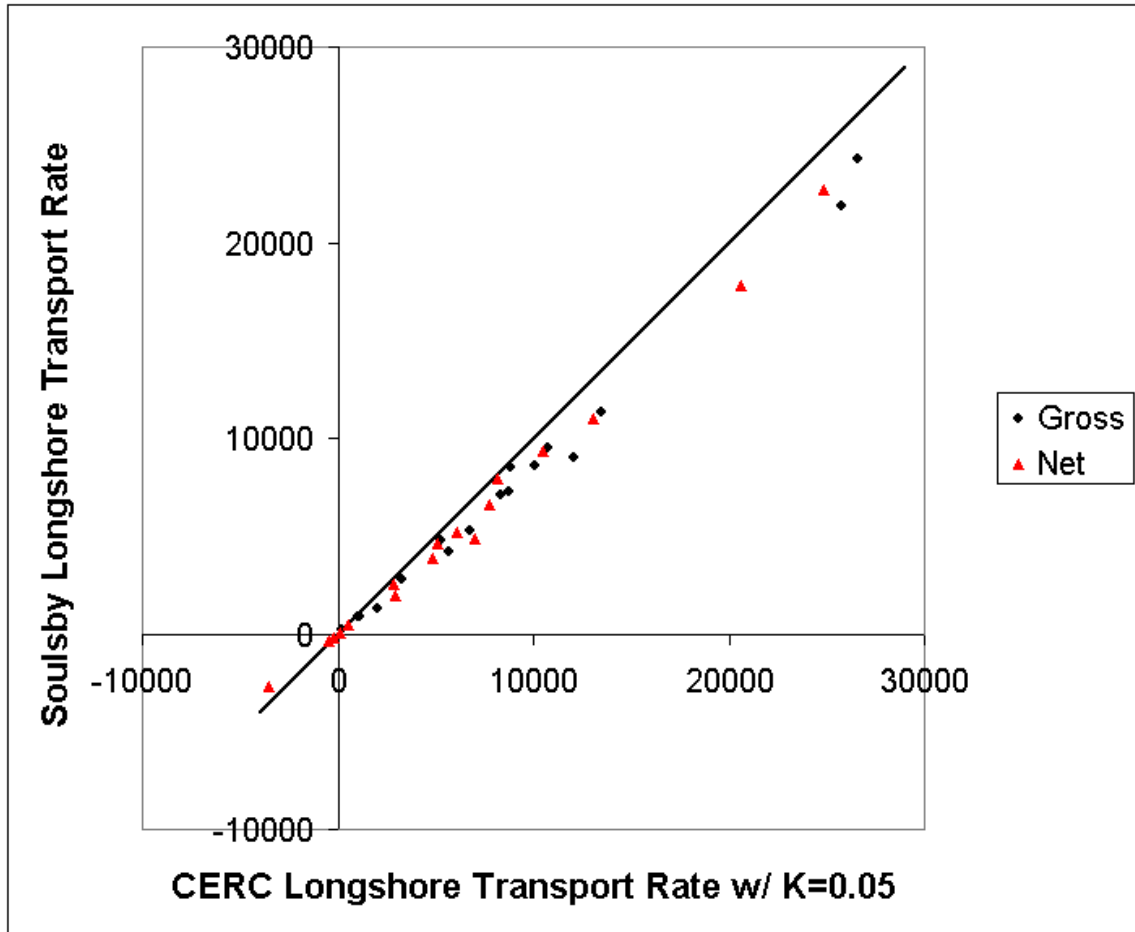


Figure 73. Comparison of Yearly Sediment Transport Rates (in yd^3/yr) between Soulsby and CERC Formulas

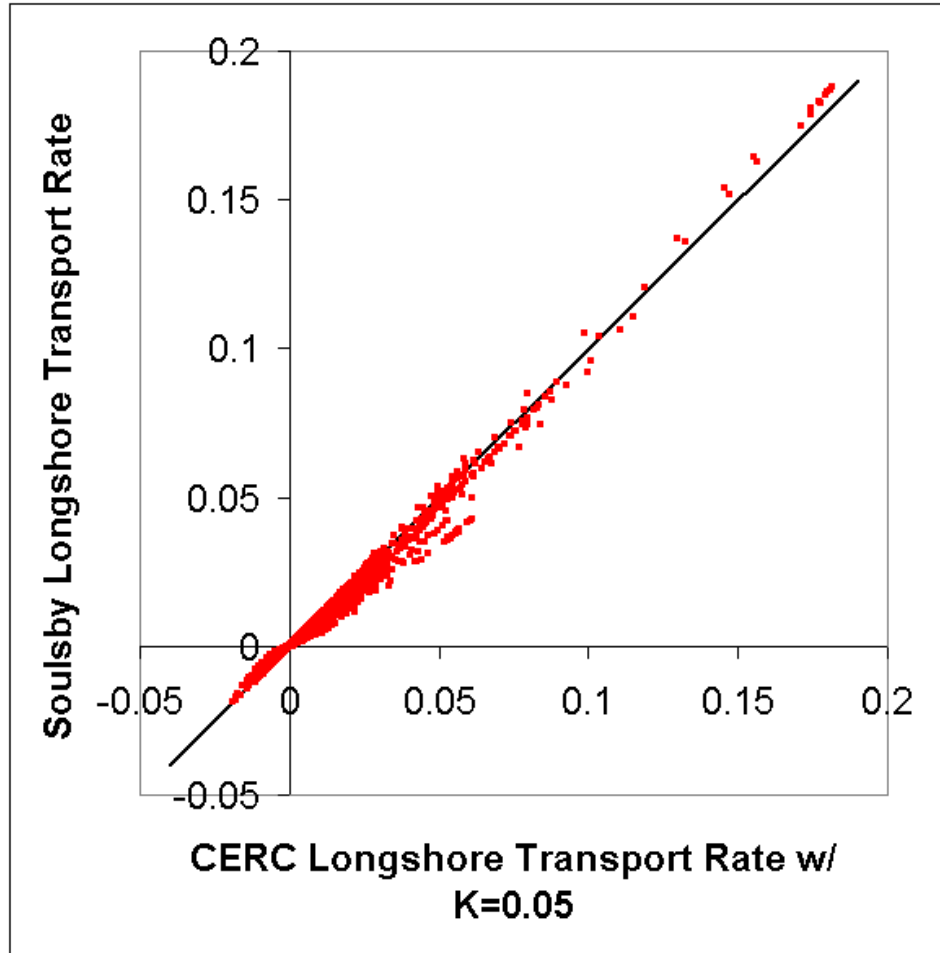


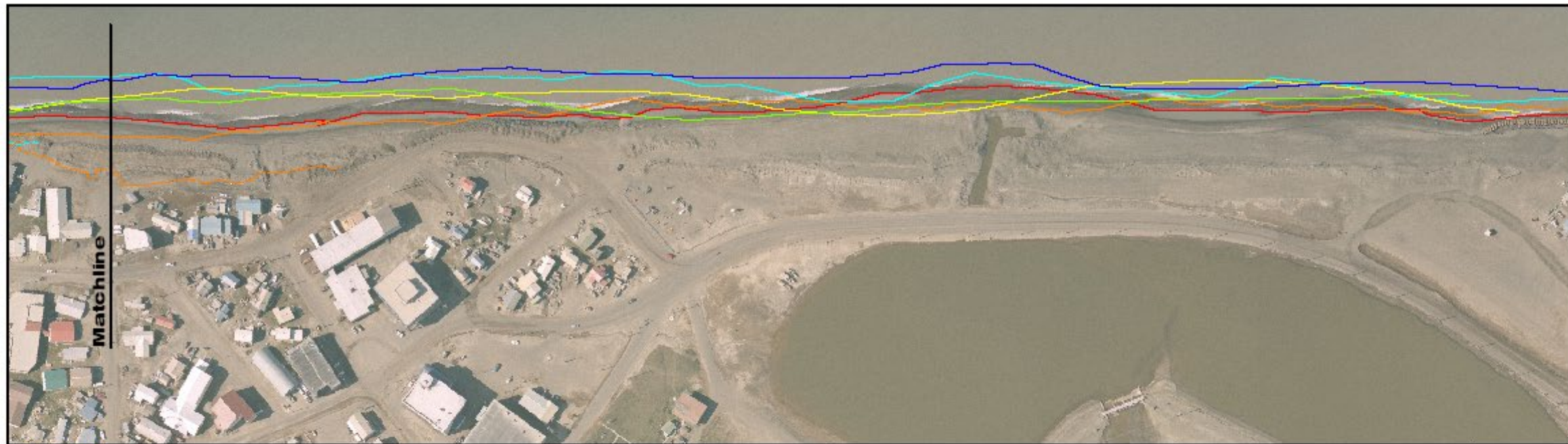
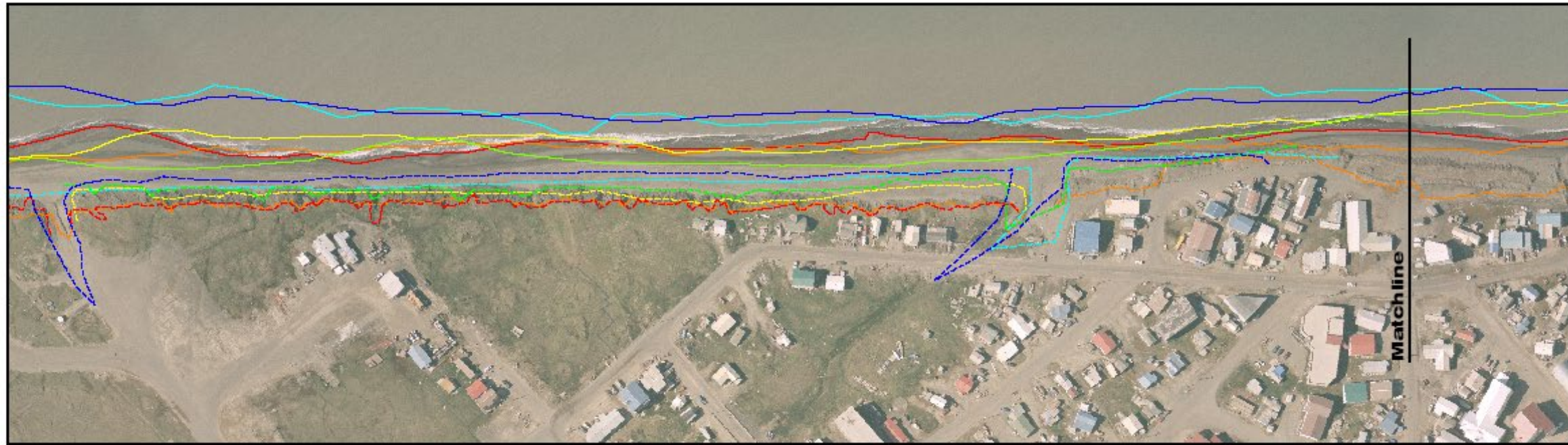
Figure 74. Comparison of Hourly Sediment Transport Rates (in yr^3/yr) between Soulsby and CERC Formulas

8. COASTAL EROSION

Analysis of aerial photography from 1948¹ to 2003 was performed by digitizing the shorelines and bluff lines. Location along the shore and bluff lines was identified by transect lines from a 1987 survey. The locations of the transect lines, with respect to the study area, are shown in Figure 70. An example of the digitized shore lines and bluff lines is shown in Figure 75. The location of the bluff line in 50 years based on that erosion rate is shown in Figure 76. Overall erosion rates based on the aerial photography analysis are listed in Table 11. ADCP observations (Figure 55) of directionally unfiltered wave data indicate that Barrow may experience wave periods longer than 10 sec, which more effectively erode the shoreline than smaller wave periods.

¹ The 1948 aerial photography was supplemented with the use of 1947 photography.

PAGE INTENTIONALLY LEFT BLANK



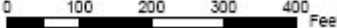
	Alaska District Corps of Engineers Civil Works Branch	Interpreted Shoreline:	 1948	 1955	 1974	 1984	 1997	 2003		
		Top of Bluff:	 1948	 1955	 1974	 1984	 1997	 2003		
				Image dated August 2003					Shoreline Study Barrow, Alaska	1

Figure 75. Example of Bluff and Shoreline Analysis

PAGE INTENTIONALLY LEFT BLANK

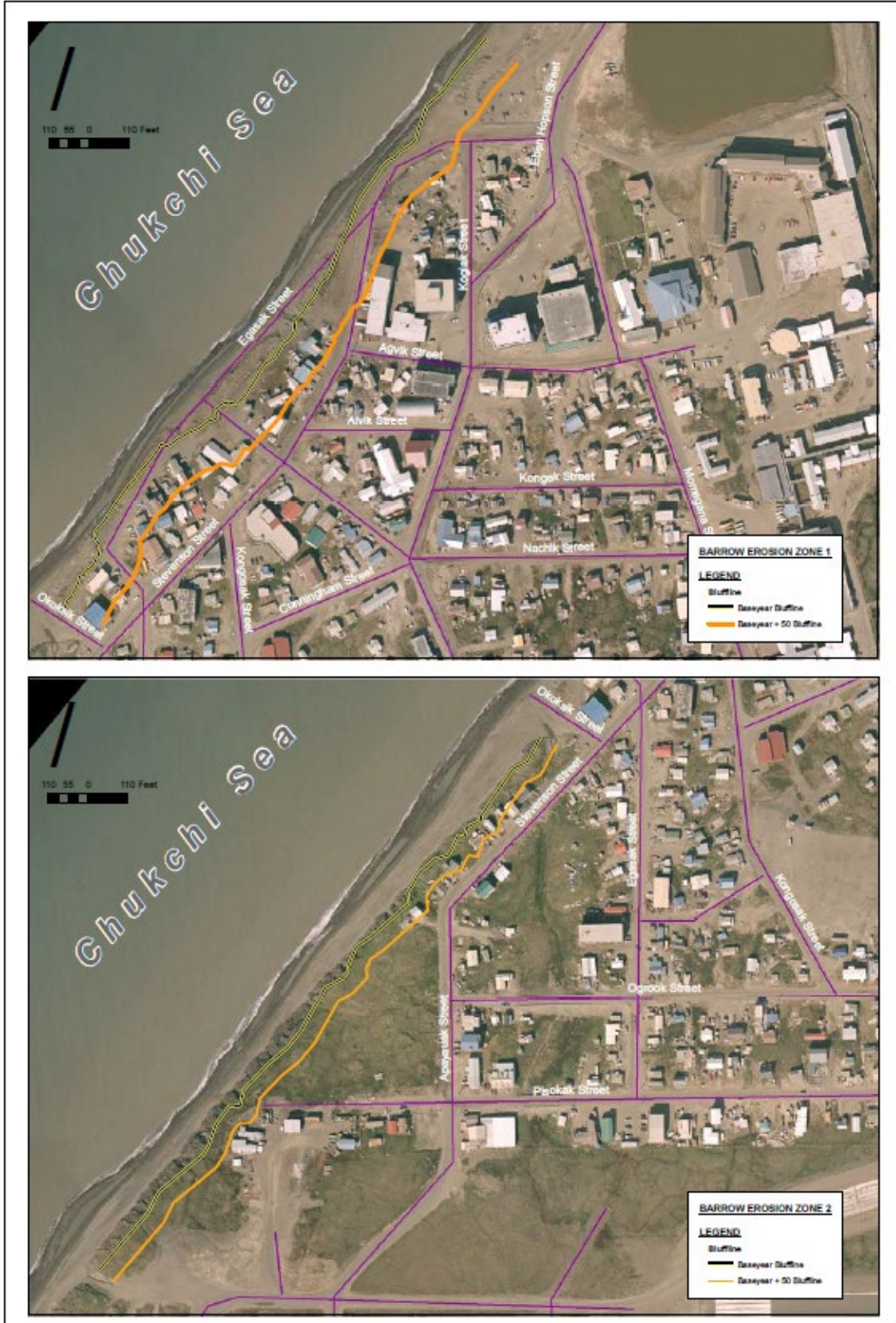


Figure 76. Location of Bluff Line in 50 Years

Table 11. Average Erosion/Accretion Rates. Analysis Based on 1943-2003 Aerial Photography.

Reach	Bluff¹ [ft/yr]	Shore³ [ft/yr]
South of Gravel Pit		-1.04
City of Barrow ²	-1.08	-1.05
Water Supply	NA	-0.72
Browerville	NA	+1.12
Landfill/Sewage Lagoon	NA	-0.61

¹ Bluff erosion was evaluated between Stations 18 and 21. Evaluation of stations south of Station 18 would be subject to interference from gravel pit activities. Aerial photography south of the gravel pit was difficult to interpret, so the bluff lines are questionable. Bluffs are not present beyond Station 21.

² Maximum bluff erosion rate is 1.5 ft/yr and maximum shoreline erosion rate is 1.93 ft/yr

Erosion noted by –
Accretion noted by +

³ Shoreline erosion rates are approximate as water elevation is highly susceptible to atmospheric effects

The coastal erosion is well documented with aerial photography. The differences in the shoreline movement were plotted in time increments to determine if the erosion along the coast is episodic or consistent through the years (Figure 77). Between 1948 and 1955 the plots indicate typical shoreline behavior with areas of erosion and accretion occurring. Between 1955 and 1974 there was a large amount of shoreline erosion that occurred along the entire study area. The 1974 and 1984 plot shows a predominance of accretion along the coast, and the 1984 and 1997 plot shows the shoreline beginning to return to a typical beach pattern with pockets of erosion and accretion.

A comparison of the overall time period of available aerial photography (1948 and 2003) indicates that there is predominance of erosion that has occurred along the coast. The areas that exhibit the greatest erosion appear to be consistent with the erosion that occurred in the 1955 to 1974 time period. The concentration of erosion during one time period indicates that the erosion that occurs along the coast is episodic, but due to the relatively small volume of sediment transport that typically occurs (Section 7.2 Longshore Sediment Transport), the beach is slow to recover when there is a large volume of material is moved or mined. This leaves the coast after the 1955 to 1974 time period with a narrow beach and the bluffs backing the beach in a precarious position of bearing the brunt of storm waves without the dissipative effects of a wide beach.

The years 1955-1974 cover the period when the highest storm water levels occurred and there were a number of major construction projects. The 1963 storm, discussed earlier in this report, is reported to have transported a large amount of beach and bluff material. Reports have put the net estimated amount of material transported during that storm as high as 200,000 cubic yards of material. In addition to the biggest storm event, this time period saw road, airport, and building construction requiring foundation material. To facilitate the construction associated with this development, there was a great deal of material borrowed from the beach.

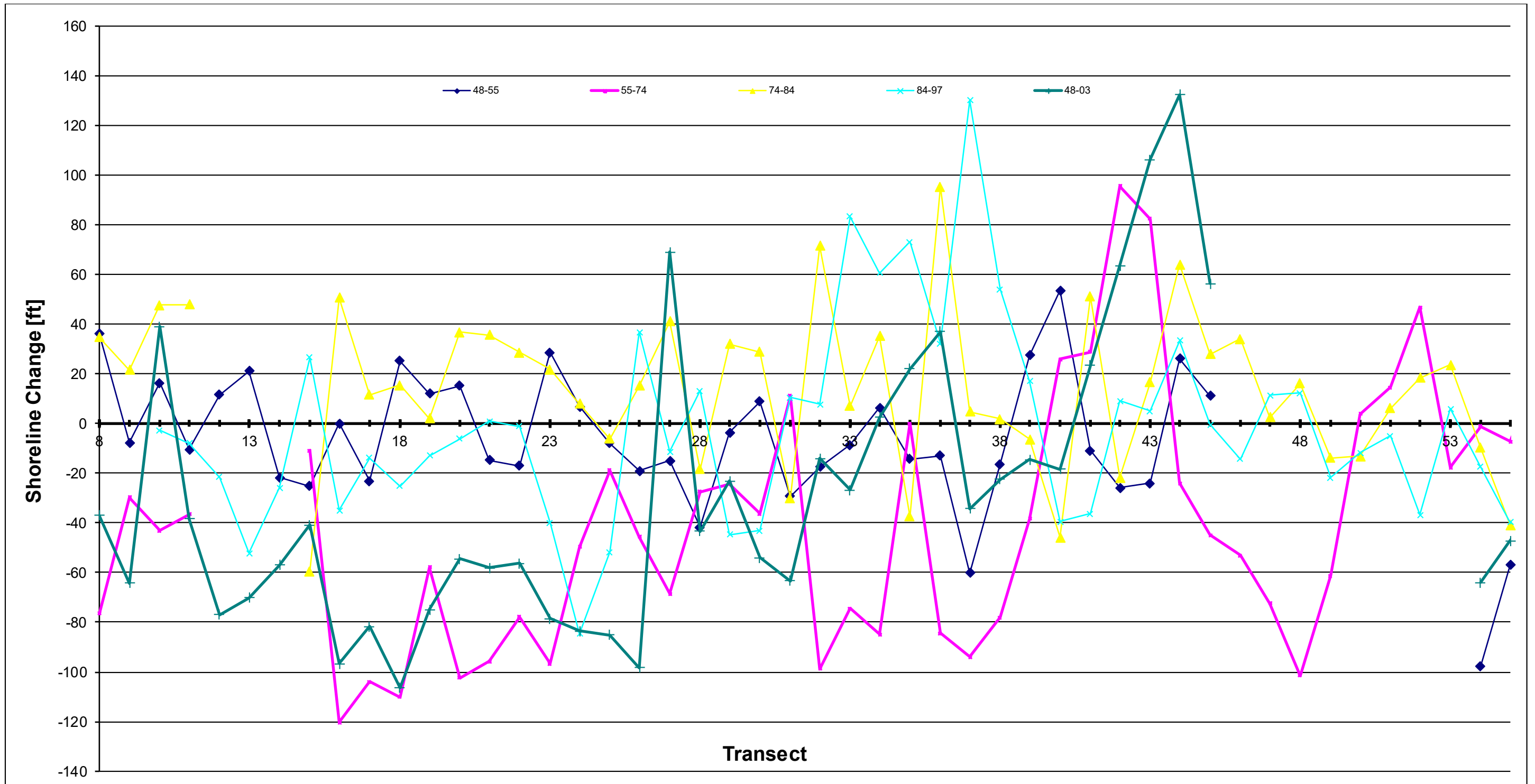


Figure 77. Shoreline Comparison

PAGE INTENTIONALLY LEFT BLANK

8.1. Shoreline Mining History

At the start of the Cold War, the United States government rapidly developed a large presence at Barrow. Part of the reason for this was to help give early warning to a ballistic missile attack from the Soviet Union. Along with a DEW line station, the NARL was established and a large, all weather, airplane runway was built. Barrow's permafrost soils were far from ideal for supporting large structures, so the beach was heavily mined to supply gravel for runway and building foundations. Figure 78 shows a dragline at the shoreline by the NARL. This borrow activity appears to have been limited to the NARL camp area although the effects of sediment removal would spread out along the beach.

Evidence of beach mining closer to Barrow was found in search of the NARL archives at the University of Alaska Fairbanks. A 1963 photograph shows trucks moving material along the beach in front of the City of Barrow and a haul road that leads to the new airport that is under construction (Figure 79 and Figure 80). In the same set of photos an oblique photo shows a scalloped coastline that looks as if it had been subject to borrowing activities (Figure 81). It was during this time period that the Wiley Post-Will Rogers Memorial Airport was built, the Samuel Simmonds Memorial Hospital was built. A comparison of aerial photographs from 1962 and 1964 shows the rapid growth that was experienced during that period (Figure 82 and Figure 83).

The head of the NARL, Dr. Max Brewer, estimated that, in all, the mining operation removed approximately 1.1 million cubic yards of material from the beach (Brigham, 1968). Also, for many years local residents took beach gravel for their use on personal property until this practice was banned, first by the Bureau of Indian Affairs, and later by the NSB (Lynch, et al., 2004).

It appears that the combination of mining of the beach for gravel and the occurrence of the largest storm on record resulted in an extreme retreat of the shoreline during the 1955-1974 period. The effects of that shoreline retreat are being experienced today through bluff erosion and flooding during storms.



Figure 78. Drag Line at NARL

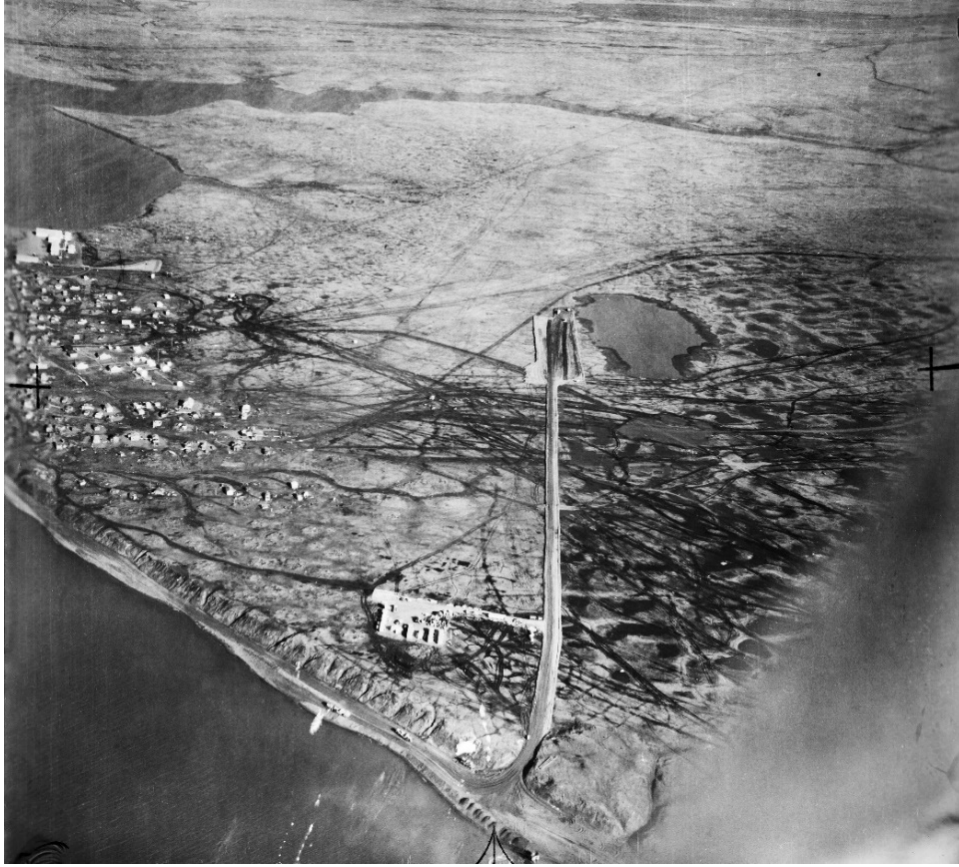


Figure 79. Haul Road from the Beach Leading to the Airport During Construction



Figure 80. Close up of Haul Road



Figure 81. Scalloped Shoreline Consistent with Beach Borrowing



Figure 82. 1962 Aerial Photography (National Snow and Ice Data Center photo)

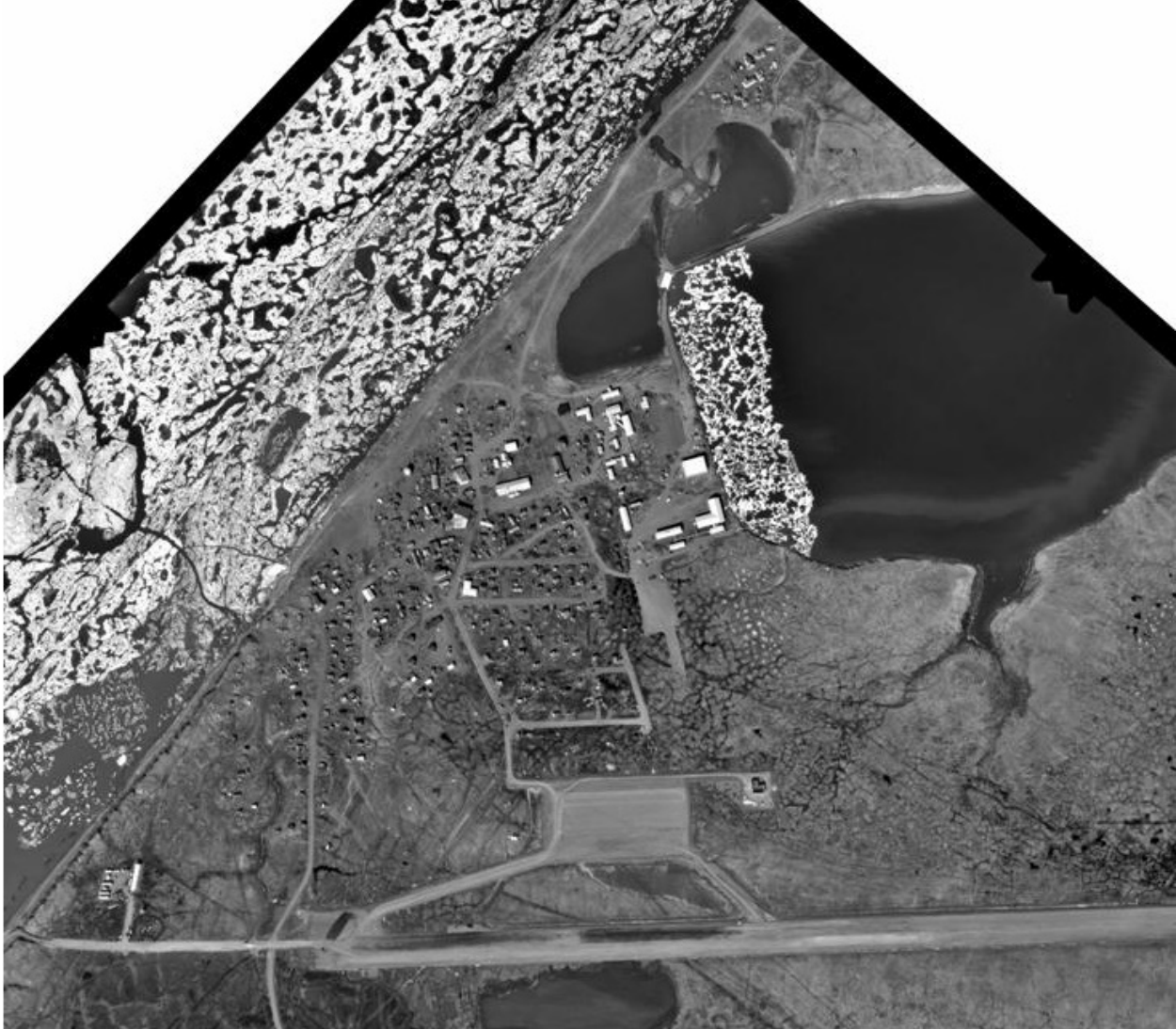


Figure 83. 1964 Aerial Photography (National Snow and Ice Data Center Photo)

Evaluation of the shoreline as a whole unit may be appropriate when looking at the entire north coast, but when evaluating the effects of erosion on a community, local erosion rates that would adversely affect the community need to be isolated and evaluated. Local “hot spots” where the shoreline continues to erode instead of experiencing the erosion/accretion cycle typical along a coast need to be evaluated. Locations that experience chronic erosion or erosional “hot spots” in the vicinity of Barrow were identified at transects 18-20, 23-27, and 29-30. Of these identified “hot spots”, the coast between transects 23 and 27 was identified as the most critical location because it covers the most shoreline, and fronts the most densely populated coast (Figure 84 and Figure 85). Evaluation of the historical coastline in this area shows a coast that has not stabilized from the initial material loss in the 1955-1974 time frame. Comparing the 1948 and 1955 beach shorelines, the beach appears to be relatively stable and since then, the beach and low lying bluffs/dunes have yet to reach equilibrium. Isolating the erosion along that section of coast for the years 1984 to 2003 shows a shoreline erosion rate of 2.2 ft per year. This is less than the erosion rate of 4 ft per year experienced between 1984 and 1997, but slightly higher than the

overall rate of 1.5 ft per year for the years 1948 to 2003 of rate. If allowed to erode unchecked at the lower rate of 2.2 ft per year and assuming the bluff/dunes will try to maintain the existing beach width, the structures along this section of coast would be impacted within the 50-year life span. The predicted beach line is shown in Figure 85. This “hot spot” section of coast is also the area of transition from a narrow beach backed by bluffs to a wide beach backed by tundra. The bluff/dune erosion is linked to the shoreline erosion because a wider beach would dissipate wave energy before it could impact the bluffs.

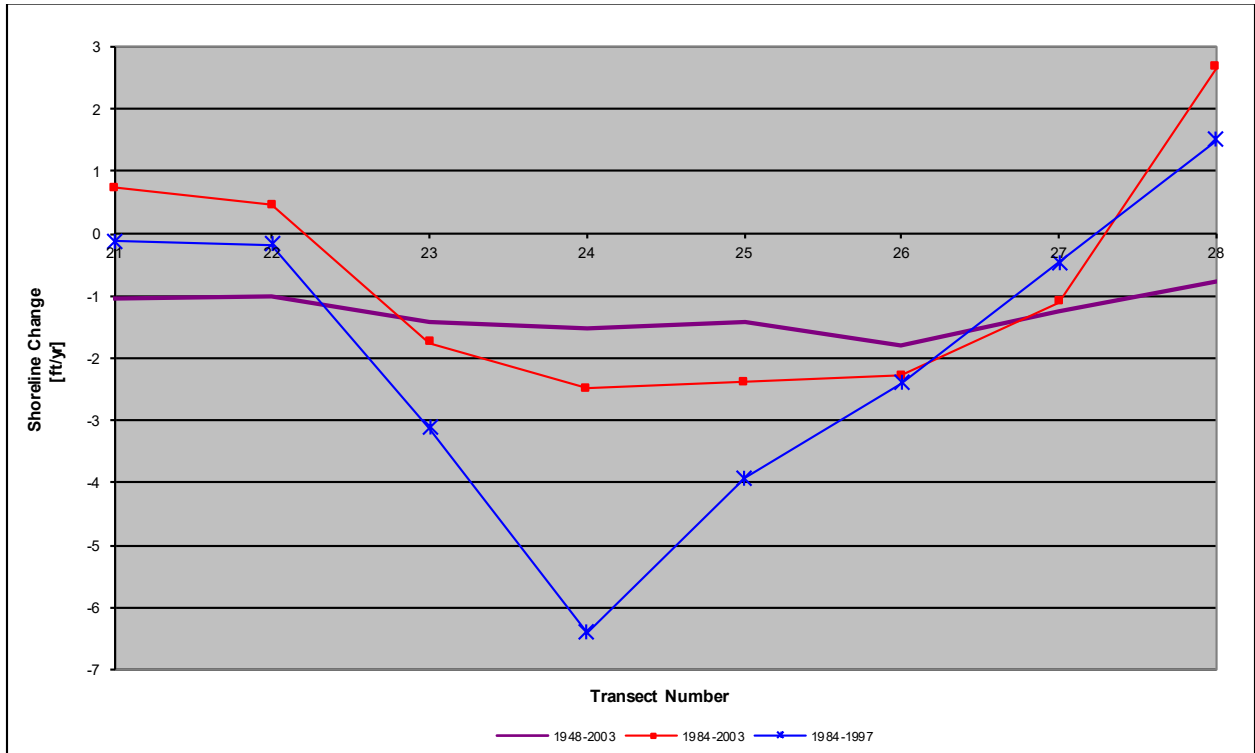


Figure 84. Plot of "Hot Spots:" Area of Persistent Erosion.

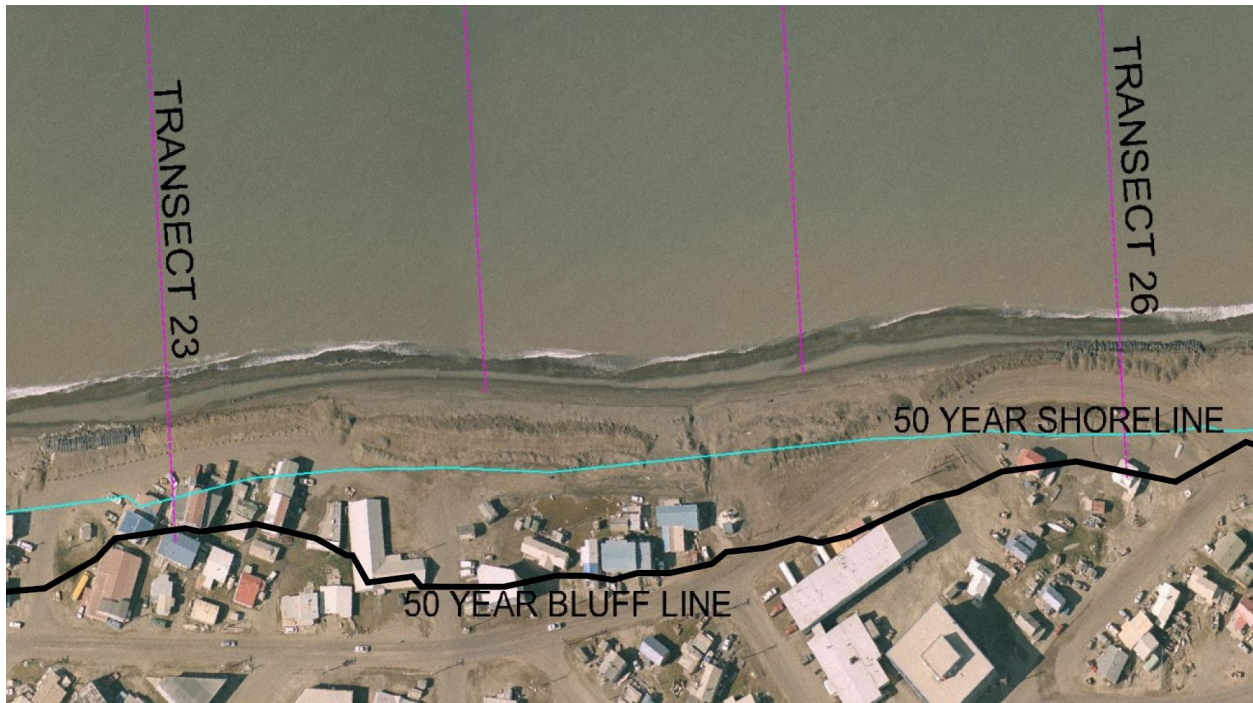


Figure 85. Aerial Photograph of "Hot Spots."

9. COASTAL FLOODING

Coastal flooding at Barrow results from wave run-up over the beach and into the upland areas. Flooding elevations were estimated with a modified version of the SBEACH model using a volume flux approach, as described below and detailed in an unpublished USACE CHL report, Longshore Transport and Shoreline Change Modeling, performed for the 2010 Technical Report (King, 2009). Fourteen damage reaches (Figure 86) were established and a representative profile was developed for each reach based on measured profile data from 1987 and 2003. The profiles on which the storms were simulated in SBEACH are provided in Figure 87 through Figure 90. (Note: The variation in berm crest between the various profiles, which influences the volume of water washed over the crest. Because the coastal flooding results from wave run-up, it is topographically controlled.) Storm data from the wave (WAM/STWAVE) and wind surge (ADCIRC) hindcasts for 28 historical events, described previously, were used as input. Twelve water level curves were generated for each storm, taking the ADCIRC predicted values and combining with three barometric and four tide curves, giving a total of 336 historically based plausible storms, which when combined with the 14 profiles resulted in 4,704 SBEACH simulations.

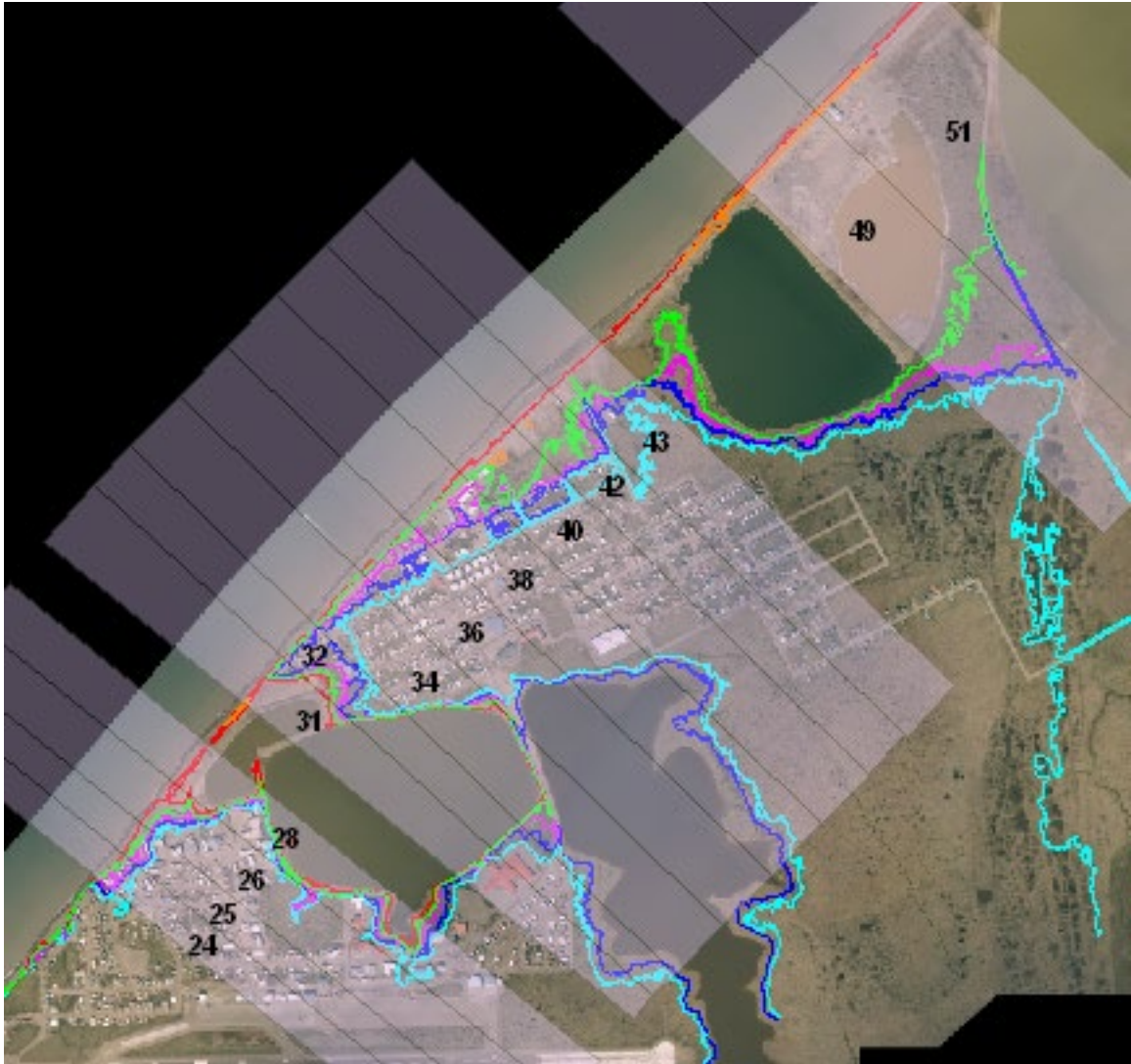


Figure 86. Study Area with Reaches 24-51 Shown. Elevation Contours (Red = 8ft, Green/Orange = 10ft, Pink = 12 ft, Blue = 14 ft, Cyan = 16ft)

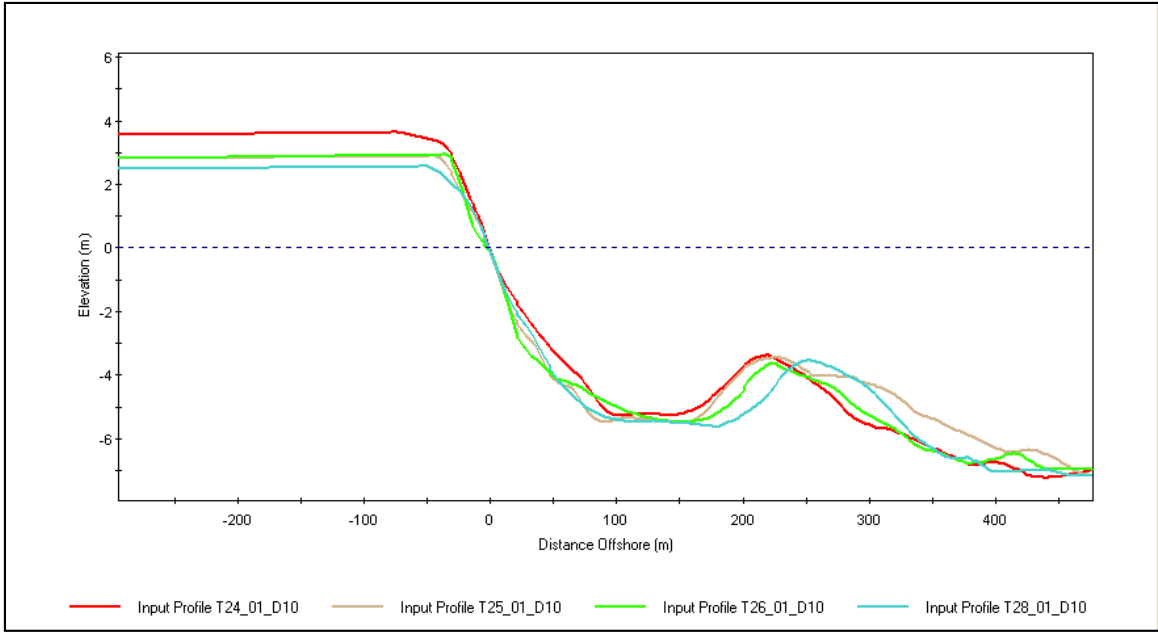


Figure 87. Beach Profiles for Reaches 24, 25, 26, and 28

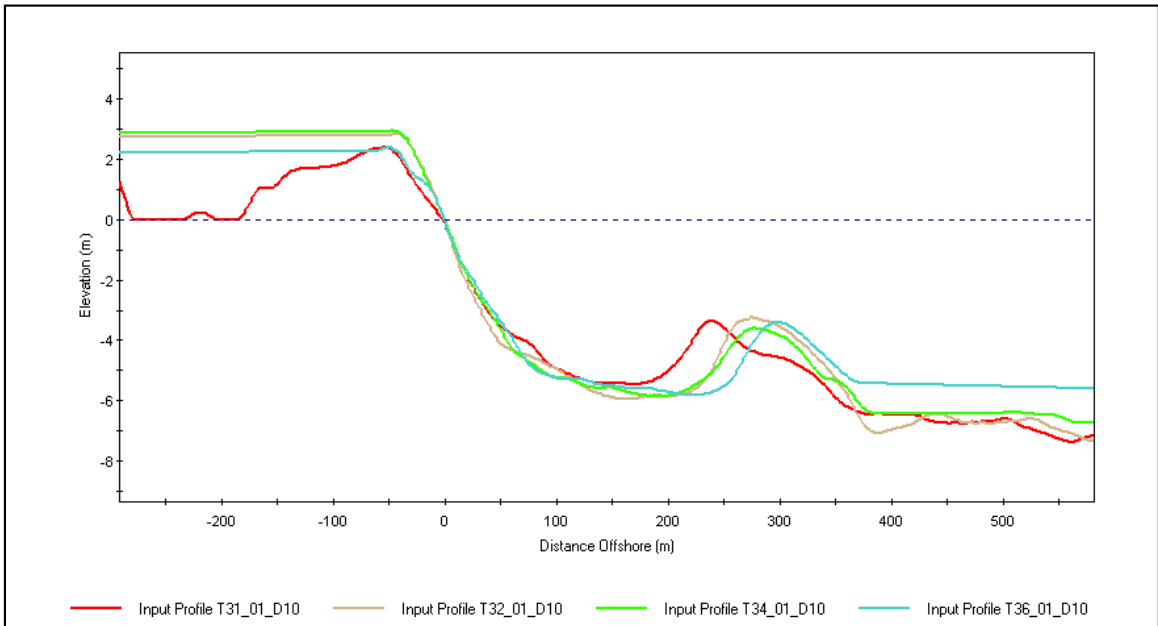


Figure 88. Beach Profiles for Reaches 31, 32, 34, and 36

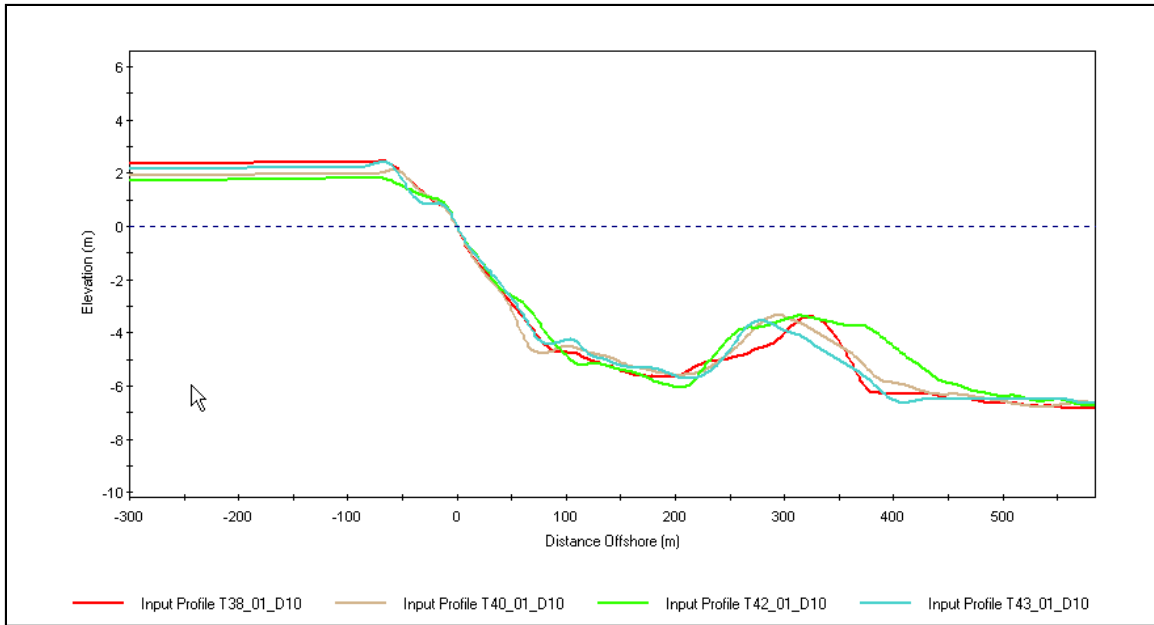


Figure 89. Beach Profiles for Reaches 38, 40, 42, and 43

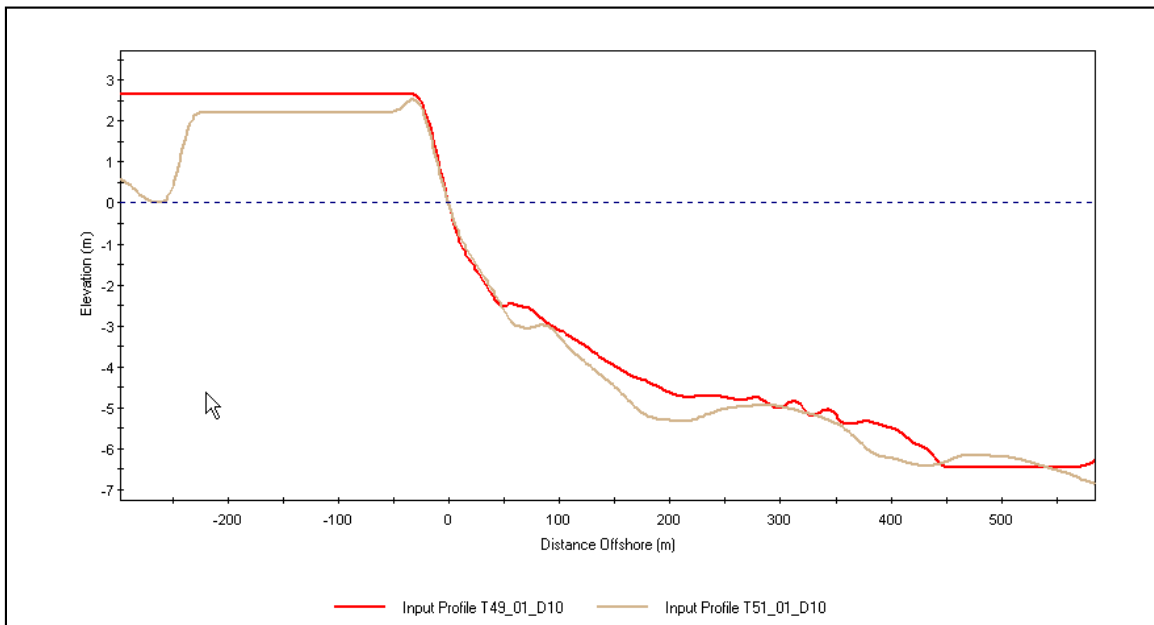


Figure 90. Beach Profiles for Reaches 49 and 51

SBEACH does not model wave run-up on complex upland areas. To estimate the run-up flooding, a modified version of SBEACH was applied to estimate the volume of water that is pumped past the berm/dune crest for each storm simulation. Estimates of volumes of water overtopping the crest were calculated using time histories of profile and hydrodynamic output from SBEACH. The modified SBEACH considers three mechanisms of flooding: (1) profile overwash, (2) profile inundation and (3) wave propagation. Profile overwash is defined here as water overtopping the dune due to calculated wave run-up that exceeds the dune crest. For the

case of overwash, the total water level (tide + wind surge + wave setup) remains below the dune crest elevation, but wave run-up exceeds the dune crest. Profile inundation occurs when the total water level exceeds the dune crest. Wave propagation occurs during profile inundation and accounts for the volume of water transmitted across the barrier island through volume flux produced by breaking waves. At Barrow, the tide + wind surge + wave setup never exceeds the berm/dune crest so only profile overwash is invoked.

The method for estimating volume of water due to overwash was formulated based on the sediment transport overwash algorithm included in SBEACH. First, the depth of the overwash bore at the dune crest was estimated by linearly interpolating between the depth of water at the surf zone/foreshore boundary in SBEACH and a depth of zero at the maximum extent of run-up calculated by the model. With this approach, the bore depth at the dune crest is zero when the maximum run-up elevation is less than or equal to the dune crest, and increases as the calculated run-up elevation exceeds the dune crest elevation.

As a first approximation, overtopping volume due to overwash was estimated according to the broad-crested weir formula:

$$q = g^{1/2} \left(\frac{2}{3} h_{bore} \right)^{3/2} \quad \text{Equation 5}$$

where q is flow rate per unit width, g is acceleration of gravity and h_{bore} is the depth of the bore at the dune crest. This approach has some limitations. For example, the weir formula assumes steady state conditions, whereas wave run-up is periodic. However, because rms run-up is employed in the model as an estimate the time-averaged run-up condition from which bore depths are computed, the steady state approximation given by Equation 5 is reasonable.

Applying Equation 5, the total volume of water overtopping each reach was estimated for each storm. The total volume of flow for each representative profile represents the volume calculated over the duration of each storm. The volume for each reach is based on a single representative profile for that reach, which can result in unrealistic discontinuities in overtopping volumes. To account for the alongshore variation across a reach and blend the volume fluxes in the longshore direction, a three-point smoothing was applied. The total volume for a given transect was calculated based on the volume calculated by SBEACH for that reach and the two adjacent SBEACH profiles according to the following formulation:

$$V_y' = (V_{x-1} + 2V_x + V_{x+1})/4 \quad \text{Equation 6}$$

where V_x' is the smoothed overtopping volume for profile x , V_{x-1} is the SBEACH calculated overtopping volume for the profile immediately to the south of x , V_x is the SBEACH calculated overtopping volume at profile x , and V_{x+1} is the SBEACH calculated overtopping volume for the profile immediately to the north of x . Figure 91 shows an example of the calculated and smoothed volume fluxes for the 1986 storm.

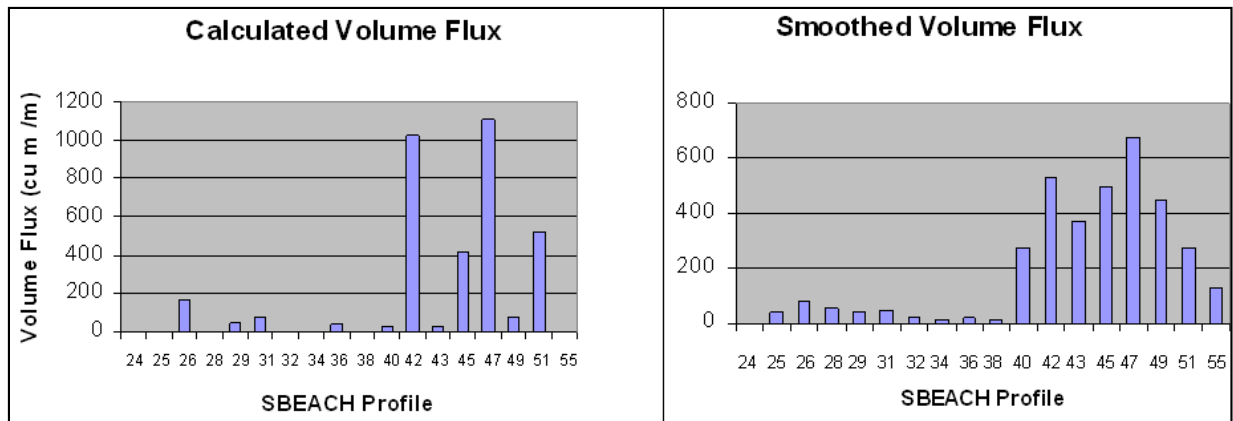


Figure 91. Volume Fluxes for September 19, 1986 Storm

The volume computed by Equation 6 is used to calculate the total volume of water that overtops the berm crest at each reach. From this volume flux, flooding elevations are calculated based upon the topography landward of the berm crest. Topographic data was analyzed within GIS to compute the storage capacity between upland contours, based on the area between those contours. The analysis assumes that the water pumped above the berm crest by wave action does not have time to drain due to irregularities in the upland profile (i.e. low areas and gullies) and the continuous overflow of water during the peak of the storms. A step function was developed for each reach, which utilized topographic characteristics and storage capacity calculations for each reach, to compute the flooding elevation. Flooding elevations were capped at 0.25 ft above the highest contour in the reach.

The calculated flood exceedance probabilities are presented in Table 12. The table presents the probability that the flooding level will exceed a given level for each reach. Stage-frequency curves were developed with the statistical Empirical Simulation Technique (EST) model. The EST assumes that past storm frequency and intensity is an accurate predictor of future storm activity. The last decade has seen an increase in storm activity, along with more ice-free days each year and the permanent ice pack being further offshore. This adds an additional level of uncertainty to the EST results and consideration of global climate change could result in more frequent flooding predictions. Because the run-up flooding is topographically controlled, the stage-frequency curve is reach-dependent. Separate curves were generated for each reach and are given in Figure 92 through Figure 105. The EST extrapolates from input data and can therefore produce results that are physically unrealistic at the upper end of the curve. Therefore, the EST results have been capped at the upper end to reflect physical constraints introduced by the topography of each reach. The bottom of each curve coincides with the beach berm crest and no flooding occurs below this level. So, on reach 24, for example, flooding is not expected to occur for storms with a return period below approximately 20 years.

Table 12. Flood Exceedance Probabilities

Reach	Berm Elev [ft]	>7ft	>8ft	>9ft	>10ft	>11ft	>12ft	>13ft	>14ft	>15ft	>16ft
24	11.99475						0.0357	0.0022			
25	9.547244				0.1741	0.0893	0.0513	0.0179	0.0067		
26	9.616142				0.1741	0.0982	0.067	0.0513	0.0223	0.0089	0.0067
28	8.458005			0.0826	0.0089						
31	7.877297		0.0938	0.0938	0.0714	0.0647	0.0625	0.0603	0.0402		
32	9.284777				0.0938	0.0714	0.0625	0.0536	0.0179		
34	9.744094				0.0558	0.0179	0.0067				
36	7.903543		0.0558	0.0558	0.0402	0.0179	0.0156				
38	8.136483			0.0558	0.0201	0.0112					
40	6.961942	0.0446	0.0313	0.0268	0.0246	0.0156	0.0089	0.0067	0.0022		
42	6.036745	0.0313	0.0268	0.0268	0.0246	0.0201	0.0134	0.0112	0.0089	0.0067	0.0045
43	7.96916		0.1607	0.0848	0.0491	0.0268	0.0246	0.0179	0.0179	0.0045	
49	8.704068			0.2946	0.0938	0.0357					
51	8.287402			0.096	0.0268						

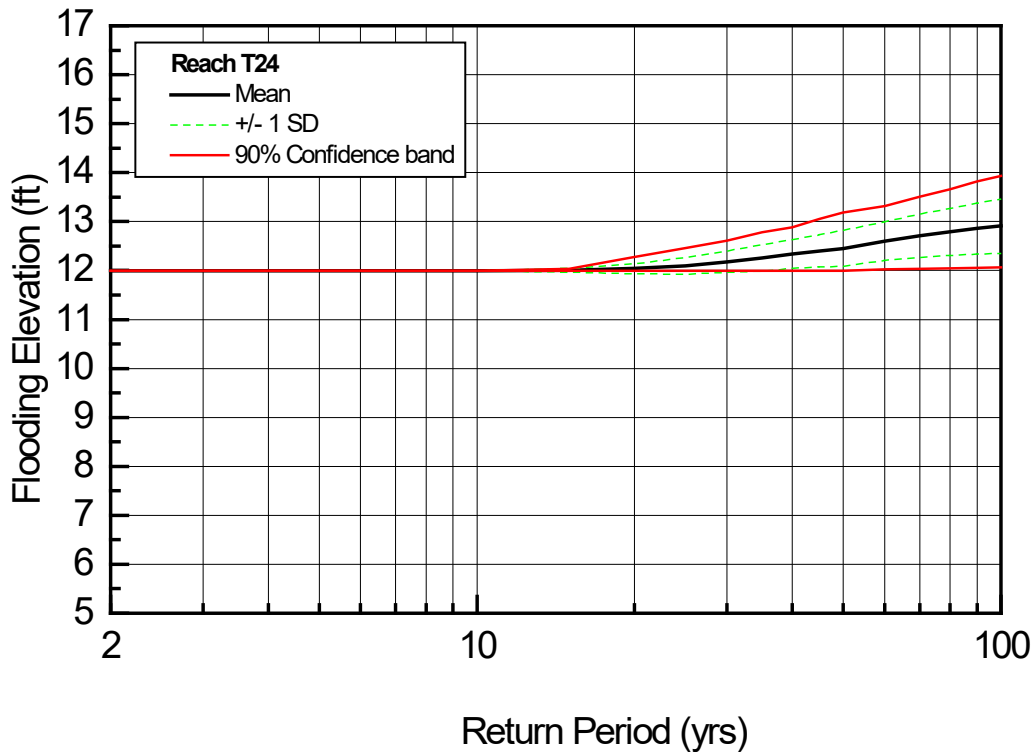


Figure 92. Stage-Frequency Curve for Damage Reach 24

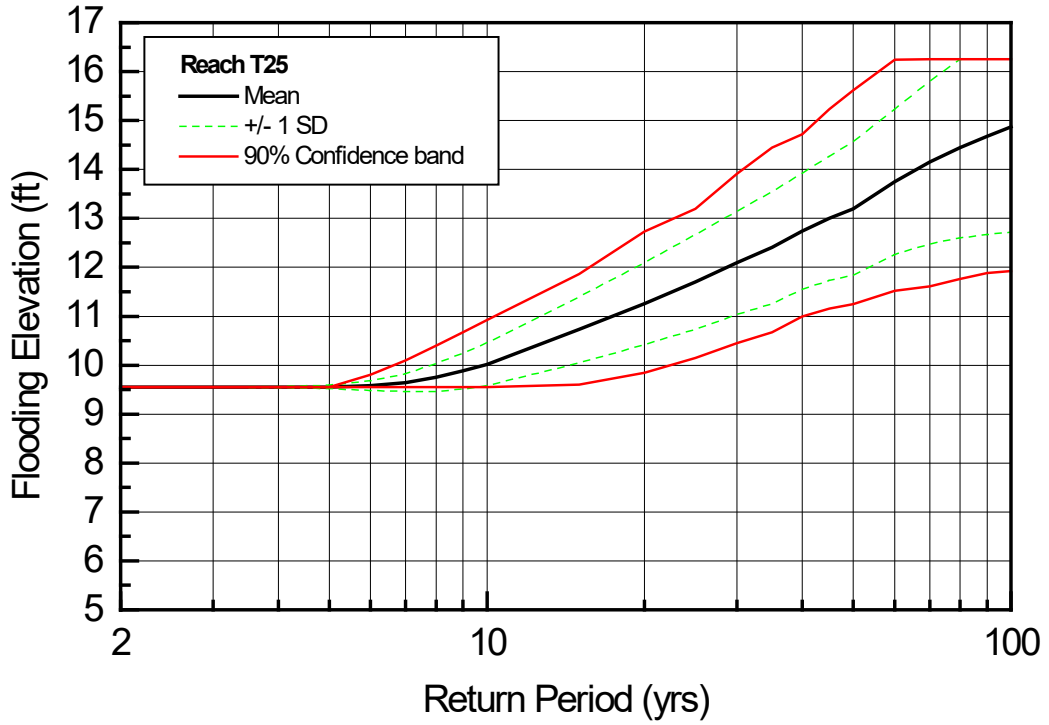


Figure 93. Stage-Frequency Curve for Damage Reach 25

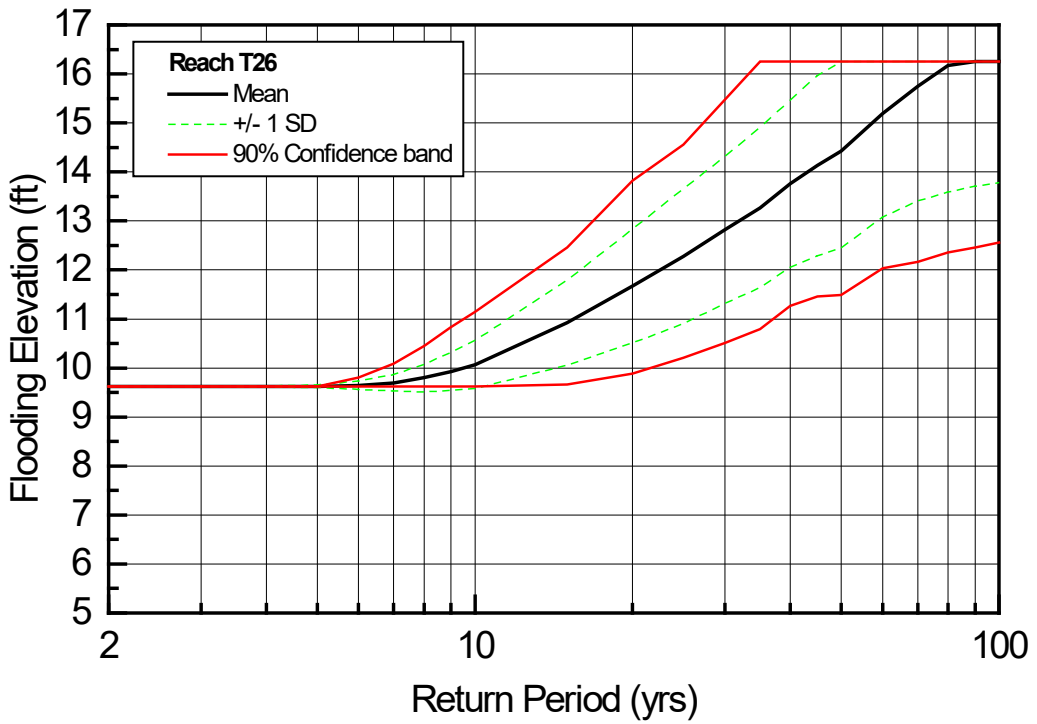


Figure 94. Stage-Frequency Curve for Damage Reach 26

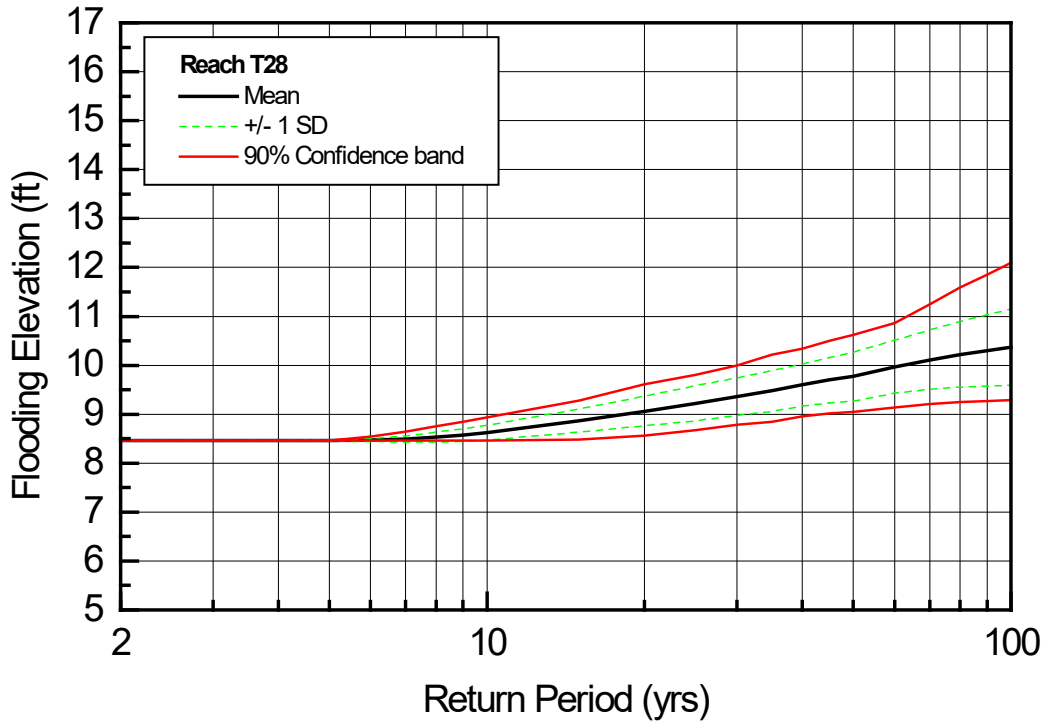


Figure 95. Stage-Frequency Curve for Damage Reach 28

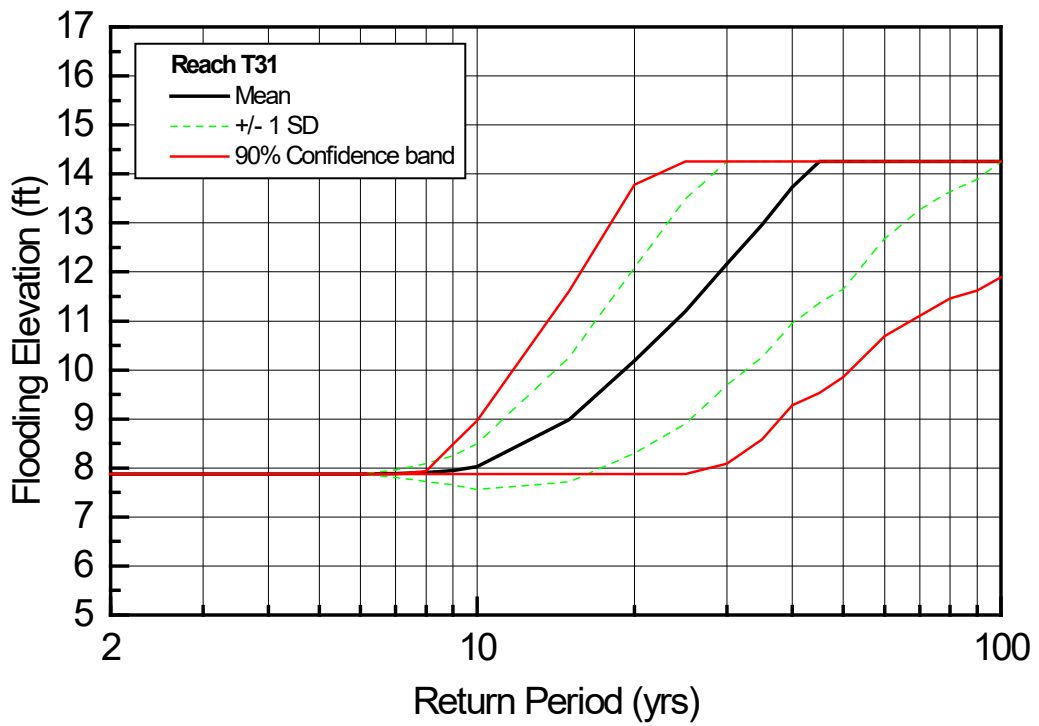


Figure 96. Stage-Frequency Curve for Damage Reach 31

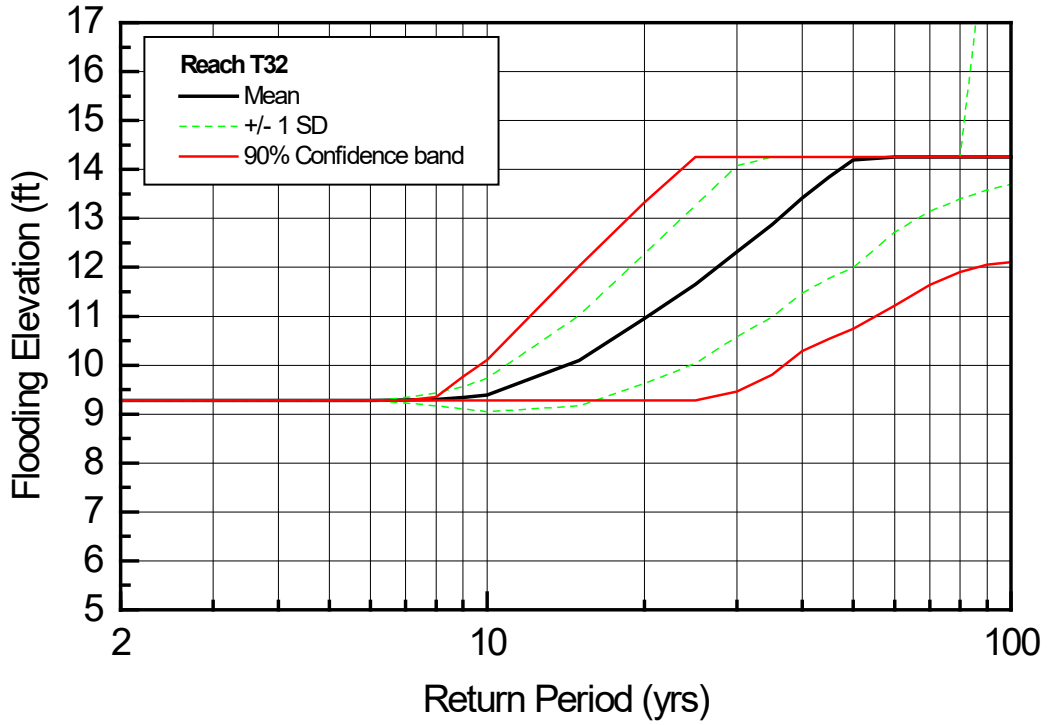


Figure 97. Stage-Frequency Curve for Damage Reach 32

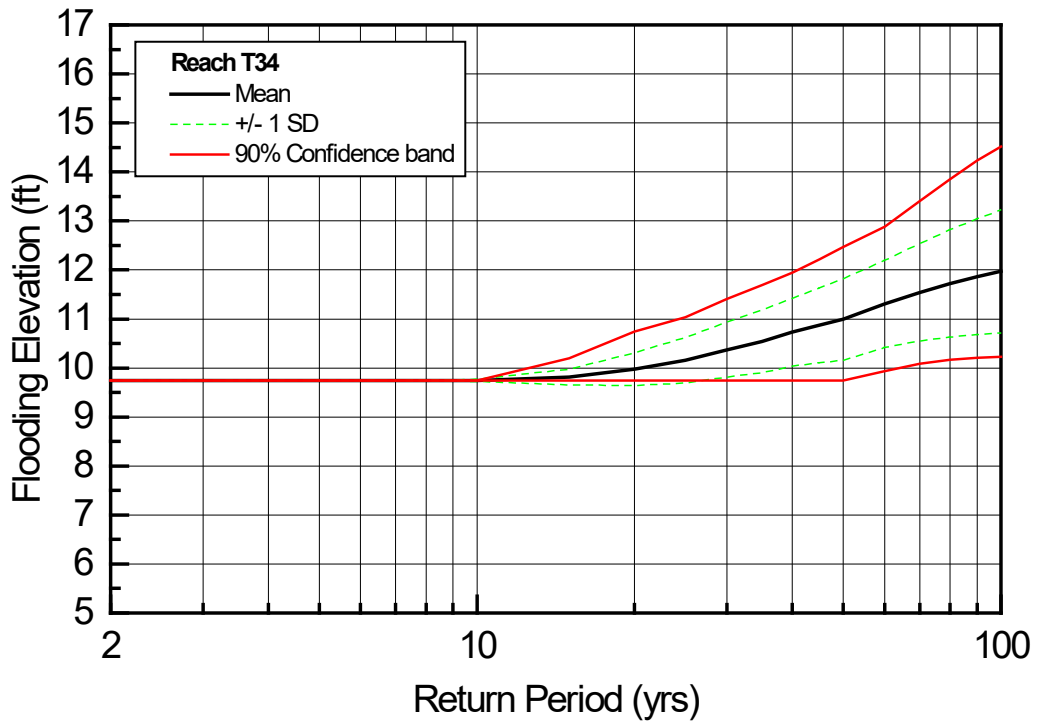


Figure 98. Stage-Frequency Curve for Damage Reach 34

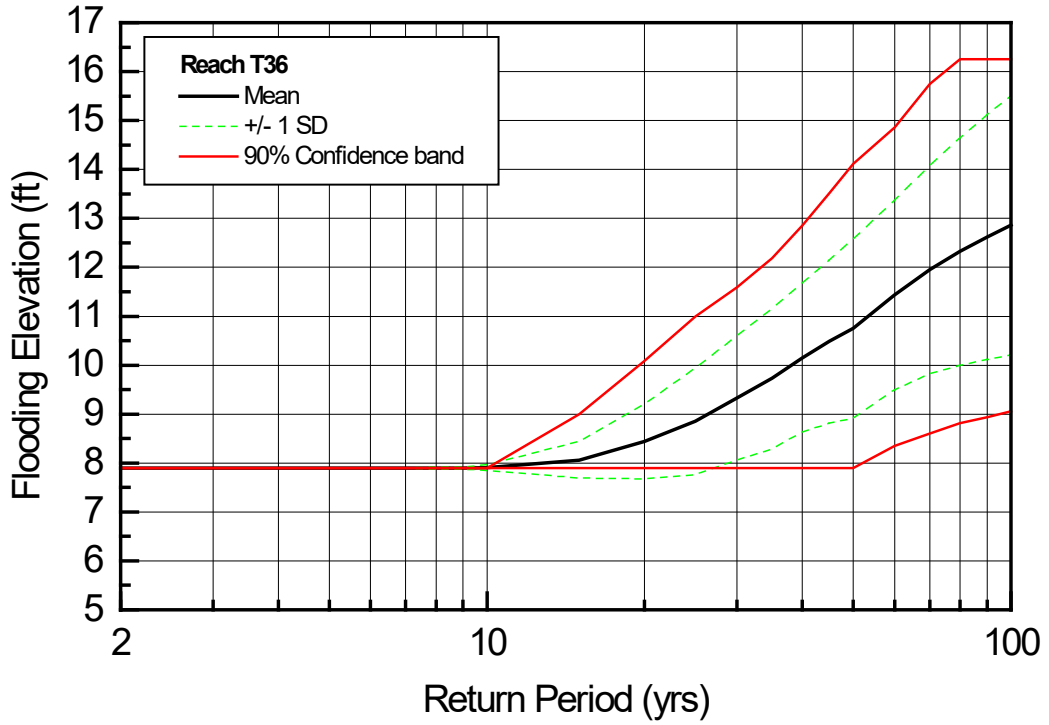


Figure 99. Stage-Frequency Curve for Damage Reach 36

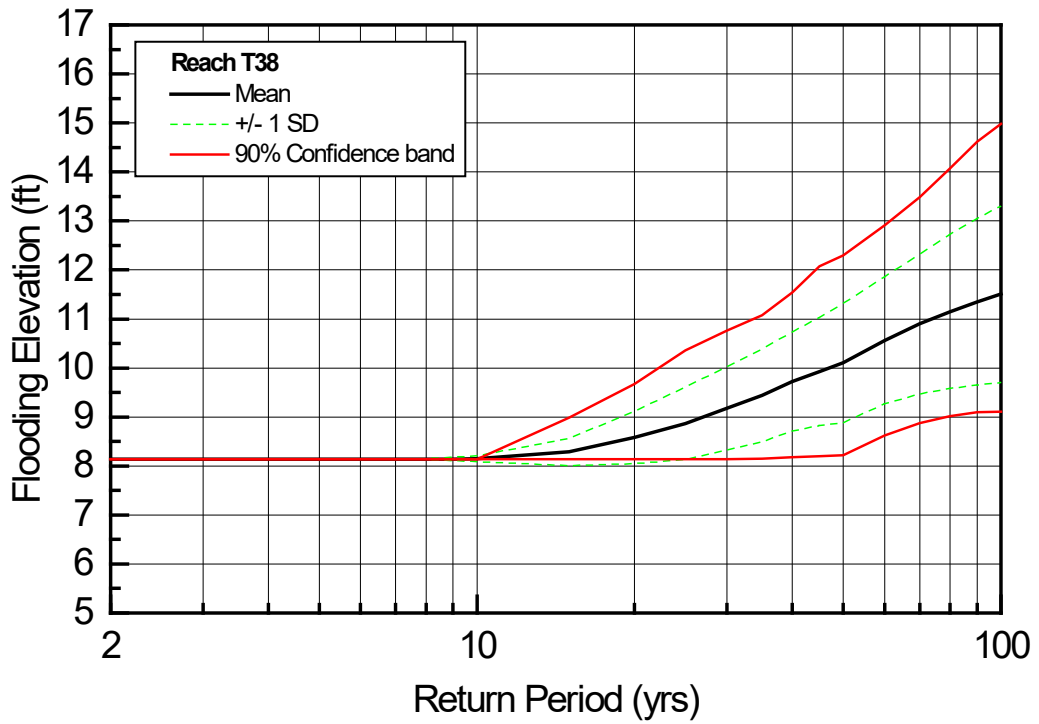


Figure 100. Stage-Frequency Curve for Damage Reach 38

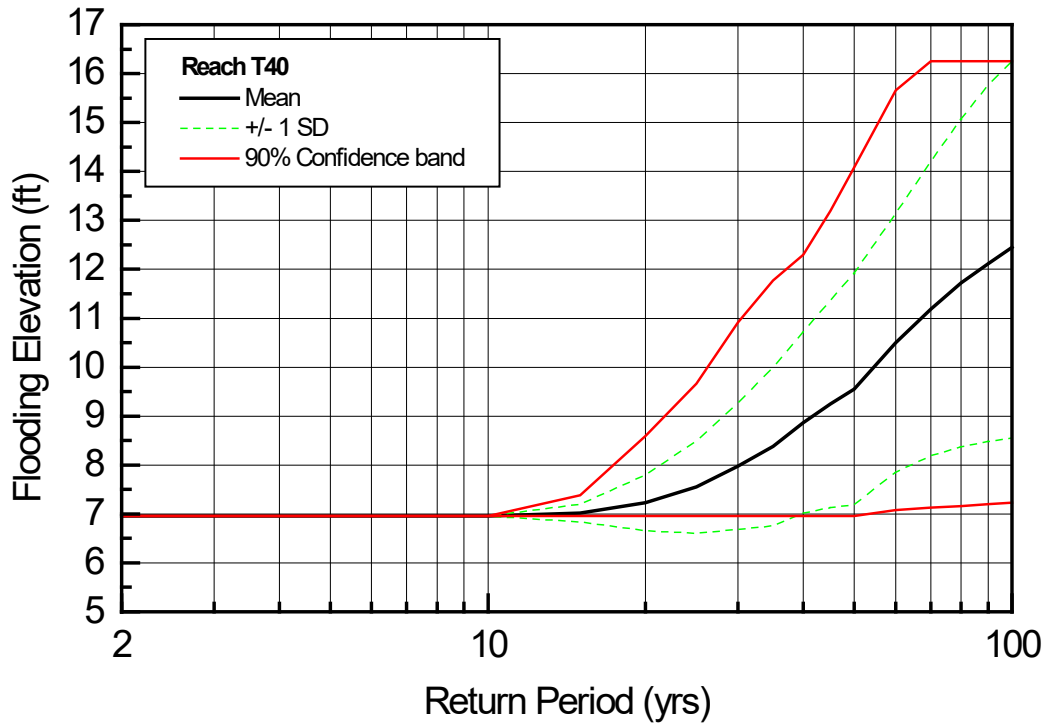


Figure 101. Stage-Frequency Curve for Damage Reach 40

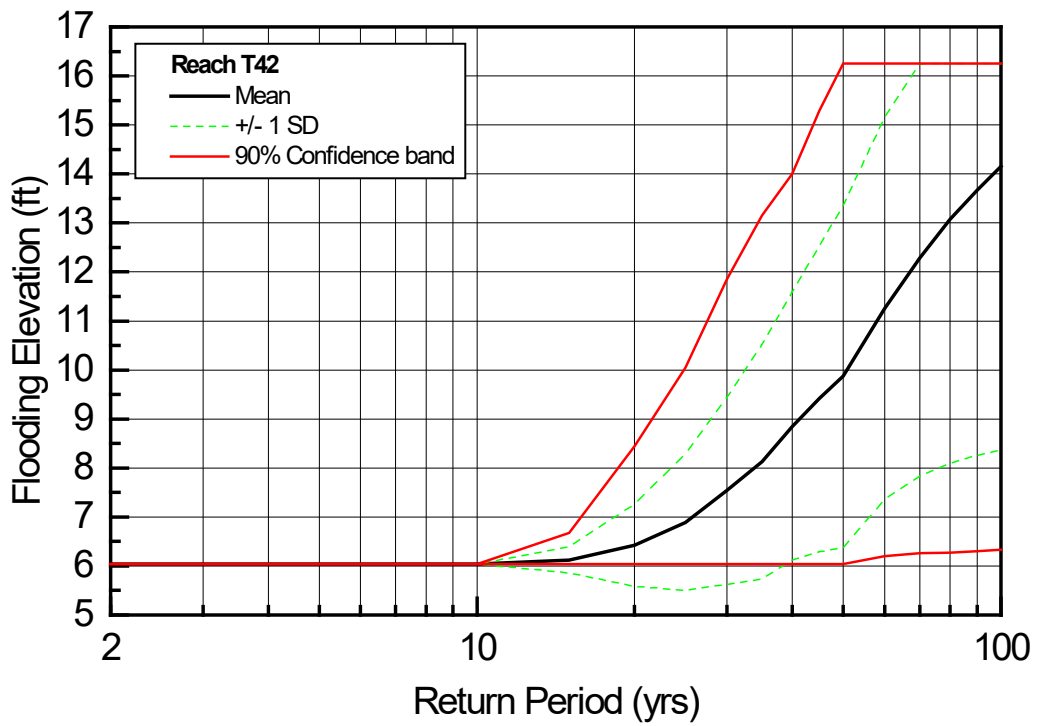


Figure 102. Stage-Frequency Curve for Damage Reach 42

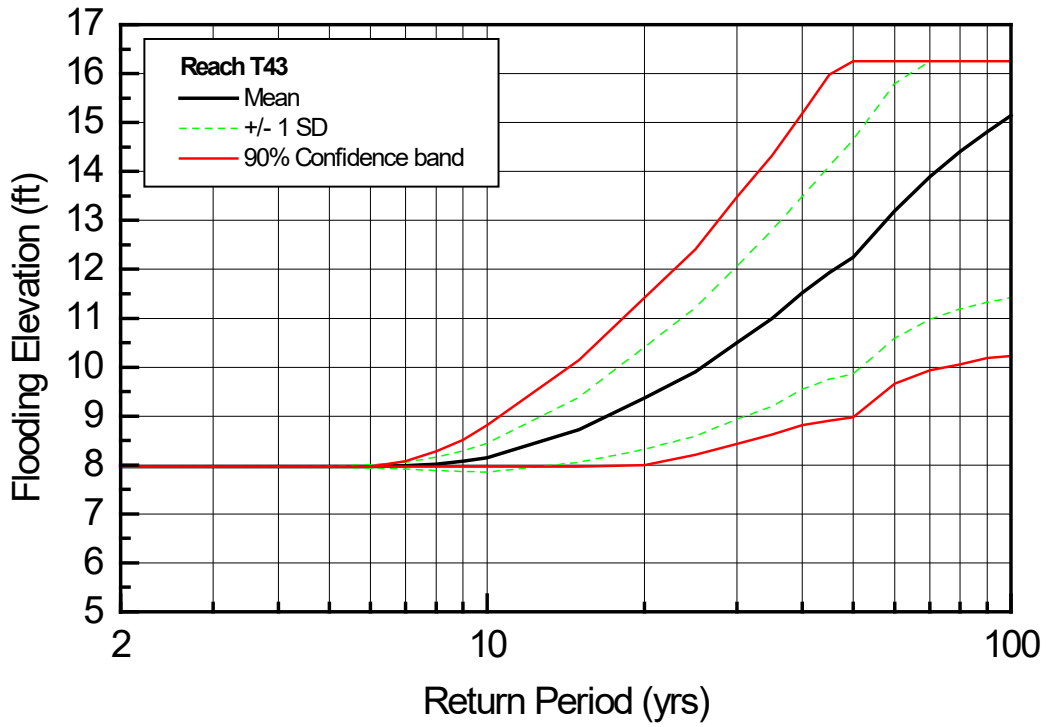


Figure 103. Stage-Frequency Curve for Damage Reach 43

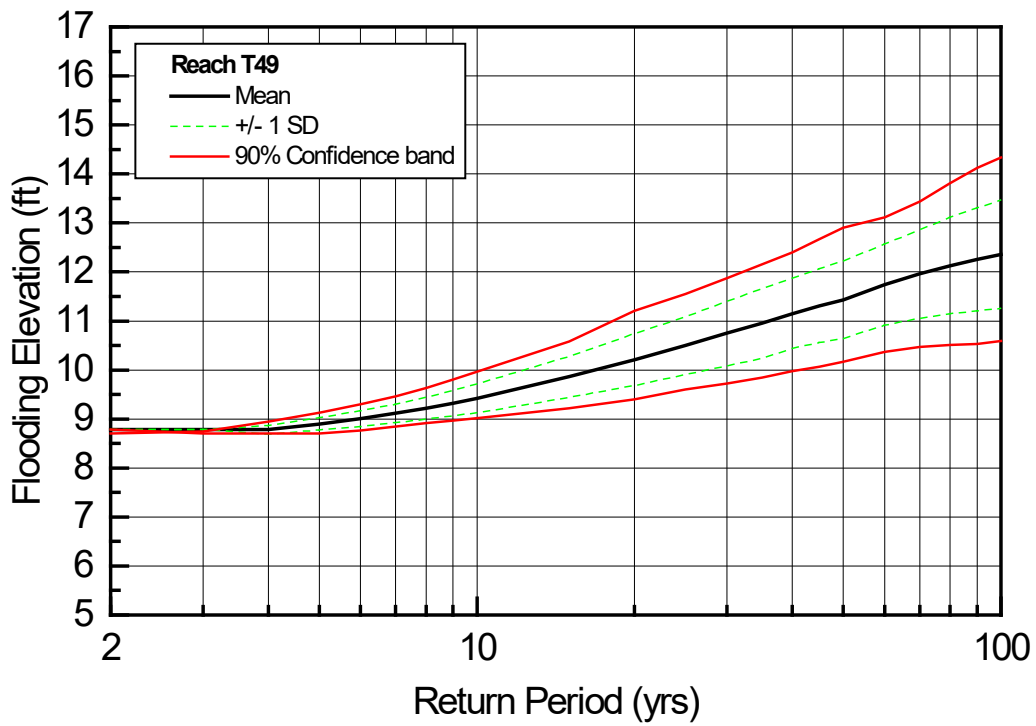


Figure 104. Stage-Frequency Curve for Damage Reach 49

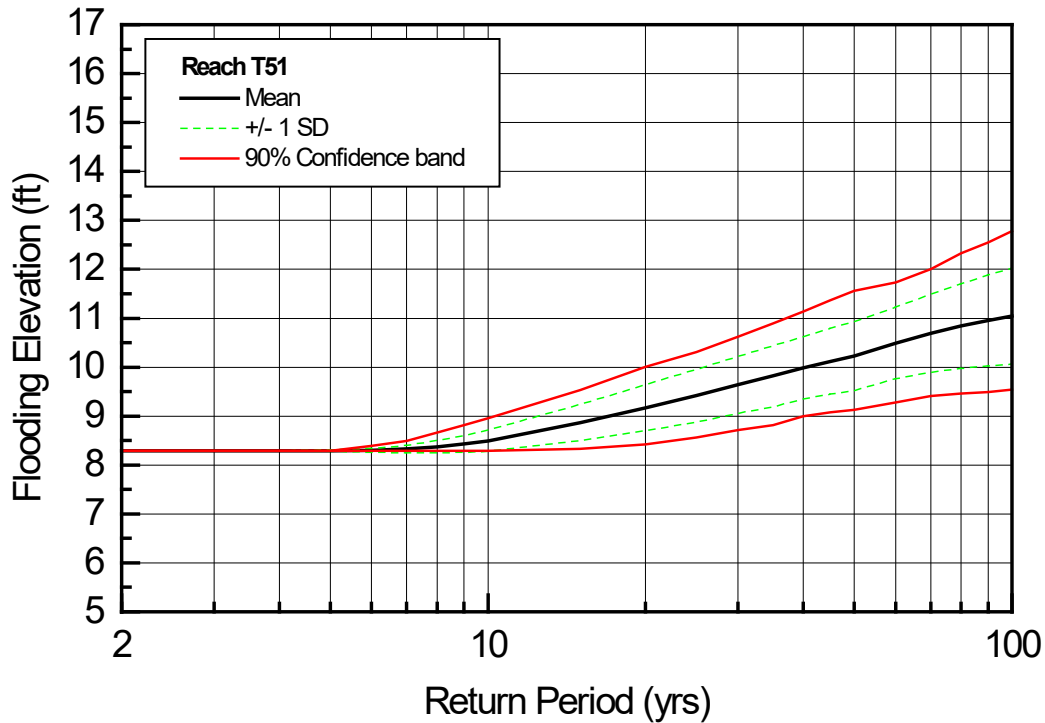


Figure 105. Stage-Frequency Curve for Damage Reach 51

For reaches evaluated south of the sewage lagoon in Barrow and Browerville, a storm with a return period of 5 to 20 years, depending on the reach, is required to induce flooding. For the reaches near the sewage lagoon, model results indicate a 3-year storm will produce some flooding. The calculated 50-year flooding elevation across the study area is approximately 10 to 14.5 ft. These calculation estimates do not include any flood risk reduction berm feature such as the temporary ones that the city puts in place during before and during a storm or any proposed structure.

9.1. Model Verification

Water level measurements during storm events against which the model results could be checked were limited because of the proactive nature of the community during storm events. The NSB actively combats flooding before and during every threatening storm event by placing sacrificial berms along the low lying coastal areas and pushing beach material up to a higher elevation during storm events. These berms are generally comprised of fine material and are easily washed away, but they last long enough to provide temporary risk reduction and are constantly being rebuilt during storms.

Prior to the procurement of the heavy equipment to actively combat coastal flooding, the community of Barrow was highly susceptible to damages from coastal flooding as seen in the damages experienced in the 1963 storm event. Evaluation of the flood potential along the coast could not account for the flood fighting activity along the coast during the storms. Papers written on the effects of the 1963 storm that impacted the coast cite debris lines measured at the 12 foot elevation at the former NARL site north of Barrow. This debris line is outside of the project area,

but the topography is similar to that in the Browerville area. The stage frequency curves indicate that a flood elevation of 12 ft is possible during an extreme storm event.

10. STORM DAMAGE REDUCTION OPTIONS

Storm damage reduction can be categorized into three options:

- options that modify existing structures or practices to prevent storm damage (also known as non-structural measures)
- options that reduce the risk due to erosion at the bluff, and
- options that reduce the risk due to flooding in low areas.

Some of these options may serve the same purpose, but for this analysis they are considered separately.

10.1. Erosion Risk Reduction

The bluff at Barrow is comprised of fine sand, silt and organic material that is bound by permafrost. Wave action on the face and at the base of the bluffs causes localized melting of the permafrost and niching at the toe of the bluffs. Once the permafrost is melted, the bluff material has no inherent strength, which leaves the bluff susceptible to two potential failure modes: slumping or block failure. Slumping occurs when the permafrost is exposed and the subsequent melting produces localized mud flows of unstable material down the face of the bluff. This material is then washed away during high water events. Block failure occurs when the base of the bluff has eroded to the point where the ice is no longer capable of supporting the weight of the bluff and a large block of bluff collapses and is washed away by high water events. The block failure can be quite large if the failure plane is along the ice wedge of a polygon.

Options considered for erosion risk reduction include:

- Non-structural Measures
- Revetment
- Beach Nourishment
- Seawall
- Breakwater
- Groins

10.1.1. Non-structural Measure

This alternative would allow the natural erosion process to take place and relocate structures, roads and utilities that would be impacted by the erosion. Alternative land parcels would need to be available for the structure relocation and utilities would need to be rerouted. No provision would be made for the preservation of archaeological remains in the bluff.

10.1.2. Revetment

A revetment would reduce niching at the bluff during storm events. Construction of a revetment has successfully reduced erosion at bluffs in many locations throughout Alaska. The limiting

factors when considering a revetment along the bluffs at Barrow are: cost of the revetment material, the resistance of the revetment material to an ivu event, and the ease of construction and maintenance. Material options being considered for the revetment include rock, supersacks, and articulated concrete mats. A revetment along the narrow parts of the beach, in front of the bluffs, would further reduce the usable beach width due to the sloping nature of a revetment design. The bluffs are also rich in cultural resources, limiting the ability to dig the revetment into the bluffs. If erosion continues at its current rate, or increases, the already narrow beach could become more inaccessible to the community. A decrease in usable beach width in the bluff area was determined to be an acceptable trade-off by the community since it is already experiencing beach loss in the bluff area. This option would not address the slumping issues associated with melting permafrost, but would shield the bluff toe from further erosion, so it was retained for further consideration.

10.1.3. Beach Nourishment

The use of beach nourishment to reduce bluff erosion has not been used widely in Alaska. Beach nourishment had been tried at Barrow, but material larger than the existing material on the beaches and in the quantities required was difficult to find. The dredge used to perform the beach nourishment was heavily damaged during a storm event in 2000 prior to the completion of the nourishment project. The nourishment program was discontinued after the loss of the dredge. The 2010 Technical Report efforts focused on finding a source of beach nourishment material for a nourishment alternative. Four potential sources for nourishment material were identified (Appendix B: Geotechnical); Point Barrow, Cooper Island, a site known as the Bureau of Indian Affairs (BIA) site, a submerged spit off of Point Barrow (Figure 106), and Colville Consolidated Use Gravel Pit.

The potential gravel source at Point Barrow is co-located with the Nuvuk archaeological site (BAR-011). The site boundaries recognized by the State of Alaska encompass the entirety of Point Barrow. The actual extent of this large subsurface site is not known, but cultural features and more than 63 human burials have been recovered by archaeologists throughout the area (Jensen, A. M., 2009). Nuvuk, which appears to have been first inhabited around 300 AD, and then continuously occupied from 800 AD until the late 1800s, was determined in consultation with local stakeholders to be too sensitive an area to disturb. Cooper Island contains more than two million cubic yards of granular material. However, this island has been a focus for climate change research and also provides nesting and breeding habitat for Black Guillemots and Horned Puffins (Ocean River Institute, 2014 referenced in PND Engineers, Inc., 2015). The BIA site has an estimated two million cubic yards of granular material at this site, however extracting that granular material will require removing approximately equal volumes of deleterious material. The submerged spit soils consist of silt or fine sand with 10-40 percent silt and no more than 5 percent gravel. Materials are considered unsuitable for beach nourishment or construction material. The ASRC Colville Consolidated Use Gravel Pit is a large out-of-bank sand and gravel mining operation in the Colville River, Nuiqsut area. The current Phase 3 mining area contains about 430 acres of mineable quantities of sand and gravel, estimated at about 15 million yd³, but is located approximately 150 miles from the project site with no road connecting the two locations.

The success of a beach nourishment alternative at Barrow is dependent on constantly renourishing the beach, if nourishment material is similar to the existing beach material, or less

frequent nourishment, if material coarser than the existing beach material is used. The lack of appropriately sized local, cost-effective material resulted in beach nourishment being dropped from further consideration.

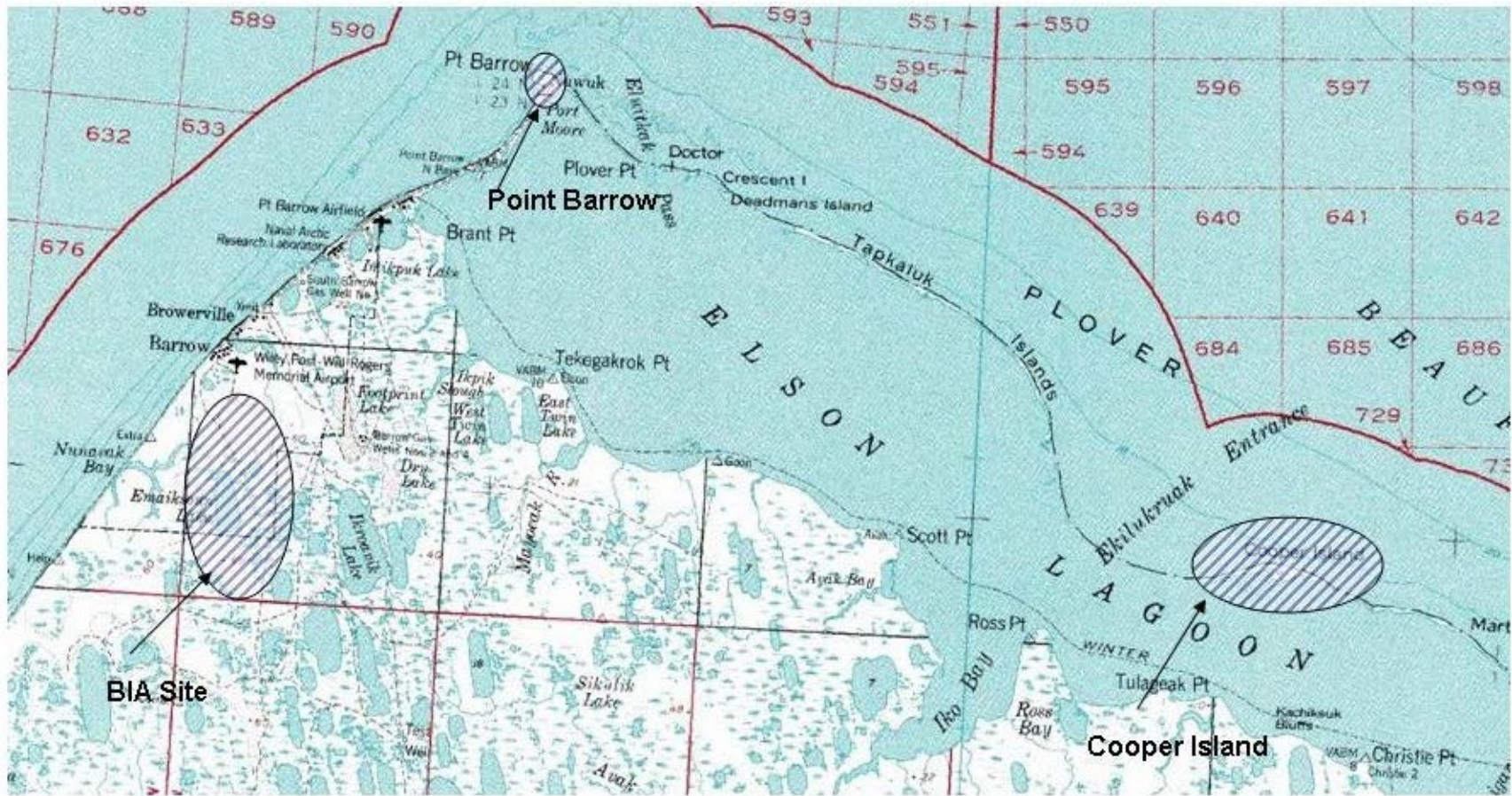


Figure 106. Potential Gravel Sites from Geotechnical Investigation

10.1.4. Seawalls

The purpose of a seawall (Figure 107) is to reduce the risk of erosion of the land behind it and reduce the risk to any developments on that land. The beach at Barrow is important to the way of life in the arctic. Boats are launched on the beach for subsistence activities and goods and supplies are landed on a barge at the beach, so it is important that the beach be maintained. The effect of a seawall is often damaging, particularly to the shoreline in the zone of the reflected wave. A number of studies have found that scour tends to develop on the beach fronting a seawall. The coastal condition at Barrow is extremely fragile since the major source of natural renourishment has been removed from the system and only a small amount of material is transported along the shoreline each year. A large storm event could take many decades of recovery in front of a seawall at Barrow. The sustained narrowing of the beach as a result of removing borrow material is evidence that the beach can obtain equilibrium, but not recover to previous widths. Taking a chance on a risk reduction measure that could possibly reduce the beach width is a risk that could result in damage to the beach from which it would not recover. A number of seawall structures in Alaska have caused scour to develop on the fronting beach. Because this option could harm the coastal environment, it was dropped from further consideration.



Figure 107. Seawall at Barrow

10.1.5. Offshore Breakwaters

Intermittent offshore breakwaters could be used to lessen the wave energy impacting the beach and the base of the bluff. Typically offshore breakwaters provide a quiet area where sediment accumulates and a tombolo forms, giving the shoreline a scalloped appearance. Due to the small amount of sediment transport, the formation of a tombolo would be a very slow process. Materials that could be used in the construction of a breakwater include rock or concrete armor

units similar to dolosse. The construction costs for this option would be higher than other options because work would need to be performed from a barge, inspection and maintenance would be more difficult, and it would likely lead to erosion outside of the project area due to the interruption of the natural sediment transport system. Consequently, it was dropped from further consideration.

10.1.6. Groins

Groins are typically placed to limit the movement of longshore sediment and build up a beach. Due to the limited longshore transport of beach material, groins would be marginally effective. Materials that could be used in the construction of a groin system include rock, steel piles, timber piles, and sacrificial supersacks. Groins would take a long time to build up sediment to increase the beach width and would limit the amount of material being transferred outside the project area resulting in increased erosion outside the project area. This option was dropped from further consideration.

Evaluation of the options considered for erosion risk reduction are presented in Table 13.

Table 13. Erosion Risk Reduction Option Matrix

Risk Reduction Type	Advantages	Disadvantages
Non-structural Measures	No maintenance costs associated with relocation. Technically easy to implement. Allows bluffs to find natural equilibrium.	There is likely local resistance to relocation. Need alternate land parcels available for relocation. Does nothing to preserve artifacts from eroding bluffs
Revetment	Provides erosion risk reduction of the entire bluff face. Easy construction with land based equipment. Easy access to inspect for damages	Susceptible to damage from an ivu event. Depending on material used, could have high maintenance requirements.
Beach Nourishment	Returns beach material that had been lost during storm events and borrow activities. Would reduce wave impact at the base of the bluff. Maintains a usable beach for community activities and shipping and receiving goods.	Would require periodic maintenance. Limited quantity of locally available nourishment material of required size.
Seawall	Provides erosion risk reduction of the entire bluff face.	Would reduce the risk of erosion of the bluffs, but possibly erode the fronting beach.
Breakwater	Would reduce the wave climate at the base of the bluff. Maintains a usable beach for community activities and shipping and receiving goods.	Susceptible to ice damage. More complex construction. Need offshore equipment. More difficult to inspect and maintain.
Groins	Would build up sediment and eventually raise beach elevation resulting in milder wave climate at the base of the bluffs. Maintains a usable beach for community activities and shipping and receiving goods.	Susceptible to ice damage. Would produce a sediment deficit down drift of the groins. Sediment transport is minimal, so beach buildup would take a considerable amount of time.

10.2. Flood Risk Reduction

The bluff at the southwestern end of Barrow provides elevation to protect that part of the coast from flooding associated with storm events. The terrain elevation decreases to the northeast, and at Tasigarook Lagoon that fronts Isatkoak Lagoon, no bluffs exist and the coast is a low-lying beach. The area of Isatkoak Lagoon and the low-lying beach along the coast are susceptible to flooding during storm events. Flooding occurs during storm events with high wave run-up elevations that exceed the elevation of the berm fronting the coast. The construction of a well-engineered flood risk reduction structure could significantly reduce the coastal flooding risk at Barrow.

Options considered for flood risk reduction include:

- Non-structural Measures
- Revetted Berm Structure
- Beach Nourishment, or a
- Seawall

10.2.1. Non-structural Measures

Homes impacted by flooding could be raised to avoid flood damage. Raising impacted homes would preserve the structure and interior; however, property kept outside such as boats, four wheelers, or snow machines would still be susceptible to damages. An alternative to raising homes above the flood level would be to relocate homes outside of the flood area. This alternative would require that parcels be available for the structure relocation. Flood damage at Isatkoak Lagoon could be addressed by raising the height of the spillway, filling Tasigarook Lagoon, or building a revetted berm in front of the lagoon to reduce the risk of saltwater contamination in the community's fresh water source.

10.2.2. Revetted Berm Structure

A revetted berm structure that would dissipate the energy associated with wave run-up could be constructed on the seaward side of Stevenson Street or Stevenson Street could be raised and the seaward side of the street could be revetted. The revetted berm would be susceptible to damage from an ivu event and could be designed to withstand ivu forces, but this would require a significant increase in the size of the armor rock, and due to a lack of information on the frequency and severity of these episodes, the associated maintenance due to ivu events is unknown. A revetted berm structure sized to address the wave run-up and not the ice forces would use considerably smaller armor rock, but would have an increased maintenance requirements. The NSB currently uses a sacrificial berm system to reduce the risk of flooding in the low lying areas which is effective, but susceptible to wave and ice damage. The revetted berm option would reduce the risk of flooding in the low lying coastal area and not harm the existing beach, so it is retained for further consideration.

10.2.3. Beach Nourishment

The use of beach nourishment as a flood risk reduction measure has not been used in Alaska. Beach nourishment would raise the beach elevation to move the wave run-up away from Isatkoak Lagoon, Browerville, and NARL. As with the beach nourishment option for erosion risk

reduction (Section 10.1.3 Beach Nourishment), the lack of appropriately sized local, cost-effective material resulted in beach nourishment being dropped from further consideration.

10.2.4. Seawall

As discussed in the erosion risk reduction option, the effect of a sea wall on the fronting beach is uncertain. Because of the importance of the beach to the activities at Barrow, and the potential damage to the beach, this option was dropped from further consideration.

Evaluation of the options considered for flood risk reduction is presented in Table 14.

Table 14. Flood Risk Reduction Option Matrix

Risk Reduction Type	Advantages	Disadvantages
Non-structural Measures	No maintenance costs associated with relocation. Technically easy to implement	There is likely local resistance to relocation. Need alternate land parcels available for relocation.
Revetted Berm Structure	Straightforward construction and maintenance. Proven success in Alaska Easy access for inspection	Susceptible to damage from an ivu event. Depending on material used, could have high maintenance requirements.
Beach Nourishment	Aids in returning the beach to its original state. Would reduce wave run-up with increased beach elevation.	Would require periodic maintenance. No economical, archaeologically, and environmentally acceptable location to provide adequate amount of material.
Seawall	Provides a large area of flood risk reduction.	Would reduce the risk of flooding in the low lying areas, but erode the fronting beach.

10.3. Selected Features

10.3.1. Bluff Erosion Risk Reduction - Revetment

A rock revetment to reduce the risk of erosion to the toe of the bluff has a proven history of use in Alaska for coastal erosion risk reduction. Several materials were evaluated to construct the revetment including the articulated concrete mats and rock. Personal correspondence with oil company personnel on the success of concrete armor units on offshore islands in the Beaufort Sea indicates that the articulated concrete mats experience chipping and breaking due to ice forces and that the mats need a well-drained underlayer to dissipate uplift forces. Articulated concrete mats are generally costly to install and maintain, and to date they have not had a good

history of erosion and flood risk reduction at coastal sites in Alaska. Rock revetments have been used successfully at sites throughout Alaska. A revetment sized for waves would be susceptible to ivu forces, but could be repaired easily if a maintenance stockpile were kept at Barrow.

10.3.2. Flood Risk Reduction - Revetment

A revetted berm structure to provide a raised shore elevation to dissipate run-up energy provides a reduction in the risk of coastal flooding at Barrow. The structure would not need to be impermeable as with a typical dike, but it would need to intercept the run-up and dissipate its associated energy. Rock would provide the most reliable, easiest to maintain, and least cost material.

10.3.3. Alternative Constraints

Due to the limited and shrinking beach width in front of the bluffs there is no bluff erosion risk reduction alternative option that includes an armor rock launchable toe or a splash apron. The final crest height, buried toe depth, and armor rock size will take into consideration RSLC and current erosion rates to incorporate resilience into the final design. Similarly, in the low lying area where there is a wider beach, there is still limitations for a robust launchable toe or enhanced splash apron due to the location of the road and lagoons limiting the landward extend of any flood risk reduction alternative. There is also a community preference for a limited structure width to limit the immediate impact that any structure would have on the width of the beach, with the understanding that the beach would continue to erode.

Alternatives that do not include beach nourishment are not designed to address current erosion rates of the beach. These alternatives are designed to reduce the risk of flooding in low lying areas and erosion along the bluff. The community recognizes that the erosion of the beach in front of any armored structure would continue to erode and reduce their access to the beach. Once the immediate risk to the community's infrastructure is reduced, the community could begin investigating methods to ensure continuing access to the beach for subsistence activities.

10.3.4. Maintenance

The frequency and severity of ivu events is generally limited to photographs and personal accounts. Statistics on the frequency of occurrence and associated ice strength, length of ice impact, and duration of ivu events has not been developed and currently there is not enough data to develop these statistics. Ivu events would be the primary reason for revetment maintenance. In the absence of statistical information, an assumption was made that regardless of the alternative chosen, maintenance in the form of rebuilding a section of revetment or revetted berm would occur every 5 years and a stockpile of rock would be maintained at Barrow to support the maintenance. Due to the extensive experience of the NSB Public Works Department in storm response and recovery and the current equipment that is maintained in the community it is anticipated that the community would perform all maintenance activities with the stockpiled material. The maintenance length was assumed to be 2,000 ft.

The project would need to be inspected for damage at least twice annually. One inspection would need to occur after the snow and ice melts and a second in the fall, before freeze up. There would also need to be post storm inspections to check the condition of the structure toe and any

displaced material. It is imperative that these inspections be performed in order to have adequate time to repair damage before winter.

10.4. Design Parameters

The governing wave height used to design the alternatives was the depth-limited wave height at the toe of any structural alternative. The depth-limited wave height is based on water depth at the toe of the structure, which is influenced by the total water level (Equation 7) and in addition to wave run-up, though RSLC and the measured tidal determination were not included in the modeling and calculations of the total water level for this feasibility study.

$$\text{Total Water Level} = \text{Wind Surge} + \text{Tide} + \text{Wave Set} - \text{Up} + \text{RSLC} \quad \text{Equation 7}$$

Wind Surge – ADCIRC Output (Section 5.1 Water Surface Modeling with ADCIRC)

Tide – +0.5ft MLLW (Section 3.3 Tides)

Wave Set-up – SBEACH Output (Section 9 Coastal Flooding)

RSLC – Not Included for Current Design (Section 6 Sea Level Change)

10.4.1. Total Water Level

The coastal flooding at Barrow is the result of the combination of tide, wind surge, wave set-up, and wave run-up, and it is only the addition of run-up that introduces flooding along the coast. As a result, the flood risk reduction structure crest elevation is based on the water depth at the toe of the structure and run-up elevation. The base water surface elevation used in the design is the ADCIRC elevation and the wave set-up and run-up elevation used in the design is the SBEACH elevation.

A hand calculation check on SBEACH elevations for wave set-up and run-up for the 20-, 50-, and 100-year events was performed using two different wave set-up equations: a method by Komar (Komar, 1998) and a method shown in the Coastal Engineering Manual (CEM) (United States Army Corps of Engineers, 2002) (Part II Chapter 4 Surf Zone Hydrodynamics). The base elevation for all calculations is the tide of +0.5ft MLLW plus wind surge level obtained from ADCIRC modeling for the 20-, 50-, and 100-year event.

SBEACH generated output to predict return frequency intervals using the EST model. This model makes the assumption that past storm frequency and intensity is an accurate predictor of future storm activity. The last decade or so has seen an increase in storm activity, along with more ice-free days each year and the permanent ice pack being further offshore. This adds an additional level of uncertainty to the EST results. The return frequency interval for storm setup (combined elevation of tide plus wind surge, plus wave setup) is shown in Figure 108.

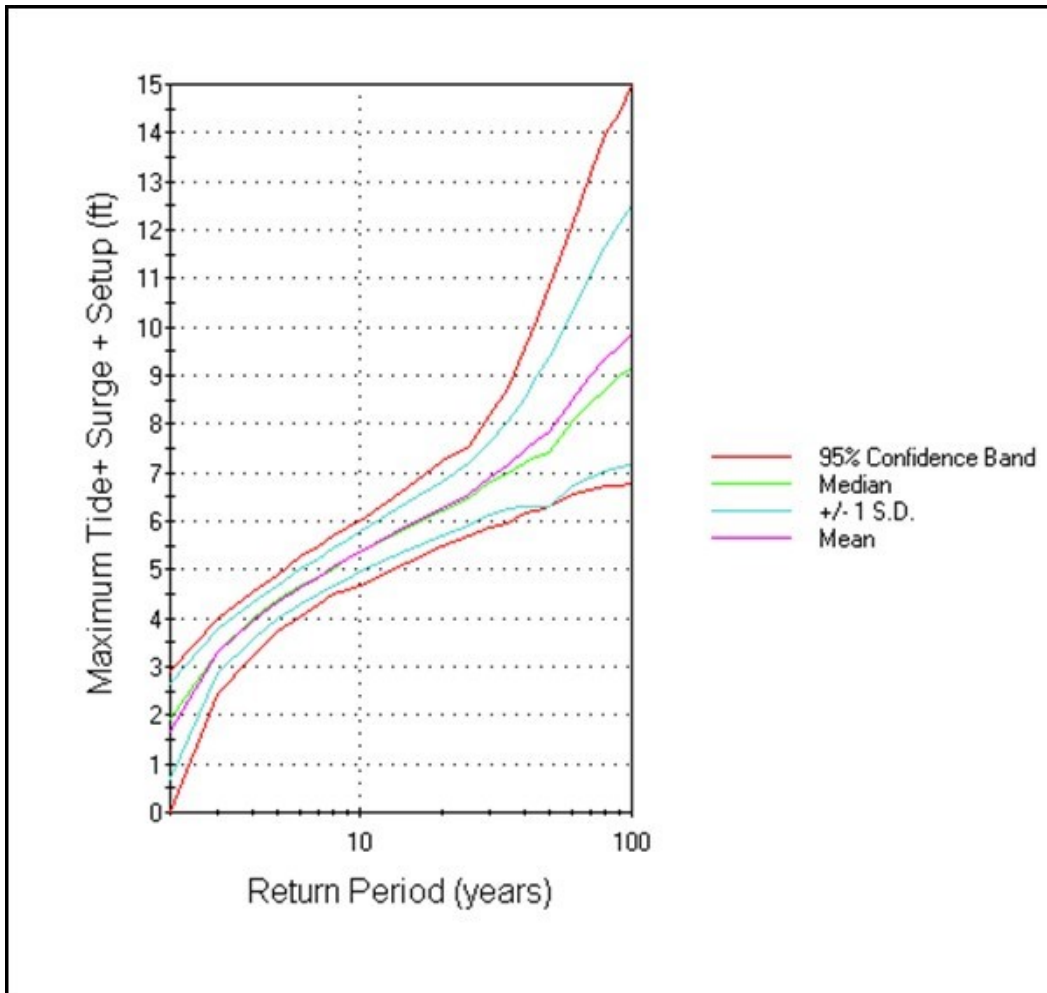


Figure 108. Stage Frequency Curve for Set-up Elevation with Maximum Tide Based on Engineering Judgment (Wind Surge, Wave Set-up, and Tide of +0.5 ft MLLW).

A comparison of the two hand calculated results is shown in Table 15. The set-up elevation with the base elevation from ADCIRC added in is shown in Table 16 and compared with the SBEACH results. The calculated difference in water surface elevation between SBEACH and the hand calculations for the 20-, 50-, and 100-year events varies between 5 and 23 inches.

Table 15. Wave Set-up

Equation	20-year Wave Set-up [ft]	50-year Wave Set-up [ft]	100-year Wave Set-up [ft]
CEM	3.3	3.7	4.0
Komar	4.26	4.5	4.7

Table 16. Total Water Level

Water surface elevation ADCIRC + Wave Set-up	20-year Wave Set-up [ft]	50-year Wave Set-up [ft]	100-year Wave Set-up [ft]
CEM	6.5	7.5	8.0
Komar	7.4	8.1	8.7
SBEACH*	6.5	7.9	9.9

* includes simple wave run-up (Section 9 Coastal Flooding)

* mean stage frequency curve (Figure 108)

10.4.2. Run-up for Low Lying Area Structure

The run-up associated with the natural beach slope was presented earlier as part of the SBEACH analysis for coastal flooding. SBEACH is not able to calculate run-up associated with a permeable rock structure so hand calculation methods were used to determine the run-up on a rock structure. The run-up associated with a permeable coastal risk reduction structure was calculated using methods described in the CEM (United States Army Corps of Engineers, 2002) (Part VI Chapter 5 Fundamentals of Design).

The risk reduction measure for flooding is set back from the near shore environment, so the calculation of run-up was made using shallow water assumptions. The larger waves will have broken by the time they reach the toe of the structure, so the significant wave height used for calculations was the maximum wave height that could be sustained at the toe of the structure with the associated total water level and wave run-up described previously using the relationship:

$$H_b/h_b = 0.78 \quad \text{Equation 8}$$

Where H_b is the breaker height and h_b is the water depth below the still water line at the wave crest at incipient breaking.

Run-up was calculated using methods for a rock armored surface shown in the CEM (United States Army Corps of Engineers, 2002) (Part VI Chapter 5 Fundamentals of Design). The run-up elevation was added to the SBEACH water surface elevation in Table 16 to obtain a minimum structure elevation for the 20-, 50-, and 100-year flood event. The minimum elevations necessary for flood risk reduction are presented in Table 17.

Table 17. Wave Run-up in the Low Lying Area (Total Water Level + Wave Run-up + Structure Run-up)

Equation	20-year Wave Run-up [ft]	50-year Wave Run-up [ft]	100-year Wave Run-up [ft]
CEM	9.5	12.5	14.0

10.4.3. Run-up for Bluff Revetment

Although the bluff area is not susceptible to flooding because of the natural elevation, wave run-up is equally important in the erosion risk reduction of the bluff. The fine material that comprises

the bluff is extremely susceptible to erosion from wave action and run-up that could remove the fine material.

The revetment elevation to reduce the risk of erosion from total water level + wave run-up + structure run-up was calculated in the same manner as for the flood risk reduction elevation described above. The profile used for this analysis was transect 18. The results of this analysis are shown in Table 18.

Table 18. Wave Run-up in the Bluff Area (Total Water Level + Wave Run-up+ Structure Run-up)

Equation	20-year Wave Run-up [ft]	50-year Wave Run-up [ft]	100-year Wave Run-up [ft]
CEM	14.5	18.5	20.0

The wave run-up elevation on the structure in the bluff area is generally higher than in the flood risk reduction area. The beach is generally narrower in the bluff area, which results in a structure that is closer to the shoreline; therefore, larger waves can reach the bluff with an accompanying higher run-up.

10.4.4. Design Wave

The armor rock was sized for a depth-limited wave impacting the toe of the structure. To accommodate the uncertainty associated with a decreasing ice season and a potential increase in storm activity, the 95 percent Confidence Interval associated with the 50-year total water level (Figure 108) was used rather than the mean water level. This was superimposed on the 2003 transect survey elevation to determine the maximum wave depth that could impact the structure. The water depth at the toe of the structure yields a maximum potential breaking wave at the toe of the structure of 8 ft.

10.4.5. Revetment Design – Armor Rock

The revetment design for shore risk reduction uses a multilayer design with two layers of armor rock, and under layers of B rock, core, gravel, and filter fabric to obtain the proper filtering, so beach material will not pipe through the structure.

Using Hudson’s equation (United States Army Corps of Engineers, 2002) (Part VI Chapter 5 Fundamentals of Design) for the largest breaking wave of 8 ft and a K_d of 2 results in W_{50} armor rock size of 2.7 ton. In addition to wave forces, any structure placed along the coast at Barrow is also going to be subject to ivu events. The survivability of a rock structure along the coast during an ivu event was studied using a physical model at the CRREL.

10.4.5.1. Armor Rock Sized to Withstand Ivu Events

A series of four model tests were conducted in the Test Basin of the Ice Engineering Facility at CRREL to simulate the impact of an ivu event from the Arctic Ocean on the proposed coastal risk reduction structure for the 2010 Technical Report. An ivu event originating from the Arctic Ocean have long been observed to occur along the shoreline at Barrow, Alaska. The objective of the model tests was to assess the integrity of the proposed structure under the impact of an ivu event by determining the stability of the rocks. A review of available data on ice conditions in

the Arctic Ocean off of Barrow indicated that representative ice covers are on the order of 5 ft thick and have a flexural strength of 600 kPa.

A 20:1 undistorted model of the proposed armor rock revetment and the immediate shoreline was constructed. The model reproduced approximately 394 ft of shoreline and covered the distance from the mean water line to the back of the revetment.

The model was supported on a rolling platform with eight wheels and was pushed by the Test Basin Carriage (Figure 109) against the stationary ice. Each test represented approximately 1,968 ft of prototype ice being driven up the shoreline against the structure. Elevation profiles of the revetment were measured before and after each test. To increase the number of variations that could be evaluated, the revetment length was split in half, so that one configuration could be built on one half, and a second configuration could be built on the other side. To enable the tests to be independent of each other, the ice sheet was cut down the middle prior to testing and an aluminum template extended out from the center of the structure to ensure that each half of the ice sheet was separate before impacting the structure. The rock placement method: random or selective, the size of the rocks, and the toe configuration were varied between tests. Selective placement of the rocks to interlock and support each other provided a much greater degree of stability during an ivu event than random placement. The size and placement of the rocks at the toe of the revetment was also found to be important in the survivability of the revetment.



Figure 109. Revetment Test Section being Pushed by Carriage

The first test was a test of armor rock sized for wave action. The armor rock was randomly placed. Results of the test indicated that the armor rock sized for waves was under sized to withstand damage during an ivu event. The armor was heavily damaged during testing.

The second test conducted compared the survivability of 8 ton rock with selective versus random armor placement. The selective placement survived with some damage, while the random placed armor suffered heavy damage. The damage appeared to start at the toe and once the ice sheet was flexed, the damage was minimal.

The third test was conducted to determine if the rock size could be decreased if heavy toe rocks were incorporated into the structure to flex the ice sheet. This test evaluated selectively placed 4 ton rock slopes with 8 ton and 13 ton toe rocks. A single layer of 13 ton and 8 ton toe rocks were used for this test. The revetment with the 8 ton toe rocks sustained heavy damage during the test while the revetment with the 13 ton toe rocks was damaged, but survived.

The fourth test evaluated 4 ton rock and 8 ton rock on the structure slope with four different toe configurations. To look at more toe rock variations, each half of the revetment slope was built with two different toe rock configurations, so a total of 4 toe rock configurations were examined (8 ton, 13 ton, and 20 ton toe rocks). The revetment slope section with the best survivability during the tests was the selectively placed 8 ton rock slope with a 13 ton toe. The 8 ton rock slope with an 8 ton toe sustained damage that would require slope repair. The 8 ton rock slope with the 13 ton toe rock sustained damage to a section of the toe that would need repair, but the bottom layers of the toe rock stayed in place and there was minimal movement on the revetment slope. The entire 4 ton rock slope survived, but experienced movement and dislodged rocks. None of the revetments tested in the fourth tests were considered failures; however, when the results are translated to prototype, three of the revetments would require extensive maintenance, and the fourth would require minor maintenance (replacement of top toe rock layer). The idealized cross section that had the best survivability and least subsequent maintenance is shown in Figure 110. Before and after pictures from the testing are shown in Figure 111 and Figure 112.

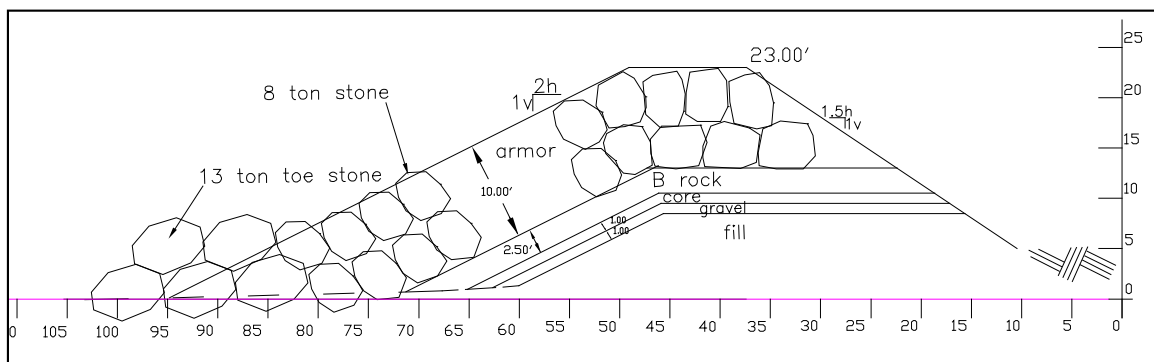


Figure 110. Idealized Cross Section from Ivu Tests with Best Survivability from Physical Model



Figure 111. Revetment before Testing. 8-ton Armor Rock (Blue Slope) with 13-ton Toe Rock (Red Toe)



Figure 112. Rock Revetment after Ivu Event Testing, some Toe Rock Moved during Test, but the Revetment Slope Stayed Intact. 8-ton Armor Rock (Blue Slope) with 13-ton Toe Rock (Red Toe)

There were many uncertainties associated with the ivu testing. The recurrence interval of ivu events and the ice strength during an ivu event are major variables. The length, speed, and duration of an ivu event are also not well documented. The tests were designed to impact the ice with a uniform strength for the entire length of the ice sheet; however, this was difficult to achieve, as the far end of the cold room was generally cooler than the front end. Random tests indicated that the ice at the back of the cold room was stronger than the front.

The results of the physical model testing provided data to size the armor rock for minimum maintenance due to ivu events. Test results highlighted the importance of the structure toe when it is set back from the beach. The toe is the first element to be impacted by the ice and cause significant ice deflection. Because of the critical nature of the toe, the smaller rock comprising the filter layers under the armor are to be buried to prevent them from being gouged out by an ivu event. Burying the filter layers leaves the armor toe rock as the initial impact surface with the ice to begin flexure.

Sizing the rock to withstand an ivu event results in an armor layer that is oversized for waves. It also set the minimum structure height. The armor rock thickness is two rock widths, which results in a revetment elevation higher than the 50-year run-up elevation along the low lying coast. In an effort to minimize the rock quantity and elevation, the B rock layer was reduced from two layers to one for a revetment designed for an ivu event (Figure 110).

10.5. Structure Design

Structures were designed with armor rock sizing governed by wave height. Structures designed to withstand most ivu events were not considered for a final design and damages due to ivu events was determined to be an acceptable risk. Due to changing sea and shorefast ice conditions (Section 3.2 Ice Conditions), ivu events could end up becoming a more infrequent occurrence. Rock sized for ivu events has prohibitively high cost and the community has a preference for structures sized for waves with the understanding that maintenance would be required in the event of an ivu event impacting any structure. This would require that the structures be inspected each year to assess damages associated with potential ivu events and maintenance performed as needed.

10.5.1. Bluff Erosion Risk Reduction Governed by Waves - Revetment

The revetment along the bluff area would consist of two layers of 2.7 ton armor rock on the structure slope and two layers of B rock (Figure 113). The B rock, core, and gravel filter layers would be buried to match the existing beach elevation. The crest height is set at 19 ft, which is 0.5 ft higher than the 50-year run-up. The bluffs would not be excavated to provide a uniform slope on which to build, rather they would be dressed with local fill material to achieve a uniform slope. The bluffs are archaeologically rich, so no excavation would be permitted on the bluff face.

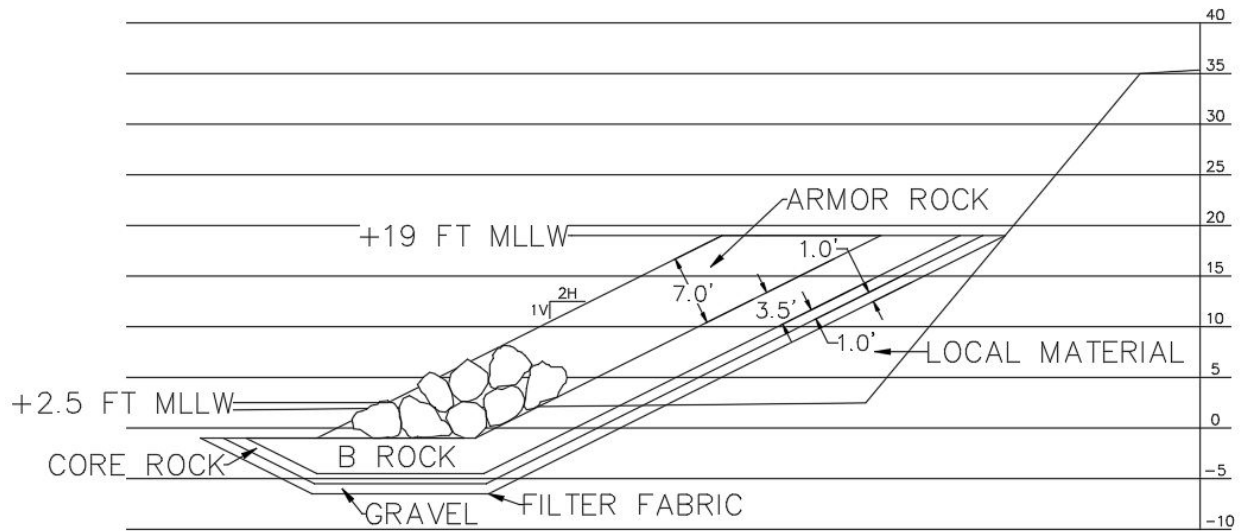


Figure 113. Bluff Erosion Risk Reduction with Armor Sized for Waves

10.5.2. Low Lying Coastal Flooding Risk Reduction Governed by Waves

10.5.2.1. Revetted Berm Structure

Coastal flooding at Barrow is the result of the combination of tide, wind surge, wave set-up, and wave run-up, with wave run-up being the water level increase that results in flooding. The coastal flood risk reduction revetted berm is designed to address flooding by reducing the wave run-up energy.

Wave run-up elevations associated with a porous structure were calculated and described previously. The crest height is set at 14.5 ft, which is 0.5 ft higher than the 100-year run-up and 2 ft higher than the 50-year run-up (Figure 114) and was chosen to increase the resilience of the flood risk reduction alternative in the low lying areas. The filtering B layer, core, gravel, and fabric would be placed below the natural beach line for ice survivability. The structure would consist of two layers of 2.7 ton rocks with a 2 horizontal on 1 vertical seaward slope and 1.5 horizontal on 1 vertical landward slope. The reduced size of the structure would likely result in increased maintenance due to ivu events, but the reduced size would make the maintenance of the structure easier to perform and a stockpile of replacement rock would be kept at Barrow for maintenance activities. The B rock would be a double layer placed on a 1 foot layer of core, 1 foot layer a gravel, and an underlayment of filter fabric. The B rock, core, and gravel filter layers would be buried to match the existing beach elevation.

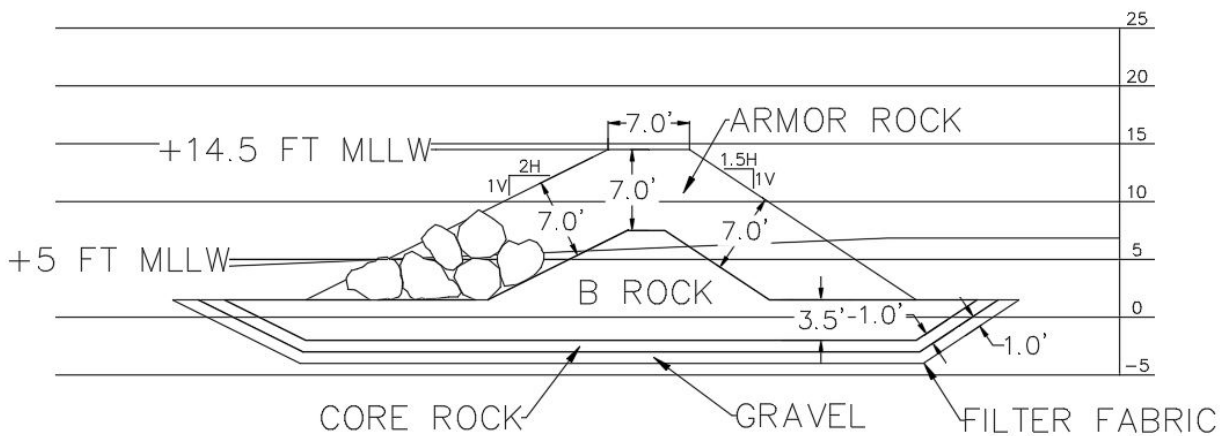


Figure 114. Revetted Berm for Flood Risk Reduction Sized for Waves

10.5.2.2. Raised and Revetted Stevenson Street

As an alternative to a revetted berm, Stevenson Street could be raised. Raising Stevenson Street as opposed to a revetted berm would decrease the quantity of armor rock and maintain a view of the ocean from the street. Stevenson Street would be raised to the elevation of the revetted berm with fill material to ensure a 100-year run-up return interval level of risk reduction. The seaward slope of the street would be revetted with two layers of 2.7 ton armor rock and two layers of B rock (Figure 115). The B rock, core, and gravel filter layers would be buried to match the existing beach elevation.

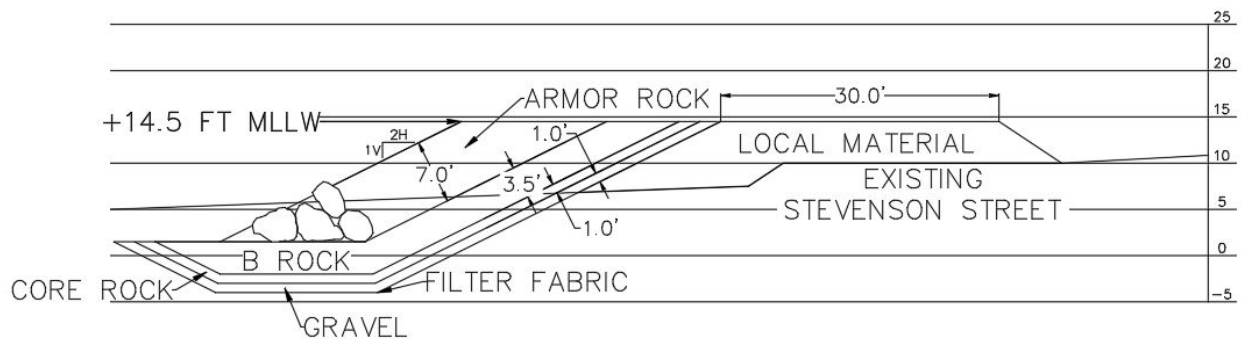


Figure 115. Stevenson Street Raised for Flood Risk Reduction with Revetted Seaward Slope Sized for Waves

10.5.3. Design Considerations for Relative Sea Level Change

RSLC is not incorporated into the final design for this feasibility study, but would be incorporated in the final design before construction. The anticipated effect of incorporating RSLC on the final design includes increasing crest height due to increased total water level. It would also increase armor rock size due to increased water depth at the toe of the structure during storm events, resulting in a larger (higher) depth-limited wave height impacting the structure. See Section 14 (Volume Sensitivity Analysis) for an estimate of the effect RSLC would have on the final design.

Figure 116 shows the three RSLC curves along with the elevations of Mean Higher High Water and Mean Lower Low Water and the average toe elevation of the proposed revetment and berm/raised Stevenson Street Alternatives, described in Section 10.5 (Structure Design), relative to Local Mean Sea Level (LMSL). Without the construction of a coastal storm damage reduction project the toe of the bluff, the beach in front of Tasigarook Lagoon, and Stevenson Street would be impacted further and to a larger extent by erosion and overtopping/flooding as RSLC is realized in Barrow (Figure 116). Based on the current elevation of the bluff toe and the estimated RSLC for the high curve, the bluff toe will be at the LMSL by year 2095 if the high curve is realized. If the bluff toe is at LMSL then the erosion rate along the bluffs will increase due to the constant attack of the toe by waves. As RSLC is realized the total water level necessary to flood the low lying areas will decrease, increasing the probability of a flood event every year.

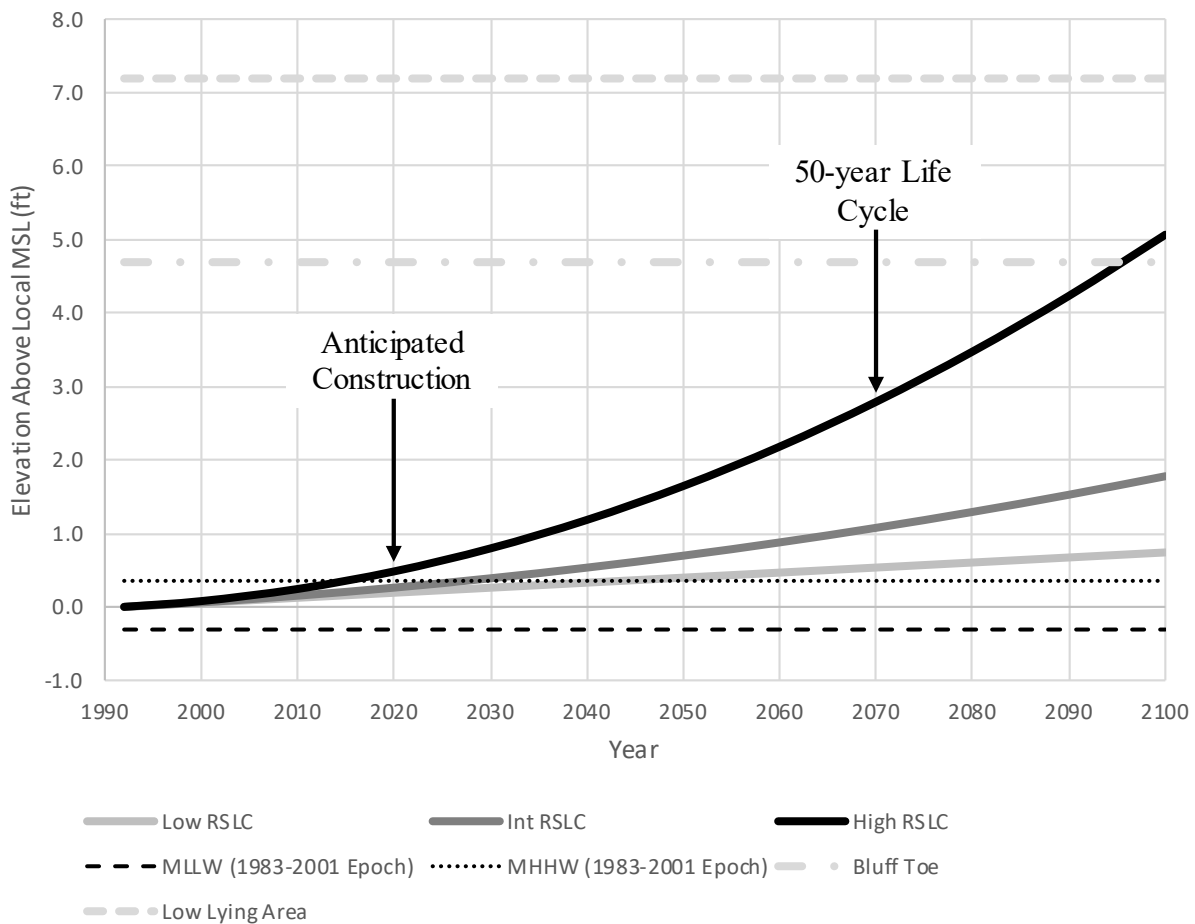


Figure 116. Relative Sea Level Change in Barrow, AK Plotted Against the Toe Elevation of the Existing Bluffs and Elevation of the Low Lying Areas. Also shown: Elevation of Mean Lower Low Water and Mean Higher High Water Referenced to Mean Sea Level.

10.5.4. Beach Access

In order to maintain access to the beach for subsistence and recreational activities, beach access ramps would be constructed with the revetted berm or raising Stevenson Street alternatives. The beach access ramp design would be completed in PED. The design for the access ramps is

anticipated to use the same rock material being used for the berm or raised street. Likely location of the access ramps would be next to The Fur Shop on Stevenson Street, the intersection of Brower Street, Tahak Street, and Stevenson Street, corner of Ahmaogak Street and Stevenson Street, and at the corner of Cakeeater Road and Stevenson Street.

10.5.5. Potential Temporary Barge Landings and Staging Areas

During construction, the contractor would need to coordinate with the community to determine both the staging areas and barge landings. For this Feasibility Study, three potential sites for staging areas and two potential sites for barge landings are proposed by the NSB. One staging area would be located on State of Alaska DOT land at the southwest end of Barrow at the end of the Wiley Post-Will Rogers Memorial Airport (Figure 117), another would be just south of the State of Alaska DOT land on City of Utqiagvik land (Figure 118), and one staging area would be located on UIC land at the southwest end of NARL (Figure 119). The barge landings would be necessary to unload contractor equipment and rock. One barge landing would be located between the State of Alaska DOT land and City of Utqiagvik land (Figure 117 and Figure 118) and another would be located just northeast of the UIC land (Figure 119).

It is anticipated that construction would take 5 years for alternatives that encompass risk reduction measures along the entire proposed stretch of coast. Based on the estimated time for construct and quantity of material, approximately 8 acres would be required as a staging area.



Figure 117. Potential Staging Area and Barge Landing at State of Alaska DOT Borrow Pit



Figure 118. Potential Staging Area South of the State of Alaska Borrow Pit. Owned by City of Utqiagvik.



Figure 119. Potential Staging Area and Barge Landing at UIC Staging Area and Location of Discharge for Middle Salt Lagoon

10.5.6. Middle Salt Lagoon Discharge

According to the NSB, the Middle Salt Lagoon, the secondary wastewater treatment lagoon, is discharges annual into the Arctic Ocean (Russell, 2019). Initial sampling of the Middle Salt Lagoon occurs in late May or early June, depending on the timing of breakup, and is required before discharge. Water quality tests are performed on the wastewater to determine compliance with Alaska Department of Environmental Conservation (ADEC) Discharge Permit Limits. Once the Barrow Utilities and Electric Cooperative, Inc. (BUECI) receives approval from ADEC for discharge, a dike is opened (Figure 119) to allow for drainage from the Middle Salt Lagoon to the Arctic Ocean until approximately the second or third week of July. The dike is then closed again to allow annual transfer of wastewater from the South Salt Lagoon to the Middle Salt Lagoon. Transfer between South Salt Lagoon and Middle Salt Lagoon ends October 1st due to freezing/ice conditions. For the final design, coordination with the BUECI would be necessary in order to determine the best design that the BUECI could maintain to ensure the continued use of the location for annual discharge of wastewater from the Middle Salt Lagoon to the Arctic Ocean.

11. ALTERNATIVES CONSIDERED IN DETAIL

11.1. General

Alternatives that provided different levels of risk reduction were considered for storm damage risk reduction at Barrow. The extents of the structural alternatives considered and the names of each reach are shown in Figure 120. Material volumes and maintenance intervals associated with each alternative are shown in Table 19 through Table 26. Each alternative is a variation on the level of risk reduction with the same measures being consistently used in each reach. Along reaches Bluff and Barrow, a rock revetment would be built to prevent further bluff erosion. In reach Lagoon a revetted berm would be constructed to reduce the risk of flooding. Along the low lying area between reach Browerville and NARL, Stevenson Street would be raised and the seaward side revetted to reduce the risk of flooding.

Sections of the bluff revetment would get very close or into the water's edge due to the narrowed beach. In these areas it is possible that sediment would accrete around the toe of the structure. Once the accretion at the base of the structure reached an equilibrium point the normal sediment transport process would continue.

Table 19. Alternative A

Barrow and Lagoon											
Armored Revetment Coverage Area	Armor [cy]	B Rock [cy]	Core [cy]	Gravel [cy]	Filter Fabric [sy]	Excavation [cy]	Local Material [cy]	Maintenance Interval / Length	Maintenance Armor [cy]	Maintenance B Rock [cy]	Maintenance Core [cy]
Barrow: Revetment	16,937	13,807	4,666	4,981	14,174	31,765	4,570	5 yrs/2000 ft	16,937	13,807	4,666
Tasigarook Lagoon: Revetted Berm	32,694	30,887	7,404	7,895	23,469	71,530	NA	5 yrs/2000 ft	22,548	21,302	5,106

Table 20. Alternative B

Barrow, Lagoon, and Bluff											
Armored Revetment Coverage Area	Armor [cy]	B Rock [cy]	Core [cy]	Gravel [cy]	Filter Fabric [sy]	Excavation [cy]	Local Material [cy]	Maintenance Interval / Length	Maintenance Armor [cy]	Maintenance B Rock [cy]	Maintenance Core [cy]
Bluff and Barrow: Revetment	38,339	30,126	10,089	10,742	30,463	82,878	5,718	5 yrs/2000 ft	21,323	16,755	5,611
Tasigarook Lagoon: Revetted Berm	32,694	30,887	7,404	7,895	23,469	71,530	NA	5 yrs/2000 ft	22,548	21,302	5,106

PAGE INTENTIONALLY LEFT BLANK

Table 21. Alternative C

Barrow, Lagoon, Bluff, and Browerville											
Armored Revetment Coverage Area	Armor [cy]	B Rock [cy]	Core [cy]	Gravel [cy]	Filter Fabric [sy]	Excavation [cy]	Local Material [cy]	Maintenance Interval / Length	Maintenance Armor [cy]	Maintenance B Rock [cy]	Maintenance Core [cy]
Bluff and Barrow: Revetment	38,339	30,126	10,089	10,742	30,463	82,878	5,718	5 yrs/2000 ft	21,323	16,755	5,611
Tasigarook Lagoon: Revetted Berm	32,694	30,887	7,404	7,895	23,469	71,530	NA	5 yrs/2000 ft	22,548	21,302	5,106
Browerville: Raise Stevenson Street	31,279	28,271	9,787	10,547	30,170	78,760	28,732	5 yrs/2000 ft	15,074	13,624	4,717

Table 22. Alternative D

Barrow, Lagoon, and South and Middle Salt											
Armored Revetment Coverage Area	Armor [cy]	B Rock [cy]	Core [cy]	Gravel [cy]	Filter Fabric [sy]	Excavation [cy]	Local Material [cy]	Maintenance Interval / Length	Maintenance Armor [cy]	Maintenance B Rock [cy]	Maintenance Core [cy]
Barrow: Revetment	16,937	13,807	4,666	4,981	14,174	31,765	4,570	5 yrs/2000 ft	16,937	13,807	4,666
Tasigarook Lagoon: Revetted Berm	32,694	30,887	7,404	7,895	23,469	71,530	NA	5 yrs/2000 ft	22,548	21,302	5,106
Salt Lagoon: Raise Stevenson Street	63,911	57,840	20,028	21,602	61,794	172,031	60,873	5 yrs/2000 ft	15,038	13,609	4,712

PAGE INTENTIONALLY LEFT BLANK

Table 23. Alternative E

Barrow, Lagoon, Bluff, and South and Middle Salt											
Armored Revetment Coverage Area	Armor [cy]	B Rock [cy]	Core [cy]	Gravel [cy]	Filter Fabric [sy]	Excavation [cy]	Local Material [cy]	Maintenance Interval / Length	Maintenance Armor [cy]	Maintenance B Rock [cy]	Maintenance Core [cy]
Bluff and Barrow: Revetment	38,339	30,126	10,089	10,742	30,463	82,878	5,718	5 yrs/2000 ft	21,323	16,755	5,611
Tasigarook Lagoon: Revetted Berm	32,694	30,887	7,404	7,895	23,469	71,530	NA	5 yrs/2000 ft	22,548	21,302	5,106
Salt Lagoon: Raise Stevenson Street	63,911	57,840	20,028	21,602	61,794	172,031	60,873	5 yrs/2000 ft	15,038	13,609	4,712

Table 24. Alternative F

F. Reduce Risk of Erosion to Bluff and Barrow and Flooding to Lagoon, Browerville, and South and Middle Salt											
Armored Revetment Coverage Area	Armor [cy]	B Rock [cy]	Core [cy]	Gravel [cy]	Filter Fabric [sy]	Excavation [cy]	Local Material [cy]	Maintenance Interval / Length	Maintenance Armor [cy]	Maintenance B Rock [cy]	Maintenance Core [cy]
Bluff and Barrow: Revetment	38,339	30,126	10,089	10,742	30,463	82,878	5,718	5 yrs/2000 ft	21,323	16,755	5,611
Tasigarook Lagoon: Revetted Berm	32,694	30,887	7,404	7,895	23,469	71,530	NA	5 yrs/2000 ft	22,548	21,302	5,106
Browerville and Salt Lagoon: Raise Stevenson Street	95,190	86,111	29,815	32,149	91,963	250,791	89,606	5 yrs/2000 ft	15,050	13,614	4,714

PAGE INTENTIONALLY LEFT BLANK

Table 25. Alternative G

G. Reduce Risk of Erosion to Bluff and Barrow and Flooding to Lagoon, South and Middle Salt, and NARL											
Armored Revetment Coverage Area	Armor [cy]	B Rock [cy]	Core [cy]	Gravel [cy]	Filter Fabric [sy]	Excavation [cy]	Local Material [cy]	Maintenance Interval / Length	Maintenance Armor [cy]	Maintenance B Rock [cy]	Maintenance Core [cy]
Bluff and Barrow: Revetment	38,339	30,126	10,089	10,742	30,463	82,878	5,718	5 yrs/2000 ft	21,323	16,755	5,611
Tasigarook Lagoon: Revetted Berm	32,694	30,887	7,404	7,895	23,469	71,530	NA	5 yrs/2000 ft	22,548	21,302	5,106
Salt Lagoon and NARL: Raise Stevenson Street	108,983	98,700	34,176	36,849	105,465	320,104	92,211	5 yrs/2000 ft	15,032	13,614	4,714

Table 26. Alternative H

H. Reduce Risk of Erosion to Bluff and Barrow and Flooding to Lagoon, Browerville, South and Middle Salt, and NARL											
Armored Revetment Coverage Area	Armor [cy]	B Rock [cy]	Core [cy]	Gravel [cy]	Filter Fabric [sy]	Excavation [cy]	Local Material [cy]	Maintenance Interval / Length	Maintenance Armor [cy]	Maintenance B Rock [cy]	Maintenance Core [cy]
Bluff and Barrow: Revetment	38,339	30,126	10,089	10,742	30,463	82,878	5,718	5 yrs/2000 ft	21,323	16,755	5,611
Tasigarook Lagoon: Revetted Berm	32,694	30,887	7,404	7,895	23,469	71,530	NA	5 yrs/2000 ft	22,548	21,302	5,106
Low Lying Area: Raise Stevenson Street	140,262	126,971	43,963	47,396	135,634	398,864	120,943	5 yrs/2000 ft	15,041	13,616	4,715

PAGE INTENTIONALLY LEFT BLANK

11.2. No Action

This alternative would be to take no action and leave the city susceptible to the effects of storm events. The bluff would continue to erode, the low lying areas would continue to flood, and the city would continue to fight to save the shoreline during events.

As RSLC is realized along the city's coast, the level of effect storms will have on the erosion rates and flooding levels will increase. Storms events that currently do not induce flooding may start flooding portions of the community and more effort would need to be expended to fight flooding and erosion.

11.3. Alternative A: Barrow and Lagoon

A rock revetment would be constructed against the natural bluff in the reach Barrow as indicated in Figure 120. A revetted berm would be constructed in front of Tasigarook Lagoon to reduce the risk of saltwater inundation of the community's freshwater source. The areas of Bluff, Browerville, South and Middle Salt, and NARL would continue to experience erosion and have the risk of flooding.

11.4. Alternative B: Barrow, Lagoon, and Bluff

As with Alternative A, a rock revetment would be constructed against the natural bluff in the reach of Barrow and a revetted berm would be constructed in front of Tasigarook Lagoon. It would also include a rock revetment constructed against the natural bluff in the reach of Bluff to reduce the risk of erosion destroying houses and cultural heritage sites. The areas of Browerville, South and Middle Salt, and NARL would continue to have the risk of flooding.

11.5. Alternative C: Barrow, Lagoon, Bluff, and Browerville

As with Alternative B, a rock revetment would be constructed against the natural bluff in the reaches of Bluff and Barrow and a revetted berm would be constructed in front of Tasigarook Lagoon. It would also include raising and revetting the seaward side of Stevenson Street as it runs in-front of Browerville to reduce the risk of flooding in the community of Browerville. The areas of South and Middle Salt and NARL would continue to have the risk of flooding.

11.6. Alternative D: Barrow, Lagoon, and South and Middle Salt

As with Alternative A, a rock revetment would be constructed against the natural bluff in the reach of Barrow and a revetted berm would be constructed in front of Tasigarook Lagoon. It would also include a raising and revetting the seaward side of Stevenson Street as it runs in-front of South and Middle Salt lagoons to reduce the risk of flooding and erosion of the landfill and sewage lagoons. This would create a discontinuous risk reduction structure with four locations where it could get flanked. The areas of Bluff, Browerville, and NARL would continue to experience erosion and have the risk of flooding.

11.7. Alternative E: Barrow, Lagoon, Bluff, and South and Middle Salt

As with Alternative D, a rock revetment would be constructed against the natural bluff in the reach of Barrow, a revetted berm would be constructed in front of Tasigarook Lagoon, and Stevenson Street would be raised and the seaward side would be revetted in front of South and Middle Salt lagoons. It would also include a rock revetment constructed against the natural bluff in the reach of Bluff to reduce the risk of erosion destroying houses and cultural heritage sites. This would create a discontinuous risk reduction structure with four locations where it could get flanked. The areas of Browerville and NARL would continue to have the risk of flooding.

11.8. Alternative F: Barrow, Lagoon, Bluff, Browerville, and South and Middle Salt

As with Alternative E, a rock revetment would be constructed against the natural bluff in the reaches of Bluff and Barrow, a revetted berm would be constructed in front of Tasigarook Lagoon, and Stevenson Street would be raised and the seaward side would be revetted in front of South and Middle Salt lagoons. It would also include raising and revetting the seaward side of Stevenson Street as it runs in-front of Browerville to reduce the risk of flooding in the community of Browerville, connecting the risk reduction measure in front of Tasigarook Lagoon and the South and Middle Salt lagoons. The area of NARL would continue to have the risk of flooding.

11.9. Alternative G: Barrow, Lagoon, Bluff, South and Middle Salt, and NARL

As with Alternative E, a rock revetment would be constructed against the natural bluff in the reaches of Bluff and Barrow, a revetted berm would be constructed in front of Tasigarook Lagoon, and Stevenson Street would be raised and the seaward side would be revetted in front of South and Middle Salt lagoons. It would also include raising and revetting the seaward side of Stevenson Street as it runs in-front of NARL to reduce the risk of flooding in the NARL neighborhood and university. This would create a discontinuous risk reduction structure with four locations where it could get flanked. The area of Browerville would continue to have the risk of flooding.

11.10. Alternative H: Barrow, Lagoon, Bluff, Browerville, South and Middle Salt, and NARL

Alternative H includes erosion and flood risk reduction measures along an approximately five mile long stretch of Barrow's coast from in-front of Wiley Post-Will Rogers Memorial Airport northeast to NARL. A rock revetment would be constructed against the natural bluff in the reaches of Bluff and Barrow, a revetted berm would be constructed in front of Tasigarook Lagoon, and Stevenson Street would be raised and the seaward side would be revetted in front of Browerville, South and Middle Salt lagoons, and NARL.

12. CONSTRUCTION CONSIDERATIONS

Construction of a coastal storm risk management structure would rely heavily on imported material. Armor rock, B rock, core, and gravel would be imported. There is a limited window during the ice free season in which barges are able to access the site. All work would need to be

performed from the beach. Archaeologically significant sites are located in the construction area so no shore side construction will be allowed and excavation into the bluffs would also be prohibited. All slope grooming would need to be performed using fill material to achieve a desired slope. There would be some excavation into the beach for construction that would have to be supervised by an archaeologist.

13. RISK AND UNCERTAINTY

The analysis performed for this appendix used historical information to assess the wind, waves, currents, sediment transport, and ice development at Barrow. The information gathered and analysis presented is the best data available at the date of the analyses. Risk and uncertainty that directly affects this project are the use of 14 year old data, annual maintenance requirements, and RSLC. It is anticipated that the use of updated data for the final design would not impact the structure design chosen but would impact the crest height of the structure. The annual maintenance may change through the life-cycle of the project from an increase in the amount of time the project would be exposed to storms due to decreased shorefast ice coverage. The waves impacting the structure would continue to be depth-limited and the height of those waves would be dependent on the realized RSLC. The proposed rock structure would be above the water line and available for visual inspection for damage from storms or ivu events.

14. VOLUME SENSITIVITY ANALYSIS

To estimate the potential impact of including RSLC on the crest elevation of the revetment, revetted berm and raised and revetted Stevenson Street designs (Sections 10.4.2 Run-up for Low Lying Area Structure and 10.4.3 Run-up for Bluff Revetment), the three RSLC curves were linearly added to the total water levels presented in Section 10.4.1 (Total Water Level). The RSLC for the low, medium, and high curves shown in Figure 69 at years 2070 and 2100, assuming construction in 2020, were added to the total water level (Figure 108) for the 50 and 100-year return intervals (7.9 and 9.9 ft, respectively) in order to update total water levels. With the total water level incorporating RSLC, the depth of water at the toe of the proposed structure at the bluffs and low lying area was determined in order to calculate updated depth-limited wave heights. Assuming an 8 sec wave and using the CEM (United States Army Corps of Engineers, 2002) (Part VI Chapter 5 Fundamentals of Design Equation VI-5-13) the run-up on a rock armored slope was calculated. The structure run-up was added to the RSLC total water levels to determine the necessary crest height to reduce the risk of over-topping of the structure with the low, medium, and high RSLC at years 2070 for the bluff and at years 2070 and 2100 for the low lying area.

Based on the calculated crest elevations two crest elevations were chosen as reasonable to perform the volume sensitivity analysis for each the bluff and the low lying area (Table 27). These elevations were chosen based on engineering judgment, the current heights of the bluffs, and what is expected to be reasonable elevations for a raised road or rock berm based on public safety.

Table 27. Crest Elevations used for Resilience Analysis in Economic Analysis

Risk Reduction Measure	RSLC Year and Curve	Current Design Crest Elevation [ft MLLW]	Crest Elevation Based on RSLC [ft MLLW]
Bluff Revetment	NA	19	19
Bluff Revetment	NA	19	21
Bluff Revetment	50-year High RSLC	19	23
Berm or Raised Road	NA	14.5	14.5
Berm or Raised Road	50-year Medium RSLC	14.5	15.5
Berm or Raised Road	NA	14.5	17

Along with a sensitivity analysis on the crest elevations, armor rock size was also evaluated. Updated armor rock sizes are based on the total water level plus RSLC at year 2070 for the 50-year design cycle if constructed in 2020 at the toe of a proposed structure at the bluff. The depth-limited wave height was larger at the bluff. The armor rock sizes based on the sensitivity analysis are shown in Table 28.

Table 28. Armor Rock Size based on Estimated RSLC at 50-years after Construction (2070)

RSLC Curve	RSLC [ft]	Design Wave [ft]	Current Design Armor Rock Size [lb]	Armor Rock Sized for RSLC [lb]
2004 Design	NA	8	5400	5400
Medium	1.08	9	5400	7600
High	2.79	10	5400	10500

15. FUTURE WORK TO BE COMPLETED IN PED

The current designs for the alternatives were based on work performed for the 2010 Technical Report that used data that ran through 2003. The hindcast is currently being updated for years 2004-2017 to include the two most recent storms in 2015 and 2017 and will be incorporated in PED. Data required to complete the storm modeling that will be used to determine the design wave height, wind surge, run-up, and inundation includes LiDAR, survey transects, and a tidal determination, which was collected in summer 2018. New ADCIRC, STWAVE, and XBeach hydrodynamic and morphodynamic processes and impacts model, which is replacing SBEACH, will be run and used to complete the final design. Toe scour will be investigated for the final design.

16. REFERENCES

- Brigham, T. G. (1968). *Barrow Gravel*. Memorandum from Chief, Division of Lands & Minerals, Program Management & Land Office, Bureau of Indian Affairs.
- Chapman, R. (2009). *Barrow Wind Driven Current and Water Level*. Not Published.
- Hume, J. D., & Schalk, M. (1976). The effect of ice on the beach and nearshore, Point Barrow, Arctic Alaska. *La Revue de la Geographis de Montreal*, 105-114.
- IPCC. (2001). *Climate Change 2001: The Scientific Basis. Contribution of Working Group I to the Third Assessment Report of the*. Cambridge, United Kingdom and New York, NY USA: Cambridge University Press.
- IPCC. (2007). *Climate Change 2007: The Physical Science Basis. Contribution of Working Group I to the Fourth Assessment*. Cambridge, United Kingdom and New York, NY, USA: Cambridge University Press.
- Jensen, A. M. (2009). *Nuvuk: Point Barrow, Alaska: The Thule Cemetery and Ipiutak Occupation*. PhD Thesis.
- Jensen, R. E. (2009). *Barrow Offshore Wind and Wave Climate*. Not Published.
- King, D. (2009). *Barrow Longshore Transport and Shoreline Change Modeling*. Not Published.
- Komar, P. D. (1998). *Beach Processes and Sedimentation*. Prentice Hall.
- Lynch, A., Brunner, R., Cassano, E., Jensen, A., Koslow, M., Lestak, L., . . . Tebaldi, C. (2004). *Barrow Climatic and Environmental Conditions and Variations - A Compendium: Technical Edition*. University of Colorado.
- Mahoney, A. R. (2018). *Landfast Sea Ice in a Changing Arctic [in Arctic Report Card 2018]*. National Oceanic and Atmospheric Administration. Retrieved from <https://www.arctic.noaa.gov/Report-Card>
- NASA Jet Propulsion Laboratory. (n.d). *GPS Time Series*. (M. Helfin, Producer) Retrieved October 2018, from NASA Jet Propulsion Laboratory California Institute of Technology: <https://sideshow.jpl.nasa.gov/post/series.html>
- Ocean River Institute. (2014, April 9). *Friends of Cooper Island*. (R. Moir, Producer) Retrieved from <https://www.oceanriver.org/partners/friends-of-cooper-island/>
- Osborne, E., Richter-Menge, J., & Jeffries, M. (2018). *Arctic Report Card 2018*. National Oceanic and Atmospheric Administration. Retrieved from <https://www.arctic.noaa.gov/Report-Card>

- Perovich, D., Meier, W., Tschudi, M., Farrell, S., Hendricks, S., Gerland, S., . . . Webster, M. (2018). *Sea Ice [in Arctic Report Card 2018]*. National Oceanic and Atmospheric Administration. Retrieved from <https://www.arctic.noaa.gov/Report-Card>
- PND Engineers, Inc. (2015). *NSB Erosion Protection: Geology and Material Resources Barrow and Point Hope*. Preliminary Investigation Report.
- Russell, T. W. (2019). *Middle Salt Lagoon Operation*. Letter Sent at the request of The United States Army Corps of Engineers Alaska District.
- Sea Ice Group at the Geophysical Institute. (n.d.). *Barrow Webcam Images*. Retrieved in 2019 from https://seaice.alaska.edu/gi/data/barrow_webcam/.
- Smith, J. M., & Sherlock, A. R. (2009). *Barrow Nearshore Wave Transformation*. Not Published.
- The North Slope Borough. (2015). *Local All-Hazard Mitigation Plan*.
- United States Army Corps of Engineers. (2002, April 30). Coastal Engineering Manual. (*EM 1110-2-1100*). Department of Army.
- United States Army Corps of Engineers. (2013, December 31). Incorporating Sea Level Change in Civil Works Programs. (*ER 1100-2-8162*). Department of Army.
- United States Army Corps of Engineers. (2014, June 30). Procedures to Evaluate Sea Level Change: Impacts, Responses, and Adaptation. (*ETL 1100-2-1*). Department of Army.
- United States Army Corps of Engineers Alaska District. (2005). *Navigation Improvements Draft Interim Feasibility Report, Delong Mountain Terminal*. United States Army Corps of Engineers Alaska District.
- Yu, Y., Stern, H., Fowler, C., Fetterer, F., & Maslanik, J. (2013). Interannual variability of Arctic landfast ice between 1976 and 2007. *Journal of Climate*, 27, 227-243.